Techno economic analysis of salt cavern hydrogen storage

Underground hydrogen storage an economic perspective

Sridharan Kandasamy



Techno economic analysis of salt cavern hydrogen storage

Final Report

by

Sridharan Kandasamy

Thesis Committee:

TU Delft Supervisor: Dr.Ir.Mahinder Ramdin Company Supervisors: Ir.Edwin Van Ruijven

Ir.Ruud Stevens

External examiner: Dr.Hadi Hajibeygi

Place: Process and Energy (3mE), Delft

Student number: 5478928

This research work was made in collaboration with Vattenfall





Acknowledgement

First and foremost I would like to express my gratitude to my TU Delft supervisor Dr.Ir.Mahinder Ramdin, for guiding me throughout the thesis and providing me with inputs to reach my goal, and the faculty of 3ME for providing me with a great quality of education.s

I would like to extend my sincere gratitude to Vattenfall Netherlands for giving me this opportunity to perform my graduation internship. Many thanks to my supervisors Ir.Edwin Van Ruijven and Ir. Ruud Stevens for supervising me throughout this thesis and providing me with some good inputs during our progress meetings. I would like to thank Ir.S.Bojert for providing me with inputs and helping me understand the gas storage. I would also like to thank the colleagues from the vattenfall for providing a comfortable environment to work.

Last but not the least, I would like to thank my parents for letting me explore my passion for energy far from home for which I'm grateful and the endless support of my friends during hardships and personal downfalls.

Abstract

With increasing interest in developing green hydrogen infrastructure as a way to decarbonize the power, transportation and heating sector the storage of hydrogen becomes a crucial component. Although most present hydrogen storage techniques are of small-scale, the intermittent nature of renewable electricity and expected future green hydrogen production and consumption makes large-scale storage an important factor.

This study evaluates the techno-economic feasibility of storing hydrogen in an already-existing underground salt cavern, one of three large-scale gas storage systems. The work starts with an overview of the large-scale gas storage methods and the challenges associated with storing hydrogen. The current existing salt cavern storage facility is discussed and the is technically assessed for hydrogen storage. The investment and operating costs related to the hydrogen storage method were calculated using models developed, certain components of the model were modeled using Aspen simulation software, which was also used to calculate the cost associated with it. For various scenarios, the cost distribution and the Levelized Cost of Hydrogen Storage (LCHS) were estimated. Based on the outcomes, the LCHS ranged from a best case scenario of 0.34 €/kg to a worst case scenario of 1.94 €/kg. Sensitivity analysis was conducted for the various storage parameters, and based on the dominant component the Net Present Value(NPV) is assessed with an increased LCHS. To conclude the study an estimate for the electrolyser capacity required for the plant to operate continuously was determined.

Contents

No	men	clature	νi
Lis	t of l	Figures	ix
Lis	t of	Tables	хi
1	1.1 1.2 1.3	Hydrogen	1 2 2 2 3 4 4
2	Bac	kground and literature review	5
	2.1 2.2 2.3 2.4 2.5	Underground gas storage Gas storage facilities Challenges in underground hydrogen storage 2.3.1 Properties comparison 2.3.2 Hydrogen embrittlemenet 2.3.3 Hydrogen loss and purity 2.3.4 Solubility of water vapour in hydrogen Compressor Thermodynamics in compression of hydrogen 2.5.1 Effect of compressibility 2.5.2 Gas equation 2.5.3 Joule-Thomson effect	5 7 9 10 11 13 13
3	Mod	lelling methodology	16
	3.1 3.2 3.3	Existing natural gas storage overview Process conversion for hydrogen storage 3.2.1 Compressor. 3.2.2 Heat exchanger. 3.2.3 Underground storage. 3.2.4 Purification Economic modelling.	19 19 22 24 25
4		ults and Discussion 3 Model implementation and cost estimation 3 4.1.1 Compressor and heat exchanger 3 4.1.2 Cavern conversion 3 4.1.3 Adsorption system 3	30 33
	4.2 4.3	Cavern injection Results 4.3.1 Effect of cushion gas on LCHS present and future scenarios 4.3.2 Effect of different percentage of purge gas 4.3.3 Effect on LCHS when two caverns and three compressors are used 4.3.4 Effect of purge gas compression on LCHS 4.3.5 Effect of cycle of operation and no of caverns on LCHS 4.3.6 Effect of regeneration gas utilization on LCHS in increased cycles of operation	

Contents

		 4.3.8 Effect of increase in LCHS on the NPV of the storage 4.3.9 Effect on LCHS when new caverns are utilized for storage 4.3.10 Effect of cavern shrinkage on LCHS 4.3.11 Electrolyser capacity estimation for hydrogen storage 	50 52
5	5.1	Conclusion and Recommendation Conclusions	
Re	efere	nces	59
A	A.1 A.2	Dendix Heat exchanger sizing	61

Nomenclature

Abbreviations

Abbreviation	Definition
CAPEX	Capital Expenditure
CAPEX _{COMP}	Capital Expenditure Compressor
CAPEX _{HX}	Capital Expenditure Heat Exchanger
CAPEX _{PSA}	Capital Expenditure Pressure Swing Adsorber
CAPEX _{SC}	Capital Expenditure Salt Cavern
NPV	Net Present Value
LCHS	Levelized Cost of Hydrogen Storage
OPEX	Operating Expense
OPEX _{COMP}	Operating Expenditure Compressor
OPEX _{HX}	Operating Expenditure Heat Exchanger
OPEX _{PSA}	Operating Expenditure Pressure Swing Adsorber
ppm	Parts Per Million

Parameters

Parameter	Definition	Unit
\overline{A}	Bare tube area of heat exchanger	[m ²]
A_b	Tube bundle area of heat exchanger	$[m^2]$
A_i	Internal crossectional area of the tuber	$[m^2]$
A_s	Tube surface area of heat exchanger	$[m^2]$
B	Pressure drop constant adsorber	[-]
C	Pressure drop constant adsorber	[-]
C_i	Concentration of particular species in the gas stream	[g/m ³]
C_p	Specific heat of the gas at constant pressure	[J/kgK]
C_{bed}	Adsorber bed constant to estimate maximum superficial velocity	[-]
d_i	Tube inside diameter	[m]
d_o	Tube outside diameter	[m]
D	Diameter of the adsorber column	[m]
D_m	Minimum diameter of the adsorber column	[m]
F_L	Life factor of the adsorber based on operation	[-]
h_1	Inlet enthalpy of hydrogen gas	[J/kg]
h_2	Outlet enthalpy of hydrogen gas	[J/kg]
h_a	Actual Height of the adsorber column	[m]
h_b	Height of the adsorber bed	[m]
h_i	Inside fluid film coefficient of heat exchanger	$[W/m^2K]$
h_o	Outside fluid film coefficient of heat exchanger	$[W/m^2K]$
h_{id}	Inside dirt coefficient of heat exchanger	$[W/m^2K]$

Contents

Parameter	Definition	Unit
h_{od}	Outside dirt coefficient of heat exchanger	[W/m ² K]
H_a	Adiabiatic head of the Compressor	[J/kg]
H_p	Polytropic head of the Compressor	[J/kg]
i	Discount rate	[%]
k_l	Thermal conductivity of gas	[W/mK]
k_w	Thermal conductivity of material	[W/mK]
K_{MS}	Particle size factor	[-]
I	Lifetime of storage	[years]
L	Length of the tube	[m]
\dot{m}	Mass flow of the gas	[kg/s]
m_a	Mass of adsorbent at equilibrium zone	[kg]
m_{H_2O}	Mass of adsorbed water	[kg]
m_i	Mass of particular species in the gas stream	[kg]
m_{MTZ}	Mass of the adsorbent in mass transfer zone	[kg]
m_t	Total mass of the adsorbent	[kg]
MW	Molecular Weight	[g/mol]
n	Polytropic index	[-]
N_c	Number of adsorber column	[-]
N_h	Adsorption cycle time	[hrs]
Nu	Nusselt number	[-]
P_1	Inlet pressure of the gas	[bar]
P_2	Outlet pressure of the gas	[bar]
P_a	Adiabatic power of the compressor	[W]
P_i	Partial pressure of a species in the gas streams	[Pa]
P_t	Tube pitch based on bundle layout	[m]
P_{ta}	Total adiabatic power of the compressor	[W]
P_{tp}	Total polytropic power of the compressor	[W]
$\frac{1}{\Delta P}$	Pressure drop across the adsorbent bed	[Pa]
ΔP_b	Air flow pressure drop in the bundle	[Pa]
	Actual flow rate of gas withdrawn from the storage	[m ³ /s]
q_g \dot{Q}	Rate of heat gain or loss in compression	[W]
\overline{Q}	Heat exchanger duty	[W]
Pr	Prandtl number	[-]
R	Universal gas constant	رتا [J/molK]
Re	Reynolds number	[-]
t	Operating years of the storage	ر-ا [year]
	Air side inlet temperature	[°C]
t_1 t_2	Air side outlet temperature	[°C]
	Operating time of the adsorber column	
t_a T_1	Inlet temperature of the gas	[s] [°C]
T_1 T_2	Outlet temperature of the gas	[°C]
	· -	
ΔT_{lmtd}	Logrithemic mean temperature difference	[K]
u_f	Face velocity of the fan	[m/s]
U_o	Overall heat transfer coefficient	[W/m ² K]
v	Velocity of the gas within the tube	[m/s]

Contents

Parameter	Definition	Unit
$\overline{v_g}$	Superficial velocity of the gas	[m/s]
v_{gm}	Maximum superficial velocity of the gas	[m/s]
V	Volume of the storage	[m ³]
$\dot{V_1}$	Inlet volumetric flow rate of gas	[m ³ /s]
$\dot{V_2}$	Outlet volumetric flow rate of gas	[m ³ /s]
V_f	Volumetric flow rate of air	[m ³ /s]
W	Working gas stored in the salt cavern	[kg]
\dot{W}	Work done by the compressor	[W]
W_f	Fan power	[W]
X_e	Equilibrium loading	[%]
X_r	Residual loading	[%]
ΔX_a	Aged equilibrium loading	[%]
ΔX_n	Net equilibrium loading	[%]
y_i	Vapor mole fraction	[-]
Z	Compressibility factor	[-]
Z_{avg}	Average compressibility factor	[-]

Greek symbols

Symbol	Definition	Units
$\overline{\eta_a}$	Adiabiatic efficiency of the compressor	[%]
η_f	Fan power efficiency of the heat exchanger	[%]
η_p	Polytropic efficiency of the compressor	[%]
γ	Specific heat ratio of the gas	[-]
μ	Viscosity of the gas	[Pas]
μ_j	Joule-Thompson coefficient	[-]
$ ho_q$	Density of the gas	[kg/m ³]
$ ho_{MS}$	Density of adsorbent	[kg/m ³]

List of Figures

1.1 1.2 1.3	Global energy demand forecast from DNV [1]	1 3 4
2.1	a) Aquifer before hydrogen injection b) aquifer water displacement after hydrogen injection [10]	6
2.2	Schematic of underground salt cavern gas storage with its tubing part which is currently used to store natural gas [16]	6
2.3	(a)Schematic of depleted gas storage (b)microscopic image of the pores in the storage (c)mechanism where the injected hydrogen occupies the pores displacing the oil [10]	7
2.4		10
2.5		11
2.6		11
2.7		12
2.8		14
2.9		15
3.1	Current existing natural gas storage process at Epe, the gas to the storage is delivered by the gas grids where it is injected in the cavern by compressing and cooling in two stages. During the withdrawal cycle, the gas is purified using a TEG dehydration unit	16
3.2		18
3.3		19
3.4	Salt cavern existing natural gas emptying process where a) shows the existing gas, b) shows	
	the brine injection and gas removal and c) shows the hydrogen injection and brine removal.	24
3.5	Two column pressure swing adsorber for hydrogen drying	25
3.6	Pressure swing adsorber operation cycles	28
4.1	· · · · · · · · · · · · · · · · · · ·	32
4.2	Cavern filling based on pressure increase when the hydrogen gas is compressed and injected	
	using the existing compressors when the centrifugal compressor operated in parallel until	
		35
4.3	Cavern filling based on pressure increase when the hydrogen gas is compressed and	
		36
4.4	Cavern filling based on pressure increase when the hydrogen gas is compressed and	
	, , , , , , , , , , , , , , , , , , , ,	37
4.5	Distribution of the CAPEX based on cushion gas investment. The scenarios are studies	
	based on the cost of hydrogen used, in (a) green hydrogen is used as cushion gas, in (b)	
	blue hydrogen is used as cushion gas and in (c) cushion gas is subsidized. When the cost	~~
	·	38
4.6	Distribution of a) annualized cost and b) levelized cost of Hydrogen storage, over three	~~
		39
4.7	5 , 5	40
4.8	, , ,	40
4.9	Levelized cost of hydrogen based on different percentages of regeneration mass. The	
	CAPEX remains the same but the OPEX increases significantly in higher regeneration	11
1 10		41
		42 42
	· · · · · · · · · · · · · · · · · · ·	42
⊤. 1∠	- Capes distribution when to whedereration das is complessed and femicined into the diff.	-T.)

List of Figures x

4.13	Cost comparison when there is H_2 loss vs without H_2 loss for a single cycle of operation based on two cases where case (a) is a single cavern single compressor and case (b) is two caverns and three compressors. From the figure, it could be observed that when the	
	volume of stored hydrogen is lower investing in the regeneration compression is not useful	
	in reducing the LCHS	44
4.14	CAPEX distribution based on 2 caverns and 2 compressors with green hydrogen as cushion	
	gas	45
4.15	Cost distribution for the hydrogen storage for 2 cavern and 2 compressors & heat exchanger	
	setup based on the different lifetimes of storage operated for 12 cycles per year	45
4.16	Cost distribution for the hydrogen storage for 2 cavern and 2 compressor & heat exchanger	
	setup based on different cycle of operation.	46
4.17	CAPEX distribution when the regeneration gas is compressed and reinjected into the storage	
	process for a 2 cavern and 2 compressor & heat exchanger setup with green hydrogen as	
	cushion gas.	46
4.18	Cost distribution for the hydrogen storage for 2 cavern and 2 compressor & heat exchanger	
	setup when the purge gas is compressed based on different cycles of operation	47
4.19	Tornado plot displaying the LCHS variation when a certain parameter is increased and	
		48
4.20	Spider plot displaying the LCHS variation based on the slope when a certain parameter is	
	increased and decreased by 50% when the other base parameters are kept constant. The	
	most dominating factor was found to be the cycle of operation and hydrogen cost	48
4.21	NPV analysis for 2 cycles of operation with different increase in LCHS percentage	49
	NPV analysis for 4 cycles of operation with different increase in LCHS percentage	49
	CAPEX distribution for two newly created caverns consisting of two compressors & heat	
	exchanger setup	50
4.24	Cost distribution of the storage for 2 new caverns and 2 compressors heat exchanger setup,	
	based on different lifetimes of storage operated for 12 cycles per year	51
4.25	Levelized cost based on different cycles of operation for new caverns	51
	Effect of cavern shrinkage on LCHS when an existing cavern is used for a lifetime of 20	
	years based on different cycles of operation	52
4.27	Effect of cavern shrinkage on LCHS when a new cavern is used for a lifetime of 40 years	
	based on different cycles of operation	52
4.28	Input parameters used to estimate the electrolyser requirement for hydrogen storage in a	
	single salt cavern	53
	ŭ	
5.1	Cavern conversion timeline	54
۸ ،	Others depend to the additional table in [40]	00
A.1	Standard tube diameters [46]	
	Face velocity design assumption [64]	60
	Adsorbent selection [53]	
	Molecular sieve capacity decline curves [53]	
A.5	Pressure drop constant for molecular sieve based on sizes [53]	62
A.6	Thickness of the column [53]	62
A.7	Cavern creation cost [65]	63

List of Tables

1.1	Green hydrogen expected demand in the Netherlands in 2030 [5]	3
2.2 2.3	Poterntial H_2 storage sites around the world	9 10
3.2	Current compressor operating parameters from the existing storage process	18
3.3	Maximum duty of the existing heat exchangers used in the natural gas storage	
	Polytropic head comparison	
	Coefficients used to calculate the overall heat transfer coefficient [47, 48]	
3.0	Coefficients used to calculate the overall heat transfer coefficient [47, 40]	20
4.1	Reciprocating compressor model inputs for hydrogen compression	30
4.2	Reciprocating compressor duty comparison	31
	Gas temperature after compression in each stages	
	Heat exchanger input parameters	
	Heat exchanger output parameters	
	Capital and operating cost of compressor and heat exchanger system	
	Cavern associated cost	
	Pressure swing adsorber input and output parameters	
	Adsorber column capital cost [59, 60]	
	operating cost of the adsorber column	
	Different colours of hydrogen cost [57, 61]	
	Maximum and minimum distribution of cost for the cushion gas scenarios	
	Maximum and minimum costs based on different regeneration percentages	
4.14	Sensitivity base case input parameters	47

Introduction

Energy has become an essential commodity within human society that is required for various activities. Currently, a significant percentage of the world's energy needs are satisfied by fossil fuels. However, the use of these fuels has resulted in an increase in emissions, which has contributed to Global warming resulting in the increase of the global temperature. Figure 1.1 illustrates the increasing demand for energy in the coming years. If the demand is satisfied with traditional fuels, it will lead to further increase in the global global temperatures. Therefore, increasing the production of renewable energy is crucial for addressing climate change and satisfying energy demands. Electricity generation is not the only sector

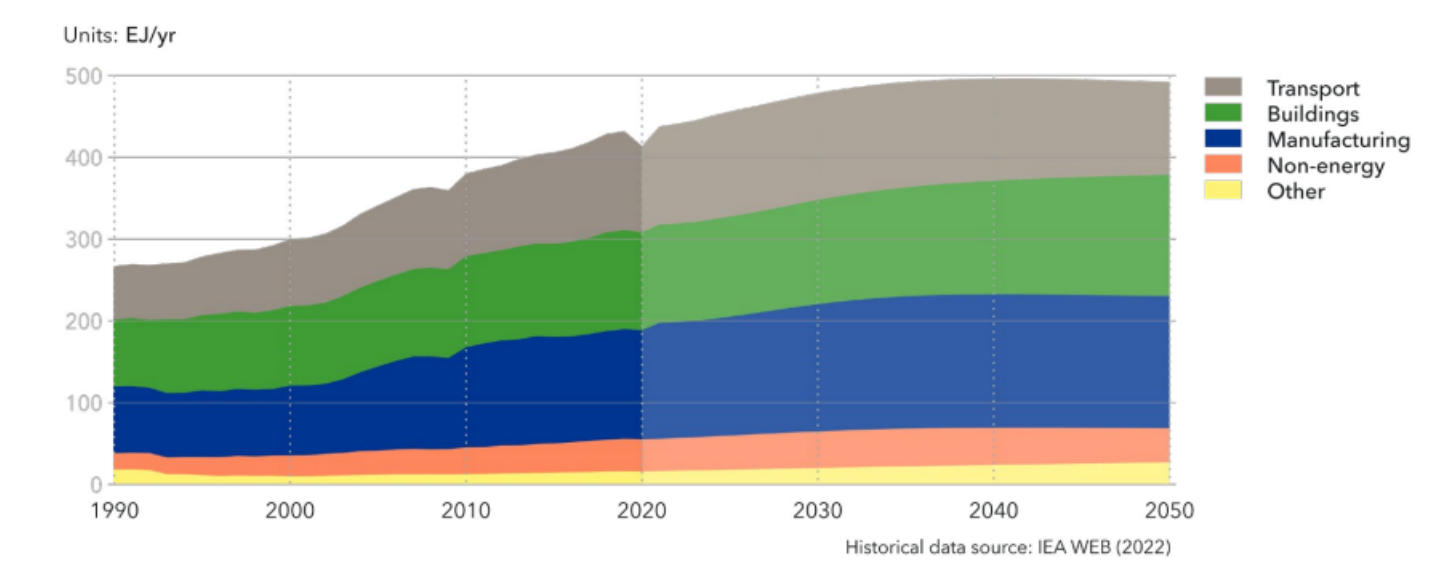


Figure 1.1: Global energy demand forecast from DNV [1]

that relies on fossil fuels as a primary source of energy. Many industries also use fossil fuel as feedstock, currently the manufacturing industry is the largest consumer of energy in the world, accounting for 133 EJ (32%) of final energy demand in 2020 [1]. The major source of energy in these industries are dominated by coal and natural gas, which are used to produce high-temperature heat or used to produce other compounds. however, direct electrification from renewable sources is often not feasible for the high heat requirement. This makes certain sectors like iron and steel, chemical industries, and refineries particularly challenging to decarbonize. To address this, alternate forms of energy such as hydrogen produced from renewable energy sources are being explored as potential solution.

1.1. Hydrogen 2

1.1. Hydrogen

Hydrogen is not new to industries, it is already extensively used as an industrial feedstock in chemical industries producing ammonia and also used in refineries. However, the hydrogen currently used is mainly grey hydrogen, which is produced from natural gas using steam methane reforming or auto-thermal reforming. In 2021, approximately 90 million tons of hydrogen was used globally as an industrial feedstock, with the chemical and refining sectors being the major consumers. However, most of this hydrogen was mainly produced from natural gas reforming, resulting in approximately 9 billion tons of CO₂ emissions worldwide. Europe is the fourth largest user of hydrogen globally, consuming around 8 million tons in 2021. As the demand for hydrogen in these industries continue to increase as well as with new demands expected like in steel industries, it is important to decarbonize the hydrogen supply chain. To achieve this, low-carbon hydrogen production methods such as blue hydrogen (produced from methane reforming with carbon capture technology) and green hydrogen (produced from electrolysis using renewable energy) are becoming increasingly important.

Green hydrogen, produced from renewable sources is preferred over blue hydrogen as it does not involve the use of traditional fossil fuels. This is an important goal in the energy transition, as reducing dependence on fossil fuels is crucial for mitigating climate change. Hydrogen also offers long-term energy storage capability, which can help address the intermittency of renewable electricity generation. During periods of excess amount of renewable energy hydrogen can be produced and stored for later use in industries and other applications. However, developing a hydrogen network requires significant infrastructure for production, transportation and storage. This includes renewable electricity sources and electrolysers for hydrogen production, a well-developed gas transportation network, and large-scale hydrogen storage capabilities. Northwestern Europe has been identified as a suitable location for a hydrogen backbone, due to its offshore wind capability, existing natural gas network that can be repurposed for hydrogen and salt cavern for hydrogen storage. The Netherlands one of the major producers and consumers of grey hydrogen in Europe, has the Infrastructure capability to develop a hydrogen backbone and is already taking steps in that direction.

1.2. Netherlands hydrogen development

In 2020, the Netherlands was the second largest consumer of grey hydrogen, after Germany. Its demand for hydrogen reached 1.3 million tons [2], with refining and ammonia production in chemical industries contributing a major share to this demand. However, given the increasing demand in these sectors, there is a growing need for low-carbon hydrogen to contribute to the energy transition. The Netherlands is working to become a pioneer in low-carbon hydrogen production, particularly green hydrogen by utilizing its offshore wind capability to start the development of the European hydrogen backbone.

1.2.1. Green hydrogen capability

The Netherlands has set an ambitious plan to increase its offshore wind energy capacity to 21GW by 2030 and to 70 GW capacity by 2050 [3]. Along with this, there is also a plan to develop an electrolyser capacity of 3-4 GW by 2030 [4]. With this increased electrolyser capacity currently the industries that consume grey hydrogen have set out plans to incorporate green hydrogen into their requirement. The estimated future demand for green hydrogen in the industries based on the proposed electrolyser capacity is given in Table 1.1.

The assumptions are based on having a steady supply of renewable electricity, but this is not possible due to its intermittent production. Green hydrogen in the Netherlands is primarily planned to be produced from wind electricity, especially offshore wind energy. In 2022 the offshore wind contributed around 40 percent of the wind electricity, with 8388 GWh of electricity produced with a total installed capacity of 2571 MW [6]. The electricity generated is distributed across the months in different quantities, Some months produce electricity more than the average, while some months produce electricity lower than the average. The offshore wind capability is planned to be increased to around 21 GW by 2030, and the electricity produced by it will also be substantially increased. The production in each month is assumed to follow the same trend as 2022 taken from IEA. Figure 1.2 depicts the forecast of electricity production in each month and the margin with respect to the average over the year.

Sector	Hydrogen (kton/year)
Steel	115
Ammonia	104
Refinery	135
Methanol	32
e-fuels	4
others	181
Total	571

Table 1.1: Green hydrogen expected demand in the Netherlands in 2030 [5]

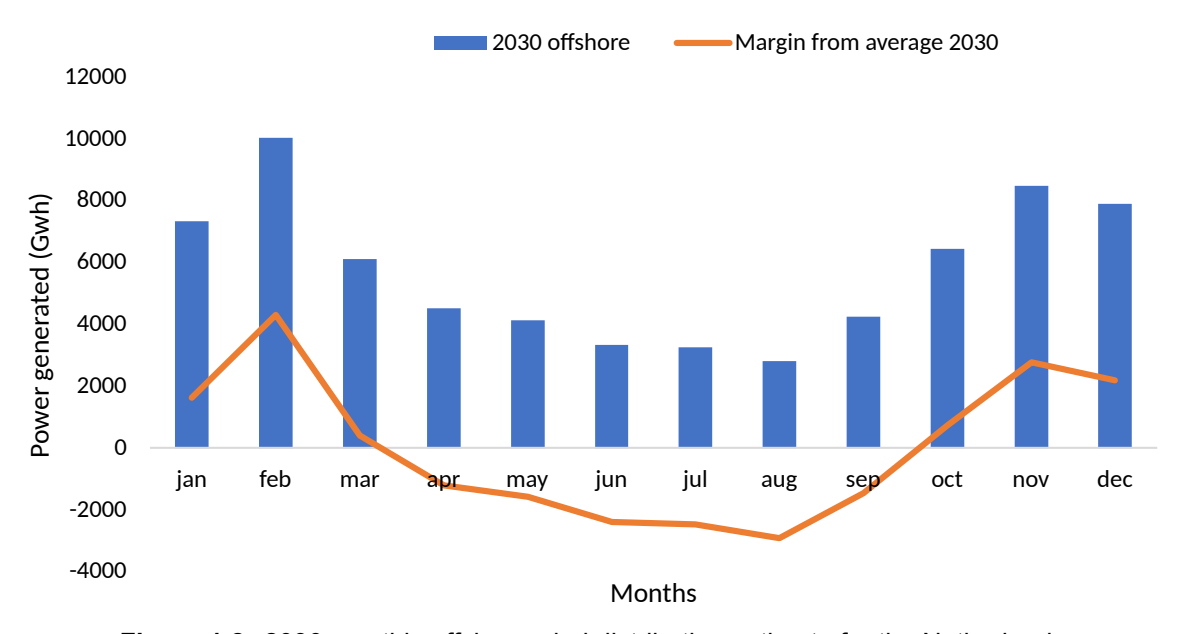


Figure 1.2: 2030 monthly offshore wind distribution estimate for the Netherlands

From Figure 1.2 it can be seen that from november to march we have higher wind generation compared to the average and the hydrogen production can be maximized during these months. Whereas in the rest of the year, the production is low and this will affect the green hydrogen production. So one possible solution to this intermittency is to have the capability for large scale energy storage.

1.2.2. Large scale energy storage

As discussed in the previous section, the intermittency in renewable energy can be solved only if we have the means to store the energy during peak hours and utilize it during off-peak hours. There are different storage methods ranging both short-term and long-term storage with different capacities. In our case, we need to store large quantities of electricity for a longer period and utilize it when required. The production of hydrogen can be done in two ways, the first method is by storing the electricity for a longer term and running the electrolyser in a base load operation. The next method would be to have a large capacity electrolyser plant to produce hydrogen and vary the production based on our available electricity.

For the first case, mechanical energy storage can be used, but in the Netherlands, pumped hydro storage is not possible due to the geological structure. Compressed air storage is possible, but instead of storing the compressed air, we could produce and store compressed hydrogen. So, the second option seems the most viable option, and the existing gas grids can be repurposed to support hydrogen transport throughout the Netherlands. However, once a large quantity of hydrogen is produced we need to have the capability for large-scale hydrogen storage.

1.2.3. Hydrogen backbone



Figure 1.3: Netherlands hydrogen gas network [7]

The hydrogen producing capability from offshore wind in the Netherlands is mainly concentrated in areas where renewable energy is located. The produced hydrogen need to be transported to various industrial clusters. Figure 1.3 shows the planned hydrogen gas transmission network in the Netherlands. The network is being developed by Gasunie in the name of Hyway27 by repurposing existing natural gas grids. The initial phase of the project starts in the Netherlands and is planned to develop throughout Europe, with initial developments in northwestern Europe. The hydrogen gas network also includes underground gas storage in this case salt cavern, to support the production and end industrial requirements. Therefore, it becomes important to study the techno-economics involved in repurposing salt caverns to support hydrogen instead of natural gas. The following research questions are answered at the end of this research.

1.3. Research questions

This research will be focused majorly on studying the techno-economics involved in converting the existing salt cavern storage at Epe to support hydrogen. At present, there are 70 salt caverns situated in Epe, Germany. Among these caverns, Vattenfall owns seven that are used for the storage of natural gas. These gas storage facilities are mainly utilized for balancing the natural gas grids. However, there remain certain caverns that are currently not being fully utilized. With growing interest in developing hydrogen infrastructure, it becomes important to access the techno-economic feasibility involved in converting the existing storage. At the end of this research, the following questions will be answered

- 1. What are the challenges involved in hydrogen storage in salt caverns?
- 2. What technical measures are required for making Epe fit for hydrogen and time taken for the conversion?
- 3. What will be the CAPEX and OPEX involved in converting the storage and operating it with Hydrogen?
- 4. What will be the Levelized cost of hydrogen storage(LCHS) in the salt cavern?
- 5. When will be the storage required and at what electrolyser capacity will it be feasible?

Background and literature review

Literature Methodology

The work is done by gathering information available from the research papers and by reviewing the existing storage process model.

2.1. Underground gas storage

Underground gas storage is an artificially created facility used to store gas at a certain depth from the surface. This type of storage is not a relatively new concept as it is already been implemented for the storage of natural gas. However certain operational differences need to be considered when storing hydrogen. The facility comprises a working gas and a cushion gas. The working gas, which in our case is hydrogen, is injected and withdrawn for customer requirements. The cushion gas, on the other hand, serves for operational purpose such as maintaining pressure during injection and extraction cycles [8]. The cushion gases that can be used are N_2 , CH_4 , CO_2 and H_2 itself, along with the working gas. The ratio of cushion gas to working gas is dependent on geological parameters including reservoir depth, and reservoir permeability. The deeper the storage, the larger the cushion gas required for operation [9]. Underground gas storage facilities are useful because they are less prone to fire and provide better safety operation, they also play a good role in space management. There are three major underground storage facilities that can be used for hydrogen storage:

- Aguifers
- · Salt cavern
- · Depleted gas fields

Aquifers

An aquifer is an underground surface made of a layer of porous and permeable rock, often several hundred feet deep, filled with fresh or saline water. Aquifers may be a viable option for hydrogen storage and an alternative when there are no depleted gas fields or salt caverns available for storage. The conditions for a good aquifer include 1) good reservoir characteristics of Host rock, and 2) the presence of an impermeable layer to prevent the gas from escaping [11].

Figure 2.1 shows the different layers of an aquifer and how the hydrogen is stored in it. When hydrogen is injected into the aquifer, which is already filled with liquid, the liquid displaces to the side due to density difference. By injecting the gas, the pressure inside the porous media is increased as the existing water is not removed. So, when hydrogen is withdrawn from the storage due to the gas-liquid interface, the liquid is simultaneously removed together with the gas, this is one of the major disadvantages of aquifer hydrogen storage [12, 13]. The mechanism for storage between an aquifer and depleted gas fields are similar because they both are classified as porous and permeable. Although the working is similar an aquifers have a high investment cost due to the detailed test required to determine the tightness of the rock because of the changes in the gas-liquid interface. There was no previous experience in the literature

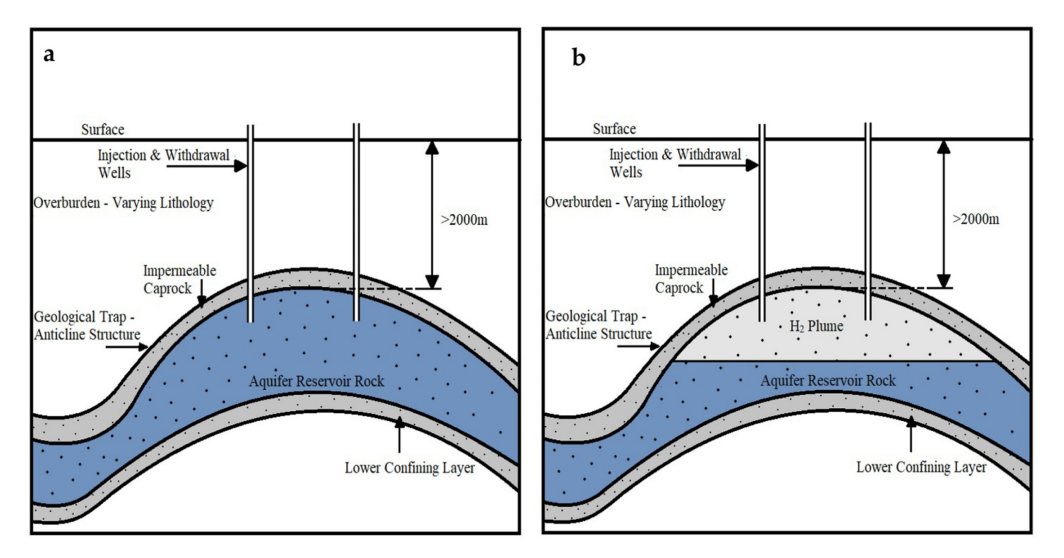


Figure 2.1: a) Aquifer before hydrogen injection b) aquifer water displacement after hydrogen injection [10]

discussing the storage of pure hydrogen in an aquifer, usually a mixture of hydrogen and natural gas is stored [14].

Salt cavern

Salt caverns are artificial chambers created within subsurface salt deposits through solution mining, which involved injecting water to dissolve salt and create a cylindrical pit. A typical salt cavern can be around 2000 m deep with a volume of 1 million m³, a height of 300-500 m, and a diameter of 50-100 m, providing the capability to store large quantities of gas. Salt caverns can be created in two types of underground salt formations: Salt domes and salt bedded formations. Salt domes are solid and homogeneous bodies made of a single material, and the cavern built in these structures is usually very robust for depths lower than 2000 m. Salt bed formation, on the other hand, consists of layers of salts present at considerably lower depths when compared to the domes. They are mostly heterogeneous in nature, mainly consisting of salt halite, with other layers of dolomite, shale, and anhydride. Salt caverns are built mainly in areas where halite is present at greater depths and the insoluble compounds are present in smaller amounts [15].

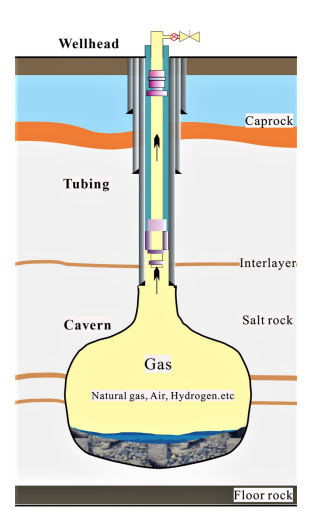


Figure 2.2: Schematic of underground salt cavern gas storage with its tubing part which is currently used to store natural gas [16]

Caverns are regarded as the best storage method for underground hydrogen compared to the other storage methods due to their lower gas permeability and good rheology, which provides good sealing

and distributes the stress developed during injection [17]. The cushion gas requirement in the salt cavern varies based on the cavern depth, when the cavern depth is larger, the cushion gas required is higher and when the depth is smaller, the cushion gas required is lower. The cushion gas requirement can vary from 22 and 33% of volumetric capacity and the maximum of 78% of working gas capacity [18]. Salt caverns are the most acceptable gas storage during peak production due to their simplicity in operation [11].

Depleted oil and gas fields

Depleted oil and gas reservoirs are porous and permeable hydrocarbon reservoirs located thousands of feet below ground, with almost all the recoverable product being extracted. In other terms, these can be characterized as a form of aquifers where there is only a residual amount of liquid within the pores but are mostly occupied by oil and gas. The major advantage of this type of reservoir is that they are a proven trapping system for gases, as it already held hydrocarbons and has a well-identified geological structure due to its exploration and exploitation history.

These types of depleted gas fields are already equipped with necessary installations both on the surface and subsurface, which can be used for hydrogen storage. The cushion gas required for this type of storage is lower than that of aquifers as the already existing remaining trapped gases will act as cushion gas. When planning for this type of storage facility, it is necessary to stop the exploitation as early as possible, so that the removed gas pores are filled with formation water, and the water can be removed. This allows us to store more gas than it has earlier with high pressures. The major disadvantage with this type of storage is that the hydrogen stored mixes with the gas in the storage and during extraction, the mixture percentage might vary. The hydrogen might also react with oil deposits in the fields, forming methane, lowering the purity, and also causing the oil to dissolve and be irreversibly lost forever [19].

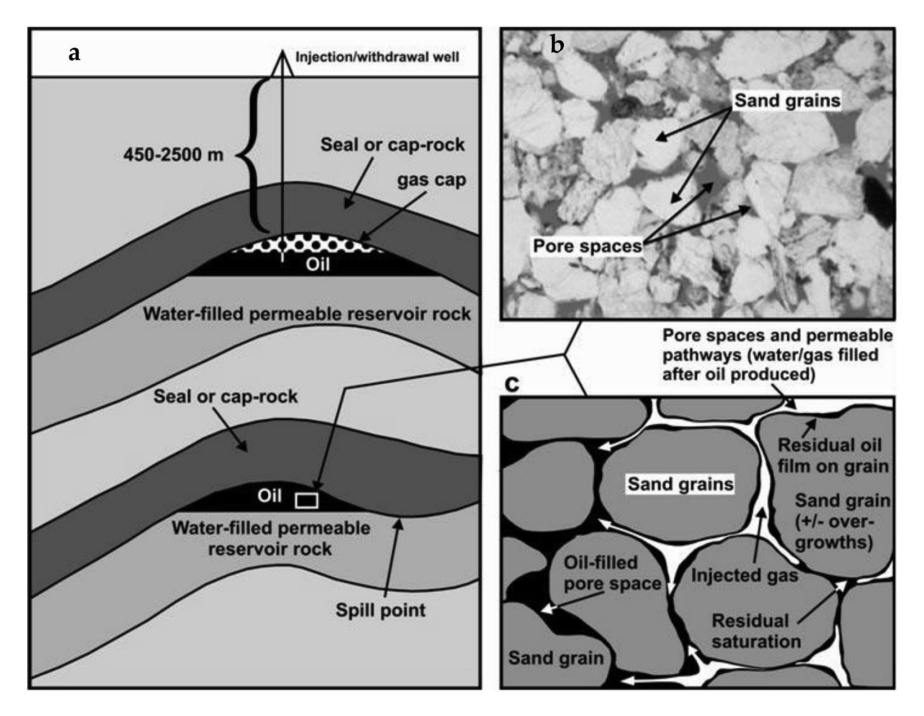


Figure 2.3: (a)Schematic of depleted gas storage (b)microscopic image of the pores in the storage (c)mechanism where the injected hydrogen occupies the pores displacing the oil [10]

2.2. Gas storage facilities

Based on the three types of underground gas storage methods that could be used for hydrogen storage, potential sites globally were discussed in some of the literature papers. Table 2.1 discuss the sites and their parameters reported in the literature.

Table 2.1: Poterntial H_2 storage sites around the world

Salt Cavern					
Country	Region	Parameters	Reference		
		Depth=525m			
Canada	Saline A2 unit	Capacity=9.5million m ³	[17]		
		Thickness=45 m			
		Depth = 400m			
Canada	Salina B unit	Capacity = 6.4 million m ³	[17]		
		Thickness = 90m			
		Operating pressure=60-180 bar			
China	Jiangsu Province-Jintan	Storage capacity = 20 Million m ³	[20]		
		Depth = 900-1100m			
		Pressure = 50-100 bar			
Denmark	lille thorup	Storage capacity = 445 Million Nm ³	[21]		
		Depth = 1270-1690 m			
	N. (1.) N. (6.1	Capacity			
0	Northern Westfalen	2.4 billion m ³	1001		
Germany	Northwest	4.6 billion m ³	[22]		
	Centrsl	1.8 billion m ³			
		Operating pressure = 59 bar-158 bar			
Spain	Castilla y Leon region	Storage Capacity = 0.1 million Nm ³	[23]		
	, 0	Depth =300m - 2000m			
		Pressure = 220 bar			
Turkey	Tuz Golu gas site	Depth = 1100-1400 m	[24]		
		Capacity = 12 x 0.63 Million m ³			
Aquifers					
		Pressure = 76bar			
Canada	Mount Simon	porosity = 15%	[47]		
Callaua	Mount Simon	Depth = 800m	[17]		
		Capacity = 725 million ton of Co ₂			
		Porosity = 14%			
Spain	San Pedro Belt	Permeability = 101.3 mD	[12]		
		Depth = 1700 m			
Depleted reservoirs					
		Pressure = 60 bar			
Cormony	Schleswig-Holstein	Porosity = 13 % -33%	[13]		
Germany	Scrieswig-Huistelli	Permeability = 2.1-572 mD	[13]		
		Depth = 500 - 3000 m			
		Capacity =48 Million m ³			
		Operating pressure =50-100 bar			
UK	Rough gas storage facility	porosity = 20%	[8]		
		Permeability = 75mD			
		Depth = 2743 m			

Several existing gas storage facilities have been studied and operated for hydrogen storage, and Table 2.2 summarizes the sites and parameters of these storage facilities. The table shows that high-purity hydrogen has only been stored in salt caverns, whereas in other storage facilities, it was stored in a mixture of other gases. So to store pure hydrogen salt caverns are the best option.

Salt caverns					
Country	Project Name	Depth (m)	Volume (m ³)	Operating conditions (bar)	H2 percentage
UK	Teesside	400	210000	45	95
USA	Clemens	1000	580000	70-137	95
USA	Moss Bluff	1200	566000	55-152	95
Germany	Kiel		32000	100	60
Aquifers					
Germany	Ketzin	200-250	-	-	62
France	Beynes	430	3.3 x108	-	50
Czech Republic	Ketzin	400-500	-	90	50
Depleted reservoir					
Austria	Underground Sun Storage	1000	-	78	10

Table 2.2: Previous experience in H₂ storage sites [10, 19]

2.3. Challenges in underground hydrogen storage

2.3.1. Properties comparison

Hydrogen is the most abundant element found in the entire universe, it is an odourless, highly reactive and non-toxic diatomic gas. From figure 2.4, we can see a comparison of lower heating value (LHV) of the various fuels based on their gravimetric and volumetric energy density. The figure shows that the gravimetric energy density of hydrogen is around 33 kWh/kg which is higher than most fuels. However, the volumetric energy density of hydrogen is lower when compared to other energy sources. To store 1 kg of hydrogen, the required volume is around 11 m 3 at standard temperature and pressure (@ 0 $^{\circ}$ C & 1 atm) condition.

Unlike natural gas, hydrogen is not an energy source but an energy carrier, which is why it is produced from other sources such as natural gas or through electrolysis. To understand the properties of hydrogen, it is compared with natural gas and is given in Table 2.3. From the table, it can be observed that hydrogen is a very light element and the density is approximately 8 times lower than methane. This property of hydrogen makes it challenging to store in the same volumes at the same pressures as natural gas. However, this issue can be addressed by compressing the hydrogen by reducing the energy gap.

2.3.2. Hydrogen embrittlemenet

Hydrogen embrittlement is a phenomenon where the ductile and tensile strength of the metals is reduced, leading to degradation over time. This occurs when hydrogen, due to its small size, enters the metal lattice of a material and accumulates resulting in the failure of the material. Higher-strength materials are generally more susceptible to hydrogen embrittlement than lower-strength materials. Materials such as iron, titanium and nickel are more susceptible to hydrogen embrittlement than materials like copper, and austenitic stainless steel [26]. Steels with high Mn content and with a strength greater than 1000 MPa are more susceptible to hydrogen embrittlement. To mitigate the effect of hydrogen embrittlement an appropriate material can be selected or the existing material can be protected by applying coatings or barriers to prevent hydrogen entering the material [27, 28]. But in large-scale applications, it is economical

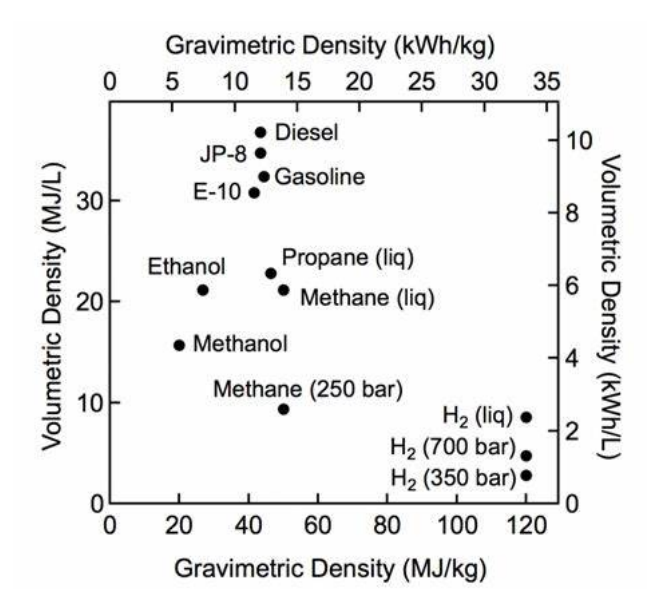


Figure 2.4: Comparison of energy densities of different fuels [25]

Table 2.3: H₂ vs CH₄ properties [10]

Properties	H_2	CH_4
Molecular weight	2.016 g/m ³	16.043 g/m ³
Density @25°C and 1atm	$0.082~\mathrm{kg/m^3}$	$0.657~\mathrm{kg/m^3}$
Viscosity @25°C and 1atm	$0.89x\ 10^{-5}\ Pas$	$1.1 \ x \ 10^{-5} \ Pas$
Normal boiling point	-253°C	-162°C
Critical Pressure	12.8 atm	-45.79 atm
Critical Temperature	-239.95°C	-82.3°C
Heating Value	33.33 kWh/kg	13.1 kWh/kg
Diffusion in pure water @ 25°C and 1atm	$5.13x10^{-9}m^2/s$	$1.85 \mathrm{x} 10^{-9} \ \mathrm{m}^2/\mathrm{s}$
Solubility in pure water @ 25°C and 1atm	$16x10^{-4}g/L$	$22.7x10^{-3}g/L$

to use materials that are inert to hydrogen embrittlement.

2.3.3. Hydrogen loss and purity

Hydrogen is a highly reactive element and when stored using underground storage methods, it has the tendency to undergo reactions that can result in loss of purity. These reactions can be caused by a variety of factors, including geochemical and microbial activity. Figure 2.5 shows the most common hydrogen reactions occurring in the subsurface hydrogen storage.

The hydrogen stored in underground reservoirs and aquifers have a risk of reacting with the fluids and rock minerals, resulting in the loss of hydrogen and a change in the chemical equilibrium of the reservoir. These reactions can also affect the permeability and porosity of the Geological rock structure [29]. Microbiological activity is another factor that can affect the purity and content of stored hydrogen. Microorganisms can be naturally present or introduced during the storage process. The major loss of hydrogen due to this reaction is due to the formation of CH_4 and H_2S which is shown in the Figure 2.5. The most common loss of hydrogen in the storage of the gas in the reservoirs is the methanogenesis reaction where the hydrogen is converted into methane.

Loss of hydrogen due to these reactions is more predominant in depleted reservoirs, but in the case of salt caverns, geochemical reactions are not as predominant. However, in the case of microbial reaction, a

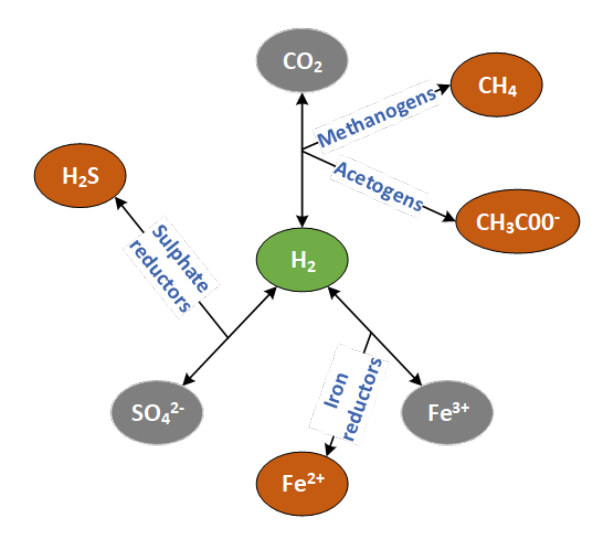


Figure 2.5: Subsurface hydrogen reactions [14]

significant amount of water can accumulate in the salt cavern during the leaching phase. The sump may contain rock impurities that allow bacteria to live in this over-saturated brine solution. As a result, bacteria can initiate a reaction between the SO_4^{-2} and form H_2S . Hydrogen sulphide above is undesirable in the gas stream above certain as it can cause corrosion [30] and also it cannot be used in fuel cell applications due to degradation of the electrode [31].

2.3.4. Solubility of water vapour in hydrogen

During the underground storage of hydrogen, the gas comes in contact with the accumulated brine solution in the cavern, and water vapour can diffuse with the stored gas over time. As a result, withdrawn gas from the storage can be saturated with water molecules, and before reinjecting it back into the grid, the gas needs to be dried. This is why most gas storage plants use a drying unit. The presence of water molecules in the gas flow can result in the formation of hydrates, which can lead to clogging of pipelines. If the water molecules content is over 5 ppm in the stream, it cannot be used for fuel cell application without drying. Figure 2.6 shows the amount of water vapour content in a compressed nitrogen and hydrogen gas at varying pressures in a constant temperature of 50°C temperature. However, one major disadvantage of the graph is that it does not account for the salinity of the water and the result is obtained for a mixture.

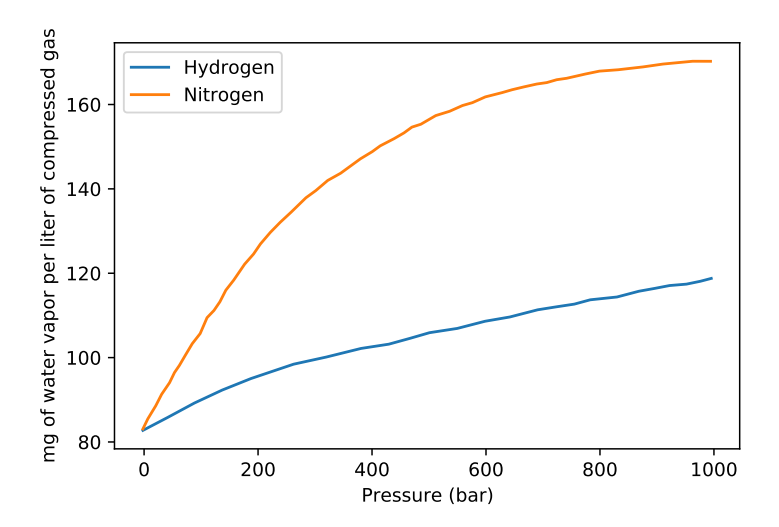


Figure 2.6: Water vapor content of a nitrogen and hydrogen gas mixture at varying pressures [32]

2.4. Compressor

2.4. Compressor

The hydrogen gas is stored at high pressures, which necessitates the use of a compressor to increase the gas pressure. However, not all types of compressors are suitable for hydrogen applications. This section discusses the different types of compressors that can be used for hydrogen applications and particularly the ones that can be used for large-scale compression. There are two major categories of compressors that can be used for hydrogen compression.

- · Mechanical Compressor.
- · Non-Mechanical compressor.

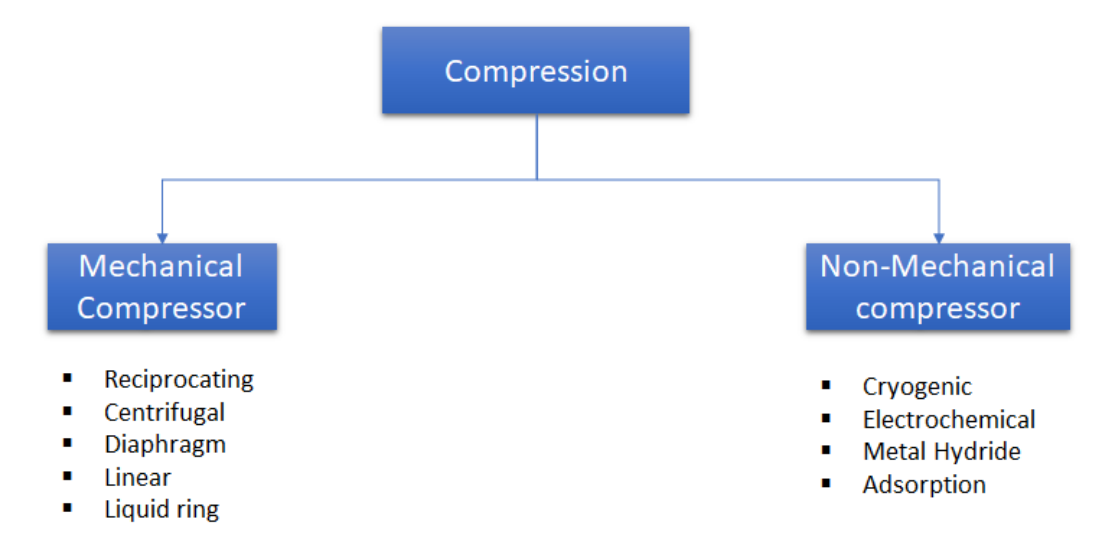


Figure 2.7: Major compressor categories for hydrogen gas application[33, 34]

As shown in Figure 2.7, mechanical compressors are typically divided into five categories, while the non-mechanical compressor can be classified into four main types for hydrogen application. It is to be noted that screw compressors are not included in the discussion due to difficulties in achieving tight tolerance and their limited pressure capabilities [35]. Table 2.4 provides a comparison of the different compressor types discussed.

Table 2.4: Different types of compressors used for hydrogen gas compression [33, 34
--

Compressor type	Flow rate [Nm ³]	Max pressure [MPa]	Compression method
Reciprocating Compressor	4800	85.9	Positive displacement
Centrifugal Compressor	50000	84.9	Dynamic
Diaphragm Compressor	581	28.1	Positive displacement
Liquid Piston Compressor	750	100	Positive displacement
Linear Compression System	112	95	Positive displacement
Cryogenic Compressor	1000	90	Thermal-positive displacement
Adsorption Compressor	560	10	Thermal
Metal Hydride	10	30	Thermal
Electrochemical Compressor	470	100	Electrochemical positive displacement

Table 2.4 highlights the fact that many compressors have low flow rates and may not be suitable for large-scale hydrogen storage. The Reciprocating compressor and Centrifugal compressor are the

only compressor types with high flow rates that are suitable for large-scale applications. while the non-mechanical are generally designed for smaller applications. In the following sections, the two major large-scale compressors for hydrogen application are discussed in detail.

Reciprocating compressor

A reciprocating compressor, also known as a piston compressor, is one of the most common types of compressor used in the process industry. Regardless of the gas densities, it is capable of producing high-pressure gas. The multistage double-acting compressor is typically used for large-scale gas compression in the process industry. The reciprocating compressors deliver gas with a low flow rate compared to centrifugal compressors but are efficient at high pressures. Currently, a double-acting, oil-lubricated piston compressor is used at natural gas storage facilities. However, for hydrogen service, a dry or oil-free compressor is recommended. The high discharge temperature of the compressor can cause issues with the sealing parts in the reciprocating compressor. As recommended for hydrogen rich services i.e. molecular weight lower than 12 by API standard 618, the temperature shouldn't exceed more than 135°C. However, to have a good life for the wearing part the temperature should stay below 120°C [33].

Centrifugal compressor

A centrifugal compressor is a type of industrial compressor that uses a rotating impeller to compress gas by increasing its kinetic energy and then converting it into a pressure energy diffuser. For hydrogen-rich services with high pressure or low molecular weight, a barrel-type casing is used to limit leakage. The low density of hydrogen gas can be a limitation for centrifugal compressors since it relies on kinetic energy to compress the gas and light gases can be difficult to compress to high pressures, because the pressure ratio for light gases is limited. However, the centrifugal compressor can deliver high flow rates than the reciprocating compressor. Centrifugal compressors can be designed to be oil-free, which will be advantageous for hydrogen compression where contamination of the gas stream is a concern. The discharge temperature of the centrifugal compressors can vary based on design and can reach a higher temperature of around 250°C if possible provided with good sealing and high-temperature O-ring.

2.5. Thermodynamics in compression of hydrogen

Hydrogen compression can be divided into two major categories based on purity. The first category involves compressing pure hydrogen produced through different electrolysis methods. The second category involves compressing hydrogen-rich gas streams found in process industries. In our case, we consider pure hydrogen produced from electrolysis.

During the compression of hydrogen, various thermodynamic phenomena come into play, which need to be considered when modelling the process. These include the effect of compressibility which relates the gas's actual volume to its ideal volume, and the gas equation that is used to compare the gas properties at two locations. Additionally, the Joule-Thomson effect can cause a change in the temperature of the gas during expansion. By accounting for these thermodynamic behaviours, accurate models for hydrogen compression can be developed for various industrial applications.

2.5.1. Effect of compressibility

Most gases, including hydrogen, exhibit non-ideal behaviour when compressed. The compressibility factor (Z) varies based on the operating pressure and temperature. Figure 2.8 illustrates the changes in the compressibility factor for hydrogen. with respect to pressure and temperature. As seen in the figure the compressibility factor of hydrogen increases as pressure increases and temperature decreases. At high pressures and low temperatures, the compressibility factor for hydrogen is greater. However, for high-pressure and high-temperature conditions, the changes in the compressibility factor are not significant.

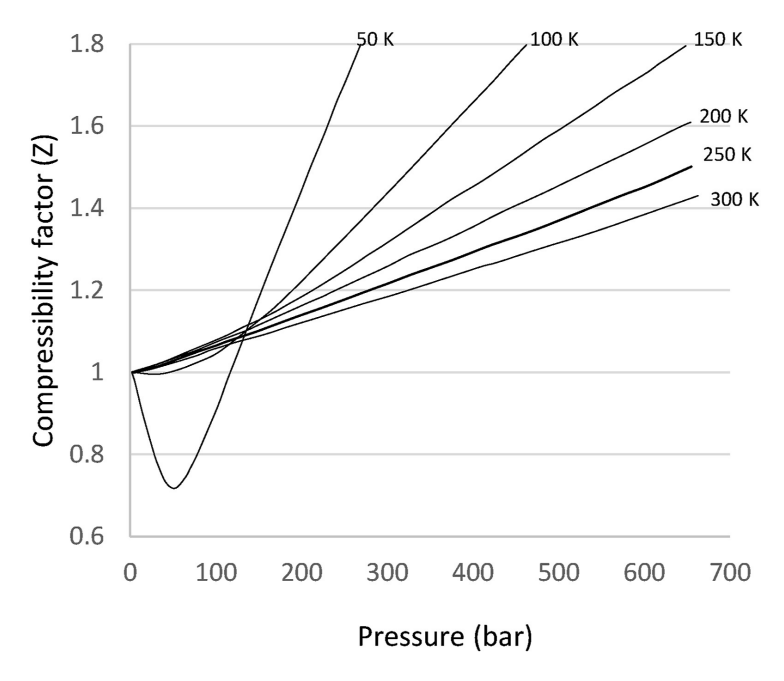


Figure 2.8: Effect of pressure and temperature on compressibility factor (Z) [36]

2.5.2. Gas equation

While ideal gas is a useful approximation for many gases, it fails to accurately predict the behaviour of hydrogen at high pressures and low temperatures. To account for this deviation the compressibility factor is used to adjust the ideal gas law, allowing for more accurate predictions of hydrogen under various conditions. The modified ideal gas law is given by the equation 2.1

$$PV = \frac{m}{MW} ZRT \tag{2.1}$$

Where P is the pressure of the gas, V is the volume of the storage, m is the mass of the gas molecule, MW is the molecular weight of the gas, Z is the compressibility factor, R is the universal gas constant and T is the temperature of the gas. The compressibility factor(Z) is calculated using the refprop or coolprop addin in python. When the equation 2.1 is represented in terms of the volumetric flow rate \dot{V} and the mass flow rate \dot{m} the equation is given by 2.2.

$$\dot{V} = \left(\frac{\dot{m}}{MW}\right) \frac{ZRT}{P} \tag{2.2}$$

When comparing gas flows under two different operating conditions, the relationship can be established using the principle of mass balance. While the total mass of the gas flow remains constant, changes in operating pressure and temperature lead to variations in volumetric flow. These changes take into account the compressibility effect of the gas. The corresponding relation between the change in the volumetric flow rate can be related using the equation 2.3

$$\frac{P_1\dot{V}_1}{Z_1T_1} = \frac{P_2\dot{V}_2}{Z_2T_2} \tag{2.3}$$

2.5.3. Joule-Thomson effect

Joule Thomson effect occurs in the case of the throttling effect when it is an isenthalpic process. The Joule-Thomson effect is the ratio of change in temperature with respect to the change in pressure at an isenthalpic process. For an ideal gas, the temperature is constant during the expansion but in the case of real gas, the temperature either increase or decreases and this varies on the type of gas used. The Joule-Thomson coefficient determines whether the temperature increase or decreases during the expansion. The Joule Thomson Coefficient is given by the equation 2.4.

$$\mu_j = \left(\frac{\partial T}{\partial P}\right)_H \tag{2.4}$$

When the $\mu_j>0$ the gas cools during the expansion and when $\mu<0$ the gas heats during the expansion. The Joule Thomson coefficient for hydrogen is shown in the graph 2.9. From the figure, we can see that the temperature of hydrogen increases when the operating range is larger than 200 K. We will be working above standard conditions so the temperature always increases when the gas is expanded during the storage.

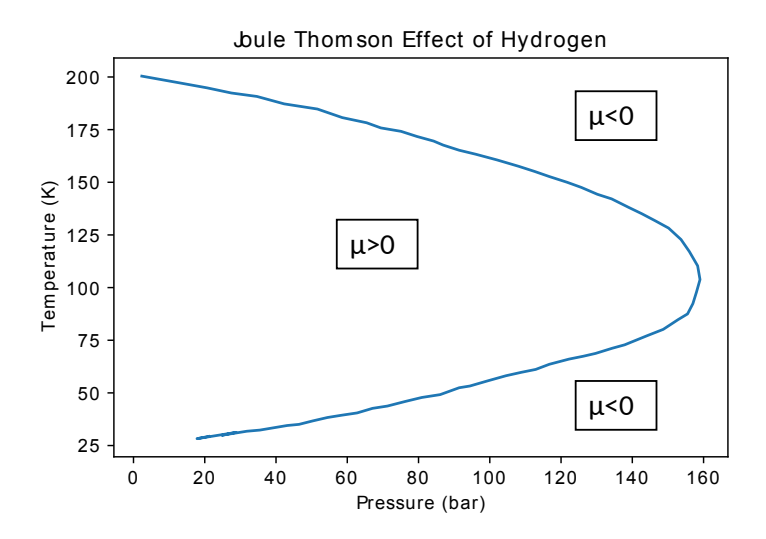


Figure 2.9: Joule Thomson coefficient behaviour with respect to temperature and pressure [37]

2.5.4. Cooling

When the gas is compressed to higher pressures the temperature of the system increases. The gas needs to be cooled to an optimum temperature before it is transferred into storage. also operating the gas at higher temperatures might result in damage to the system. A heat exchanger is used to remove the excess heat from the system by using a medium of low temperature. The amount of heat that needs to be removed from the gas is given by the equation 2.5.

$$Q = \dot{m} C_p (T_2 - T_1) \tag{2.5}$$

Where Q is the amount of heat that needs to be removed, C_p is the specific heat constant of the gas, T_1 and T_2 are the temperature at the inlet and outlet conditions of the gas. The heat exchangers are mainly used to reduce the excess temperature of the gas. The value of Q will be negative and this means that the heat is removed from the gas.

Modelling methodology

This chapter provides an overview of the current natural gas storage process, and then the storage is divided into main parts and the modelling is discussed for each part separately. The main focus of this section is to discuss the methodology and technical measures involved in hydrogen storage. The modelling methodology discussed in sizing the equipment is used to estimate the cost in later stages.

3.1. Existing natural gas storage overview

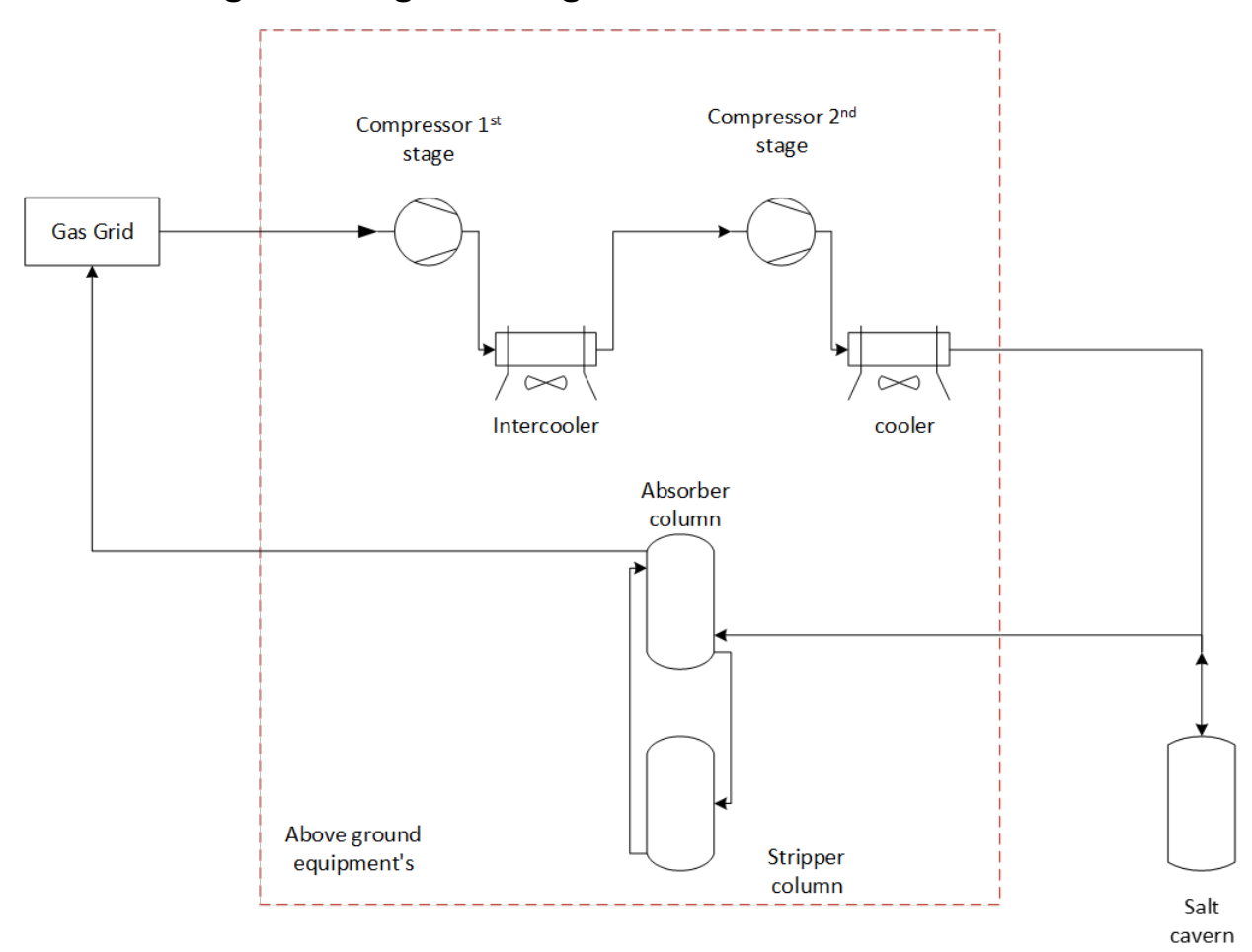


Figure 3.1: Current existing natural gas storage process at Epe, the gas to the storage is delivered by the gas grids where it is injected in the cavern by compressing and cooling in two stages. During the withdrawal cycle, the gas is purified using a TEG dehydration unit

The gas storage plant is located in Epe,(Germany), The storage process is shown in Figure 3.1. The storage plant consists of seven caverns and is connected to the natural gas grids operated which is operated by Gasuni. Upon delivery, the natural gas is compressed to increase its pressure using compressors. The temperature increase resulting from the compression is then reduced using an air cooler. The pressurized gas is then stored in the underground salt caverns. When the gas is withdrawn from storage, it contains diffused water molecules that need to be removed before it can be injected back into the grid. To achieve this, a glycol dehydration unit is employed, and TEG-glycol is the typical choice for gas dehydration in most industrial natural gas processes. The steps and constraints involved in the storage process will be discussed in further detail in the following subtopics.

Compression

In order to be injected into storage, natural gas from the grid must first be compressed to a pressure of 40 to 50 bar. Reciprocating and turbocompressors on a large scale are employed to raise the pressure for large gas streams, as was covered in section 2.4. These compressors can deliver a discharge pressure of approximately 205 bar. To achieve the required discharge pressures, the compressors are operated in two stages, and after each stage, a heat exchanger is utilized to remove the heat generated during compression. This step helps to keep the allowable temperature below 170°C, which is within the safe operating temperature for the compressors. Table 3.1 displays the operating parameters of both the reciprocating and turbocompressors.

Table 3.1: Current compressor operating parameters from the existing storage process

Parameters	Reciprocating Compressors	Turbocompressors
Inlet pressure (bar)	33-77	40-50
Outlet pressure 1st stage (bar)	125	100-105
Outlet pressure 2nd Stage (bar)	205	205
Flowrate Series (Nm³/hr)	30,000	100,000
Flowrate Parallel (Nm³/hr)	50,000	270,000

The compressors consist of two stages and are operated in parallel for low pressures and in series for high pressures. The flow operation of the compressors is depicted in Figure 3.2. From the figure, it can be observed that the compressor stages operate on the same shaft, and the series and parallel operation is operated by controlling the flow to the stages. The actual flow rate of the gas is related to the nominal volumetric flow rate using the equation 2.3. The actual volumetric flow rate of the hydrogen gas is given in Table 3.2, and from the table, it can be observed that the centrifugal compressor plays an important role in gas storage as it delivers high volume of high-pressure gas.

Compressor Actual volumetric flowrate parallel (m³/hr)

Reciprocating 433 129
Centrifugal 2922 1082

Parallel

Parallel

Series

Table 3.2: Actual volumetric flow rate of compressors

Figure 3.2: Parallel and series operation of a single compressor

Heat exchanger

An air-cooled heat exchanger is used in the storage process to reduce the temperature of the compressed gas in each stage. The increased temperature is brought down to a working temperature of 60°C in the first stage and 50°C after the second stage and then the gas is injected into the salt cavern. These types of heat exchangers are most commonly used in the process industries, where the removed heat has no direct use locally. This type of heat exchanger does not require investment in the cooling medium as it simply uses forced convection to reject heat from the source to the atmosphere. The amount of heat removed from the storage when the compressors are operated in parallel operation is given in Table 3.3

Table 3.3: Maximum duty of the existing heat exchangers used in the natural gas storage

Compressors	Maximum heat removed(MW)
Reciprocating	1.09
Centrifugal	5.53

Salt cavern Constraints

The salt caverns at Epe have a total capacity of 2 million m³. The maximum permissible pressure of the caverns ranges from 193-205 bar, and gas injection into each cavern is halted once the maximum pressure is reached. The depth of the caverns ranges from 1260-1400 m leached in the salt deposits and the caverns need to be maintained at minimum pressure to maintain their integrity and this depends on the depth and the duration of the storage. The minimum pressure in the caverns ranges from 5 MPa for one month to 11 MPa for a storage period of nine months.

Another constraint of the caverns is the mass inflow and outflow, which is maintained at a maximum of around 1 MPa per day [38]. Using the properties of methane from Table 2.3 and the salt cavern constraints, the storage capacity of natural gas in the salt caverns is 3.8 TWh. the total energy capacity includes both the working gas and cushion gas of the storage. But if only the working gas capacity is considered assuming that the grid operates at 40 bar, it is approximately 2.9 TWh of energy, with 0.9 TWh of energy used as cushion gas.

Drying

When the stored natural gas is pumped out of the storage, it is immediately dehydrated to prevent the formation of hydrates. Triethylene glycol (TEG) is commonly used in natural gas processing for gas dehydration, which works through physical absorption. The TEG then moves to the stripper column where the water molecules from the desiccant are removed by increasing the temperature. The dried TEG is recycled back to the absorber columns. Once the natural gas is dried from the water molecules the dried gas is injected back into the gas grid.

3.2. Process conversion for hydrogen storage

Technical measures need to be performed when converting the storage process to support hydrogen. This conversion may require the installation of new equipment, leading to new economic considerations, or it may provide the possibility of reusing the existing facility. In this section, an examination is conducted to assess the feasibility of the existing storage and equipment for hydrogen gas operation and modelling methods are discussed in case new equipment is needed. The study is conducted in four major parts, as shown in Figure 3.3.

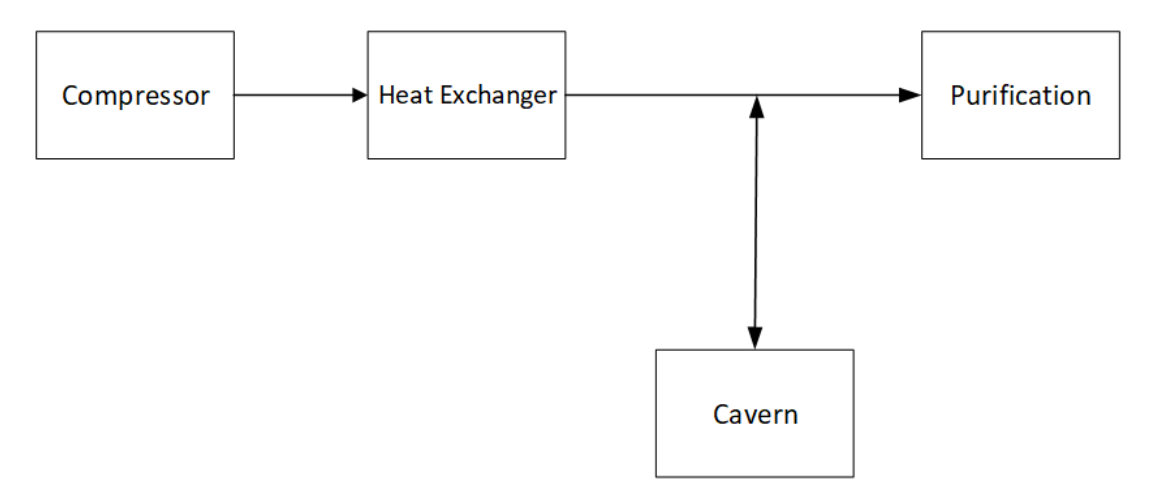


Figure 3.3: Major parts involved in hydrogen storage

3.2.1. Compressor

The first major equipment involved in the storage process is the gas compressor, which pressurizes the hydrogen gas delivered by the gas grids. As discussed in section 3.1, there are currently two large-scale reciprocating and centrifugal compressors used for compressing natural gas. The compressor section deals with two parts, the first part discusses the modelling involved in the compressor duty calculation and the second part discusses the current best suited technology for hydrogen compression.

Compressor work

The compressors need to be sized and this is performed by calculating the compressor duty which can also be represented as the compressor work. From the first law of thermodynamics for an open system the compression work is given by the equation 3.1

$$\dot{W} = \dot{Q} + \dot{m}(h_2 - h_1) \tag{3.1}$$

Where, W is the work done by the compressor, Q is the heat loss during the compression, m is the mass flow rate of the gas, h_1 and h_2 are the enthalpy at the inlet and outlet of the compression. The major compressor work used in estimating the duty is based on the adiabatic process and polytropic process and the relation in the following sections.

Adiabatic compression

When there is no heat loss or gain during the compression of the gas, the process is known as adiabatic compression. In this case, the value of \dot{Q} from the equation 3.1 tends to zero. Adiabatic compression is also be known as isentropic compression as we can consider the compression of the gas process to reversible. During this process the equation of the open system 3.1 becomes

$$\dot{W}_a = \dot{m}(h_2 - h_1) = \dot{m} \, dh \tag{3.2}$$

The equation 3.2 can also be written in the form of the adiabatic head (H_a), which is defined as the work done per unit weight of the gas being compressed and the equation is written as

$$\dot{W}_a = P_a = \dot{m} H_a \tag{3.3}$$

For a quasi-static adiabatic process the gas equation must satisfy the equation 3.4

$$PV^{\gamma} = Constant \tag{3.4}$$

Where γ is the adiabatic gas constant. By using the equations 3.2 and 3.4 the adiabatic head (H_a) of the compressor can be determined and is given by the equation 3.5

$$H_a = Z_{avg}RT_1 \frac{\gamma}{\gamma - 1} \left(\left(\frac{P_2}{P_1} \right)^{\frac{\gamma - 1}{\gamma}} - 1 \right)$$
 (3.5)

Where,(Z_{avg}) is the average compressibility factor, P_1 and P_2 are the pressure at the inlet and outlet of the compressor. The total adiabatic power is related using the adiabatic efficiency (η_a) and is given by the equation 3.6.

$$P_{ta} = \frac{\dot{m} H_a}{\eta_a} \tag{3.6}$$

By substituting the equation 3.5 in equation 3.3 the power consumed by the compressor is calculated. The relation between the pressures, temperatures and volume is given in the equation 3.7

$$\frac{T_2}{T_1} = \left(\frac{P_2}{P_1}\right)^{\frac{\gamma - 1}{\gamma}} = \left(\frac{V_2}{V_1}\right)^{\gamma - 1} \tag{3.7}$$

Polytropic compression

The adiabatic process occurs very rapidly without any transfer of heat to or from the system, while an isothermal process occurs very slowly with inter cooling to maintain the gas temperature constant. In practical application, this is not achievable, so an intermediate process known as the polytropic process is used. The polytropic process is an isentropic (i.e. an irreversible adiabatic) process that takes place in multiple stages, with inter cooling in between to maintain the temperature of the gas in acceptable ranges. The polytropic gas equation is similar to the adiabatic equation but is represented with the polytropic index(n) and is given by the equation 3.8

$$PV^n = Constant (3.8)$$

When $n = \gamma$ it is adiabatic process and when n = 1 it is isothermal process. The polytropic index and the isentropic index are related together by using the polytropic efficiency (η_p) and is given the equation 3.9

$$\left(\frac{n-1}{n}\right) = \left(\frac{\gamma-1}{\gamma}\right) \frac{1}{\eta_p} \tag{3.9}$$

Since the equation 3.8 is of the same form as 3.4 equation the polytropic head is in the same form as the adiabatic head but with the polytropic coefficient. The polytropic head is given by the equation 3.10

$$H_p = Z_{avg} R T_1 \frac{n}{n-1} \left(\left(\frac{P_2}{P_1} \right)^{\frac{n-1}{n}} - 1 \right)$$
 (3.10)

The polytropic exponent n is a measure of the deviation of the polytropic process from an ideal adiabatic process and can vary depending on the specific conditions of the process. This equation can be used to calculate the work required to compress the gas during a polytropic process and can be a useful tool for designing and analyzing gas compression systems. The total power of the compressor is related using the polytropic efficiency 3.11

$$P_{tp} = \frac{\dot{m} H_p}{\eta_p} \tag{3.11}$$

Existing compressor utilisation for hydrogen application

Reciprocating compressors are constant volume compressor which compresses the gas that is sucked into the chamber and compress it and delivers it at higher pressures. The gas density does not play a major role in the compression process involving the reciprocating compressor. Reciprocating compressors are good at high-pressure applications especially when the comparison is made between hydrogen and natural gas [39]. But the compressors built for natural gas application might not be directly suitable for the hydrogen application this is due to the following reasons

- The material of construction for the natural gas which in case high-strength materials are not suitable for hydrogen application as this will lead to hydrogen embrittlement.
- The small size of the hydrogen molecule than natural gas can lead to leakage through seals and gaskets. This will reduce the efficiency due to loss and might result in safety hazards.
- The lubricant used currently in the comparison need to be studied whether it is suitable for hydrogen application.

Centrifugal gas compressors pressurize the gas using centrifugal force, they are called dynamic compressors as the gas flows continuously through the compressor and the pressure is increased due to the impeller tip speed. When the gas is compressed using the tip speed of the compressor the large molecule gas like natural gas requires a lower tip speed and the small molecule gas such as hydrogen requires a larger tip speed. So for compressing hydrogen a tip speed of more than 3 times is required than in natural gas [40]. The head required for compressing the hydrogen gas is higher than that required for natural gas. The current compressor head will not be sufficient for compressing hydrogen gas and this can be related using the polytropic head equation 3.10. The conditions are taken from Tables 3.1 and 2.3 and the polytropic head comparison between natural gas and hydrogen is given in Table 3.4.

Table 3.4: Polytropic head comparison

Parameter	Natural gas	Hydrogen
Polytropic head(Wh/kg)	79	886

From Table 3.4 the polytropic head required for hydrogen is approximately eleven times more than that of methane. So if the existing centrifugal compressor was used for compressing hydrogen there needs to be approximately 11 compressors. This becomes ineffective from a cost perspective, so centrifugal compressors are only possible only if the compressor has a larger tip speed. **As a conclusion:** The existing compressor used for natural gas cannot be used for hydrogen storage and investment towards new compressors has to be made.

3.2.2. Heat exchanger

The current existing air cooled heat exchanger is able to provide the required cooling load for reducing the temperature of the hydrogen gas. But the material of construction is carbon steel which is susceptible to hydrogen embrittlement and the fins welded to the heat exchanges might harden the material and cause hydrogen embrittlement so good tolerance and allowance are required for hydrogen application. So the current heat exchanger needs to be changed using suitable material. The most common material used for high pressure hydrogen service is austenitic stainless steel namely 316L [41, 42, 43].

Since the material of the construction of the heat exchanger needs to be replaced this entirely affects the heat exchanger as the thermal conductivity of the material changes which result in different heat transfer effect from the heat exchanger. A comparison of the thermal conductivity of the carbon steel and the stainless steel is given in Table 3.5. Similar to the natural gas storage process an air cooled heat exchanger is selected for the hydrogen storage as well the reason being that there is no other easily available cooling fluid present.

Table 3.5: Thermal conductivity of materials used in heat exchanger [44, 45]

Material	Thermal conductivity(W/mK	
Carbon steel	45	
Stainless Steel 316L	16.3	

Air cooled heat exchanger sizing

The heat exchanger acts both as an inter-cooler after the first stage and as a final cooler before the gas is injected into the cavern. The sizing of the heat exchanger is performed for the maximum heat load, as the compressors are operated both in series and parallel operation. The heat exchanger after both stages of the compressor is used to reduce the temperature of the gas to around 50° C. The first step involved in sizing is calculating the amount of heat that needs to be removed and it can be considered as the duty(Q) of the heat exchanger and is given by the equation 3.12.

$$Q = \dot{m} \, C_p (T_1 - T_2) \tag{3.12}$$

The calculations are performed using the design procedure from Sinnot and Towler [46] with providing inputs from different sources. To calculate the overall area required for heat transfer the overall heat transfer coefficient (U_o) of the heat exchanger is calculated using the equation 3.13

$$\frac{1}{U_o} = \frac{1}{h_o} + \frac{1}{h_{od}} + \frac{d_o \ln\left(\frac{d_o}{d_i}\right)}{2k_w} + \frac{d_o}{d_i} \times \frac{1}{h_{id}} + \frac{d_o}{d_i} \times \frac{1}{h_i}$$
(3.13)

The internal heat transfer coefficient (h_i) for the equation is calculated using the Nusselt number (Nu) using the relation given by the equation 3.14

$$Nu = 0.021Re^{0.8} * Pr^{0.33}$$
 (3.14)

$$Nu = \frac{h_i d_i}{k_l} \tag{3.15}$$

By using the equations 3.14 and 3.15 the internal heat transfer coefficient is calculated based on the Reynolds number (Re) and Prandtl number (Pr) where the initial velocity within the tubes is assumed. Since the atmospheric air is used as the cooling fluid external dirt coefficient (h_{od}) is neglected. The outside fluid film coefficient (h_o) and the internal dirt coefficient (h_{id}) were taken for literature and are given in Table 3.6.

Table 3.6: Coefficients used to calculate the overall heat transfer coefficient [47, 48]

Parameter	Coefficient (W/m ² K)	
h_o	500	
h_{id}	11344	

The pipe diameter for the sizing was assumed from Figure A.1 and is given in the Appendix 5.2. Since the austenitic stainless steel is used it needs to be verified whether the operating pressure is suitable for the selected tube sizes. So the standard ASME 31.3 [49, 44] is used to verify the pressure conditions. Once the suitable diameter and thickness are selected an overall heat transfer coefficient for the heat exchanger design is calculated using the equation 3.13. The duty of the heat exchanger can also be expressed by the equation 3.16 which relates to the overall heat transfer coefficient (U_o), required bare tube area (A) and the mean temperature difference (ΔT_{lmtd}).

$$Q = U_o A \Delta T_{lmtd} \tag{3.16}$$

The logarithmic mean temperature difference which relates the temperature change of the process fluid and the cooling fluid which is used to calculate the duty is given by the equation 3.17, and the temperature of the cold fluid at both the inlet (t_1) and outlet (t_2) is assumed initially.

$$\Delta T_{lmtd} = \frac{(T_1 - t_2) - (T_2 - t_1)}{\ln \frac{(T_1 - t_2)}{(T_2 - t_1)}}$$
(3.17)

With the known duty, overall heat transfer coefficient and the mean temperature difference, the bare tube area of the heat exchanger is calculated using the equation 3.12. With the calculate bare tube area of the heat exchanger the number of tubes (N) that is required for the heat exchanger is calculated by relating with the surface area (A_s) of the tube and is given by the equation 3.18

$$N = \frac{A}{A_c} \tag{3.18}$$

After the number of tubes is calculated, a pitch (P_t) between the tubes based on the layout is assumed. The tubes are bundled together and the corresponding bundle area (A_b) for the provided layout of tubes is calculated using the relation 3.19

$$A_b = L * P_t * N \tag{3.19}$$

With the known volumetric flow rate (V), the number of tubes and internal cross-sectional area (A_i) calculated using the internal diameter (d_i) of the tube, the velocity of gas (v) within the heat exchanger tubes is estimated using the relation 3.20.

$$v = \frac{\dot{V}}{A_i} \tag{3.20}$$

The corrected internal heat transfer coefficient is determined by establishing a relationship with the obtained and the initially assumed tube velocity. Using this corrected internal heat transfer coefficient, the corrected overall heat transfer coefficient can be estimated. This estimation then facilitates the determination of the new bare tube area and the number of tubes required.

The next set of calculations is performed for the air side to determine whether the initial assumed condition for the air side is satisfied. The volumetric flow rate of the air (V_f) is calculated using the bundle

area and an assumed face velocity (u_f) taken from Table given in appendix A.2. The volumetric flow rate of air required for cooling is given by the equation 3.21.

$$V_f = u_f A_b \tag{3.21}$$

Once the volumetric flow rate of air in the bundle is calculated it is used to determine the required fan power (W_f) and is given by the equation 3.22.

$$W_f = \frac{V_f \Delta P_b}{\eta_f} \tag{3.22}$$

To have an acceptable temperature change on the air side of the heat exchanger the bundle area plays a role but the volumetric flow rate of the air is the main factor to achieve an acceptable temperature difference. So to have a better layout and considering the space constraints the velocity of the air needs to be increased which in turn requires a large fan power.

3.2.3. Underground storage

To maintain cavern integrity, the cushion gas is always maintained at minimum pressure, typically around 40-50 bar, depending on the specific cavern characteristics. However, with the expectation of achieving at least 98% hydrogen purity for the hydrogen grid [50], the existing natural gas must be removed from the cavern. This process also involves replacing the existing gas pipeline and cavern seals, which were designed to support natural gas operations. Consequently, this adds to the capital expenditure involved in the project. The natural gas removal process is shown in Figure 3.4.

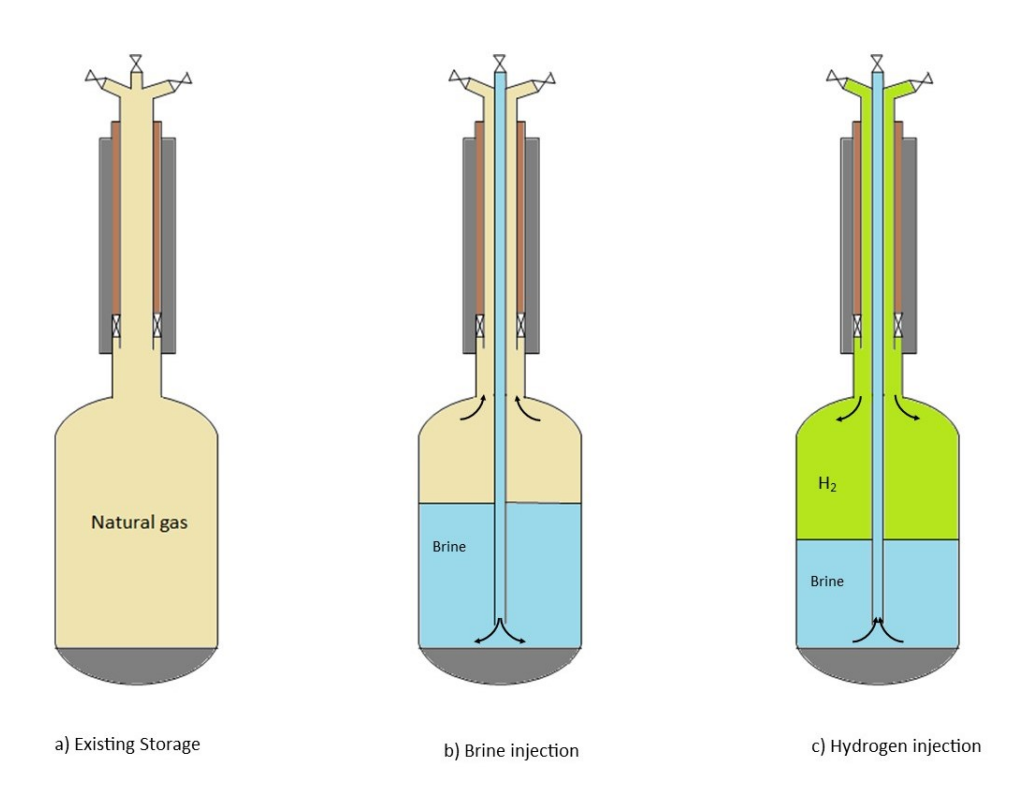


Figure 3.4: Salt cavern existing natural gas emptying process where a) shows the existing gas, b) shows the brine injection and gas removal and c) shows the hydrogen injection and brine removal.

Figure 3.4 shows the process involved in emptying the natural gas and injecting hydrogen. The first process shows only the cushion gas within the cavern when the working gas is completely withdrawn (a),

next the brine pipeline is introduced and the water is injected through the pipeline (b). When the brine starts fluting the cavern the natural gas present inside the cavern starts to exit through the gas pipeline. Once the natural gas is removed from the salt cavern the gas pipeline is replaced with a hydrogen-suitable material and in recent research screwed tube connection is preferred over the welded joint. Once the pipelines are replaced the hydrogen gas is injected through the new gas pipeline and the debrining phase starts (c). When the hydrogen is injected during the debrining phase the compressors need to be operated in series which delivers pressure at 205 bar this is because due to hydrostatic pressure the water pressure inside the cavern is around 170 bar. So to remove the water from the fluted cavern the hydrogen need to be inserted above 170 bar.

The reason for the gas temperature to be reduced by the heat exchanger is that the wall temperature at the salt cavern will be around 40-60°C at the depth of 1300m [51]. An average lifetime of a salt cavern is 30-50 years [52] but since these caverns are already in operation the lifetime of the caverns will be lower. When the gas is injected in the cavern the gas expands and this creates a throttling effect (i.e.) gas expands with constant enthalpy, which results in an increase in temperature based on the operating range this occurs due to the Joule-Thompson effect. In the current operating condition for the hydrogen gas, the temperature increase will be a maximum of 7°C which does not have a significant effect on the temperature. So the Joule-Thompson effect is neglected in the calculation.

3.2.4. Purification

In the early operation of storage, there is a high probability for the stored gas to be wet with water. This occurs mainly because, during the fluting of the cavern, to remove natural gas a certain amount of brine will be left out at the end. This left our brine solution might cause the gas withdrawn from the cavern to be wet and the gas needs to be dried. A Pressure Swing Adsorption(PSA) technique is a commonly used industrial technique and the TEG dehydration is not well established for hydrogen application so the sizing is made for PSA [53] and the adsorption column is shown by Figure 3.5. Due to the presence of the bacteria especially the sulphate-reducing bacteria, the hydrogen gas when stored has the tendency to form hydrogen sulphide but a multi-component sizing was not considered and the sizing focuses just on drying.

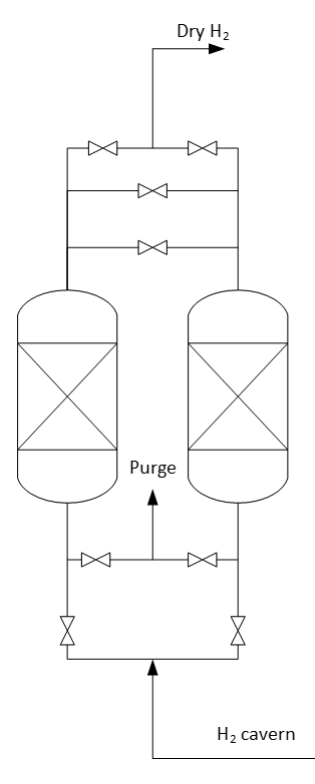


Figure 3.5: Two column pressure swing adsorber for hydrogen drying

The water content that is permissible within the gas pipeline is -8°C dew point and this translates to less than 100 ppm of water within the gas withdrawn from the storage. The presence of salt in the brine reduces the amount of water that is diffused in the hydrogen gas but the design is made for the worst-case scenario when there is no dissolved salt in the brine. From the previous research, the maximum water content of the gas was identified to be at 0.1 mol% or 1000 ppm. The sizing primarily starts with identifying the partial pressure (P_i) of water within the hydrogen gas stream and it is calculated using Dalton's law which relates the partial pressure to the total pressure (P) by means of vapour mole fraction (y_i) and is given by the equation 3.23.

$$P_i = y_i P = \mathsf{ppm}\,P \tag{3.23}$$

By using the ideal gas law relation the concentration (C_i) is related to the partial pressure and it is given by the equation

$$C_i = \frac{m_i}{V} = \frac{P_i MW}{RT} \tag{3.24}$$

A suitable adsorbent for the storage application was selected by using the comparison Table given in the appendix A.3. Hydrogen from the salt cavern includes water and in some cases the formation of hydrogen sulphide when stored for a longer time. Due to this reason, the adsorbent 3A cannot be selected and the adsorbent that is suitable for adsorbing H_2S and water needs to be selected. So the adsorbents from 4A to 13X can be utilized to adsorb both species in this sizing, the adsorbent 4A was selected. The equilibrium loading of the adsorbent was calculated using the partial pressure and was around 24% for adsorbent 4A. A residual loading of 2-4% is assumed for the molecular sieve and a net equilibrium loading (X_n) is calculated by the difference between the equilibrium loading (X_e) and residual loading (X_r) which is given by the equation 3.25

$$\Delta X_n = X_e - X_r \tag{3.25}$$

During the continuous operation of the adsorption column the loading of the adsorbent decreases so the column needs to be designed by taking this into factor. So a life factor (F_L) is used to find the aged equilibrium loading (X_a) . The factor is determined using the number of cycles a single column when operated for a fixed lifetime and the factor was taken from the plot from the appendix A.4 assuming an average performance. Then by using the equation 3.26 the aged equilibrium loading (X_a) of the desiccant is determined.

$$\Delta X_a = \Delta X_n F_L \tag{3.26}$$

The maximum superficial velocity (v_{gm}) through the adsorber column can be approximated using the adsorber bed constant (C_{bed}) and the density (ρ_g) of the hydrogen gas and is given by the equation 3.27

$$v_{gm} = \frac{C_{bed}}{\sqrt{\rho_q}} \tag{3.27}$$

The minimum column diameter (D_m) is related using the actual flow rate (q_g) of the gas through the tower and the maximum superficial velocity (v_{gm}) of the gas through the adsorber column and is given by the equation 3.28

$$D_m = \sqrt{\frac{4q_g}{\pi v_{gm}}} \tag{3.28}$$

With the obtained minimum diameter a suitable diameter of the column is approximated and using that

the actual velocity of the gas (v_g) through the column is determined. The next step in the sizing is the determination of the mass of the adsorbent and to start with that we estimate the amount of water that needs to be removed. The mass of water $(m_{\rm H_2O})$ that is required to be removed is given by the equation 3.29

$$m_{\mathsf{H}_2\mathsf{O}} = C_i q_q \tag{3.29}$$

The mass of adsorbent (m_a) required is calculated using the mass flow of water, the time of operation (t_a) and the aged adsorbent loading factor (X_a) , which is given by the equation 3.30

$$m_a = \left(\frac{m_{\mathsf{H}_2\mathsf{O}} t_a}{\Delta X_a}\right) 100 \tag{3.30}$$

When the adsorber column is operated not all the desiccant will be saturated with water, some of the desiccants will still be able to adsorb more water and to take the mass of underused desiccant into account, the relation 3.31 is used

$$m_{\text{MTZ}} = (v_g/C_{bed})^{0.3} (K_{MS}) \left[\frac{\pi D^2}{4} \right] (\rho_{MS}/F_L)$$
 (3.31)

The total mass of the adsorbent (m_t) is given by relating the adsorbent mass at equilibrium zone (m_a) and the mass at the mass transfer zone (m_{MTZ}) and is given by the equation 3.32

$$m_t = m_a + 0.5 m_{\mathsf{MTZ}} \tag{3.32}$$

The bed height (h_B) can be determined based on the total mass of the adsorbent and the diameter of the column and is given by the equation 3.33

$$h_B = \frac{4m_t}{\rho_{MS}D^2} \tag{3.33}$$

The actual height (h_a) of the column will be the bed height and the additional height that provides support and ensure good flow distribution, This is usually between 1-1.5m. the actual height is given by the equation 3.34

$$h_a = h_B + 1.5 (3.34)$$

When the gas is transported through the adsorbent for a certain length of the bed there will be some loss in pressure (ΔP) which needs to be taken into account and is given by the equation 3.35.

$$\frac{\Delta P}{h_B} = B\mu v_g + C\rho_g v_g^2 \tag{3.35}$$

The constants B and C are estimated using the table given in the appendix A.5. The thickness of the column is estimated through the Table from appendix A.6. The operation of the PSA for the case is given by the process given in Figure 3.6.

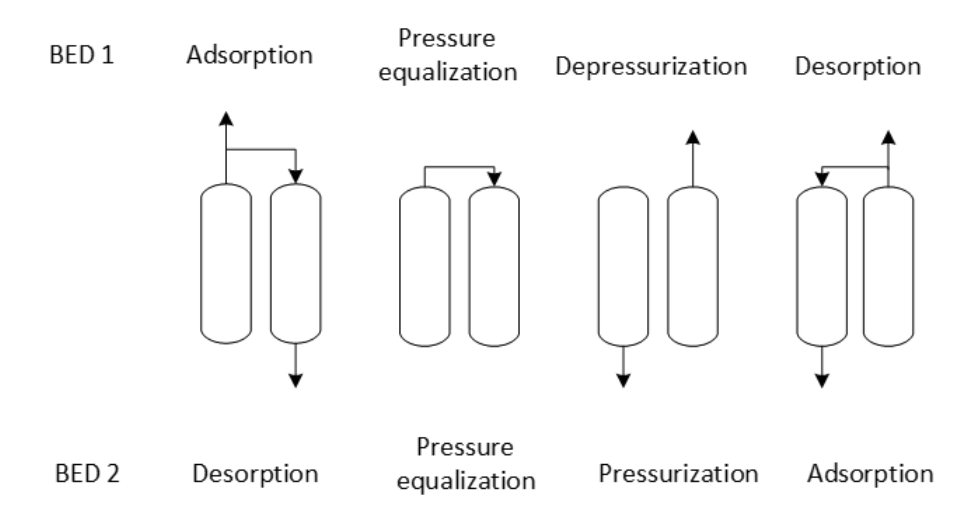


Figure 3.6: Pressure swing adsorber operation cycles

3.3. Economic modelling

To economics involved in the hydrogen storage process is studied by calculating the annualized and the levelized cost. To determine the economics as an initial step the capital expenditure (CAPEX) and the operating expenditure (OPEX) of each part of the storage process are determined. The total capital expenditure (CAPEX) of the storage is the sum of four major individual sections shown in Figure 3.3 and is given by the equation 3.36.

$$CAPEX = CAPEX_{COMP} + CAPEX_{HX} + CAPEX_{SC} + CAPEX_{PSA}$$
(3.36)

The total annual operating expenditure (OPEX) involved during the operation of the storage includes the electricity cost for the compressor and the heat exchanger and the hydrogen loss involved in the purification step. The salt cavern does not contribute towards the operating expense it contributes only towards the capital expenditure. The operating expense of the storage is given by the equation 3.37.

$$OPEX = OPEX_{COMP} + OPEX_{HX} + OPEX_{PSA}$$
 (3.37)

The annualized cost is a good estimate to identify the expense that is incurred during a particular year (t) throughout the lifetime (l), it is related using the capital recovery factor and is given by the equation 3.38

$$Annualizedcost = (CRF \times CAPEX) + OPEX$$
 (3.38)

The capital recovery factor (CRF) is used to estimate the annualized CAPEX throughout the lifetime of the plant and is given by the equation 3.39

$$CRF = \frac{i}{1 - (1 + i)^{-l}}$$
 (3.39)

The levelized cost is another economic parameter that is used to evaluate the net present cost required to run the plant during its operational lifetime. In this case, the levelized cost of hydrogen storage (LCHS) is used and is given by the equation 3.40. The formula relates the initial CAPEX of the project and OPEX involved during the operating year with the total amount of working hydrogen gas that is stored in the cavern during that year [54].

$$LCHS = \frac{CAPEX + \sum\limits_{t=1}^{l} \frac{OPEX}{(1+i)^t}}{\sum\limits_{t=1}^{l} \frac{W}{(1+i)^t}}$$
 (3.40)

When the storage is operated based on the levelized cost the storage will not generate any new revenue (i.e.) there will be no profit obtained from the project over the lifetime. This is because the net present value (NPV) of the project equals zero at the end of its lifetime. To identify a profitable range the levelized cost of the hydrogen needs to be increased and based on the increase the NPV for the storage needs to be studied, The NPV is given by the equation 3.41.

$$\mathsf{NPV} = -\mathsf{CAPEX} + \sum_{t=1}^{l} \frac{\mathsf{CF}}{\left(1+i\right)^t} \tag{3.41}$$

Results and Discussion

In this chapter, the modelling methodology from chapter 3 is implemented and results were obtained. The CAPEX and OPEX involved in the process are estimated using the outputs from the model and based on the results different scenarios were studied to determine the annualized and Levelized cost of Hydrogen Storage (LCHS).

4.1. Model implementation and cost estimation

4.1.1. Compressor and heat exchanger

The first part of the modelling involves the compressor and as discussed in Chapter 4 the reciprocating compressor is selected for compressing the hydrogen gas. To determine the duty of the compressor, both the compressor head equation and Aspen HYSYS software were used. The operating parameters of the compressor are assumed to follow the currently available compressor that is used in the natural gas storage and the input parameters are given in Table 4.1. The efficiency of the reciprocating compressor is usually from 80-90% for hydrogen application and is larger when compared to natural gas compression [39], But to understand the cost at worst case scenario an adiabatic efficiency of 80% was used for the calculation. The inlet temperature and pressure of the hydrogen gas were taken from Gasuni's quality specification for the hydrogen gas network [55].

Table 4.1: Reciprocating compressor model inputs for hydrogen compression

Parameter	Inputs Parameters
P_1 (bar)	50
P_{inter} (bar)	125
P_2 (bar)	200
T (o C)	20
\dot{V} (Nm 3 /hr)	30,000
\dot{m} (kg/hr)	2,668
η_a (%)	80
R (kJ/kgK)	4.1242
γ	1.4

By implementing the input parameters from Table 4.1, the duty is calculated using the polytropic head equation 3.3 and compared with the results from Aspen HYSYS software calculation. The comparison between the duty is given in Table 4.2. From the comparison, it can be observed that there is less variation between the results. So the results from Aspen were used in the further calculation.

Table 4.2: Reciprocating compressor duty comparison

Method	Power (kW)
Aspen HYSYS	1893
Compressor Head	1890

The increase in temperature of hydrogen gas during the compression is reduced to the acceptable range using an air cooled heat exchanger. The air cooled heat exchanger is modeled using the modelling procedure given in the chapter 3.2.2 and aspen exchanger design. There are two stages of compression in which the pressure reached 200 bar so two heat exchangers are required where one acts as an intercooler between the stages. The increase in temperature is different in both stages due to the pressure ratio and the temperature of the gas at the end of each stage is given in Table4.3.

Table 4.3: Gas temperature after compression in each stages

Stage	Temperature (°C)	
1 st stage	133	
2 nd stage	110	

From Table 4.3 it can be observed that the gas temperature reaches more than 100°C after both stages of compression. This temperature needs to be brought down to a cavern temperature of 50°C. The compressor stages are operated in parallel operation till the cavern pressure reaches 125 bar, In the parallel operation the temperate of the gas reaches the maximum temperature of 133°C. So the heat exchanger for both stages is designed for the maximum temperature case. The duty of the heat exchanger is calculated using the equation 3.12. The input conditions for the heat exchange are given in Table 4.4. By using the inputs from Table 4.4 the following outputs were calculated using the methodology given in

Table 4.4: Heat exchanger input parameters

Inputs			
Parameters	Value	Parameters	Values
Process stream		Heat Exchanger	
T ₁ (°C)	133	d _o (mm)	25.4
$T_2(^{\circ}C)$	50	d _{in} (mm)	21.2
Q(MW)	0.897	L(m)	6
Air side		$P_t(mm)$	76.2
t ₁ (°C)	25	$\eta_f(\%)$	70
t ₂ (°C)	28	$\Delta P_b(Pa)$	150

section 3.2.2 as well as using the aspen exchanger design rating. In both cases, the heat exchanger is designed with a single bay with two fans delivering the required air flow rate to maintain an air temperature difference of 3°C. The heat exchanger consists of tubes of two rows with a single pass and the results given in Table 4.5 were obtained from the model.

Table 4.5: Heat exchanger output parameters

Parameter	Model	Aspen
N	125	100
W_f (kW)	54.5	57.14

From Table 4.4 it can be that the number of tubes required for the heat transfer is less in the Aspen model than it is in the numerical calculation and this discrepancy in the calculation is due to the exclusion of the fin dimension in the numerical calculation which increases the surface area of the tube. The Aspen model for the compressor and the heat exchanger was integrated together in an Aspen model. The model consists of two stages of compression with inter-cooler and end cooler and the developed model is shown in Figure 4.1.

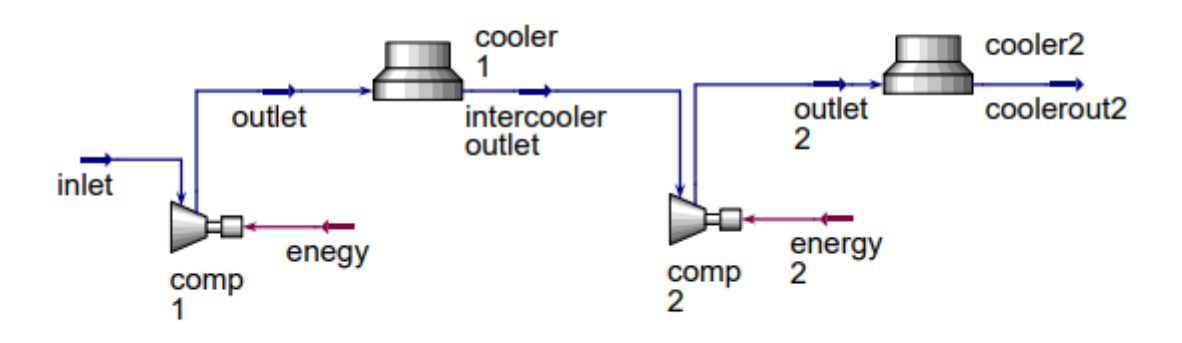


Figure 4.1: Aspen HYSYS compressor and heat exchanger process model

The model was developed in Aspen HYSYS and it was imported to the Aspen process economic analyser to estimate the capital and operating expense. The costs were estimated considering a compressor with two stages having two heat exchangers as a single unit, which delivers 2668 kg/hr of hydrogen at 200 bar. The operating cost is given initially for 1000 hrs but this will be modified in the results section for further study. Both the capital cost from the process economic analyser is based on the cost from the first quarter of 2019, so the CEPCI index needs to be accounted for when estimating the capital cost [56]. The capital cost and the operating cost of the setup are shown in Table 4.6

Table 4.6: Capital and operating cost of compressor and heat exchanger system

Parameter	Cost (million €)
CAPEX(2019)	9.63
CAPEX (2022)	12.8
OPEX(1000 hr)	0.32

4.1.2. Cavern conversion

The existing natural gas in the cavern is used to maintain a minimum pressure within the cavern. During the process of removal of gas from the cavern as described in section 3.2.3 there is a cost associated with it. These costs are purely a contributor towards capital investment. The capital expenditure from the cavern conversion contributes towards the CAPEX $_{SC}$ in the initial investment. The capital cost associated with the cavern conversion is given by the equation 4.1

$$CAPEX_{SC} = Brine cost + Pipeline cost + Cushion gas-Natural gas cost$$
 (4.1)

From the equation 4.1 it can be observed that the main contributors in the cavern are the brine cost involved in fluting the cavern, the gas pipeline replacement cost in the cavern and the cushion gas cost concerning towards maintaining the integrity of the cavern. Due to purity reasons, hydrogen is used as cushion gas in this study and the initial investment is associated with the cost of green hydrogen which is currently 6.03 euro/kg [57]. The existing natural gas that is removed from the cavern can be sold and this will reduce the CAPEX involved in the cavern. The cost of natural gas taken for the calculation is 33.17 euro/MWh [58]. The cavern calculations were performed for a cavern volume of 260,000 m³ with a minimum pressure of 50 bar and a temperature of 50°C. The lower heating value of the gas is utilized everywhere to determine the cost per kilogram of hydrogen.

Cost ParameterCost (Million €)Brine0.5Pipeline4.5Cushion gas5.72Natural gas-3.8Total6.92

Table 4.7: Cavern associated cost

From Table 4.7 it can be observed that a total initial net investment of 6.92 million euros is required for the cavern. In the view of timeline for the conversion, the water for the cavern fluting is delivered at 50 m³/hr through the existing water network. The injection and removal of the brine based on the injecting flow rate takes nearly 1.2 years provided the emptying process occurs continuously.

4.1.3. Adsorption system

As discussed in the section 3.2.4 a pressure swing adsorber is modelled and the input parameter and the output from the results from the model are given in Table 4.8. As there will be H_2S formation in the cavern so from Table A.3 the selected adsorbent is 4A. The amount of water content present in the hydrogen stream withdrawn was taken from a previous study and is taken as 0.1 mol% and this converts to 1000 ppm of water in the gas stream. The pressure drop that is desirable is 1 MPa per day [38] which is approximately 200 tons per day for a cavern volume of 260,000 m³. So the flow rate is determined for a 50% withdrawal limit which is 100 tons per day. The loading conditions for the water on the adsorbent were taken from the loading curve for 4A adsorbent [53]. The number of hours(N_b) and the number of columns(N_c) for the adsorber was considered as an assumption.

The Adsorber system accounts for both the capital and operating costs of the storage. The capital contributed is the CAPEX $_{PSA}$ and is calculated by taking the cost associated with the weight of the adsorber vessel and the mass of the desiccant given by the equation.4.2

$$CAPEX_{PSA} = Vessel cost + Desicant cost$$
 (4.2)

Inputs		Outputs	
Parameter	Value	Parameter Value	
y _w (ppm)	1000	v _{gm} (m/min)	38.73
$V_w(Nm^3/hr)$	50,000	v _g (m/min)	10.34
X _e (%)	24	D(m)	1.5
$X_r(\%)$	4	m _t (kg)	4650
N _h (hr)	12	h _a (m)	5.23
N_c	2	Δ P(kPa)	2.43

Table 4.8: Pressure swing adsorber input and output parameters

The material of construction chosen is 316L austenitic stainless steel with a material cost of 4.99 Euro/kg [59]. The cost of the adsorbent 4A is taken as 1.08/kg adsorbent [60]. The capital cost involved in the pressure swing adsorber is given in Table 4.9

Table 4.9: Adsorber column capital cost [59, 60]

Parameter	Cost (Euro)
Vessel cost	113093
Adsorbent cost	9340
Total	122,433

The capital cost of the Adsorber system is not very high when compared to the other initial investments. But the Operating cost of the pressure swing adsorber will have an impact on the LCHS as there will be hydrogen loss occurring during the depressurization and desorption cycle of the column. The operating expense of the adsorber column is given by the equation 4.3. Due to purity reason hydrogen is preferred as the regeneration purge gas.

$$OPEX_{PSA} = (Depressurization loss + Regeneration loss) \times H_2 cost$$
 (4.3)

Based on the mass of the purified hydrogen used in the regeneration cycle the operating cost of the adsorber increases and as an initial condition the mass of hydrogen used in regeneration is assumed to be 2% of the total mass of purified hydrogen. Based on the current green hydrogen cost the OPEX of the adsorber column is given in Table 4.10. The regeneration gas percentage can reach between 10-15% of the feed stream and this is discussed in the result scenarios.

Table 4.10: operating cost of the adsorber column

Process	H ₂ loss(kg/12hr)	Cost(€/12hr)
Depressurization	34	205
Regeneration	1064	6415
Total	994	5994

4.2. Cavern injection

The hydrogen injection and withdrawal in the cavern can be considered a mass balance. When the hydrogen gas is injected at high pressures, it expands inside the cavern and when the mass is increased in a fixed volume the pressure subsequently increases as well. The increase in the pressure follows a linear profile and is related through the ideal gas law given by the equation 2.1. Based on the cavern pressure the compressors are operated in series and parallel operation given in Figure 3.2 and the limiting conditions are taken from Table 3.1. Based on the different cases of compressor operation and the cavern injection time varies and is given in the section below.

Injection using existing compressors

At present, there are two reciprocating and two centrifugal compressors and these compressors are considered in this case. Although the centrifugal compressor is neglected for compressing hydrogen but to understand the limiting condition for the cavern the first case is made with an assumption that the existing compressors can be used for gas injection. Initially, all the seven caverns have been used for the gas injection cycle and the pressure increase and the duration of the injection are given in Figure 4.2

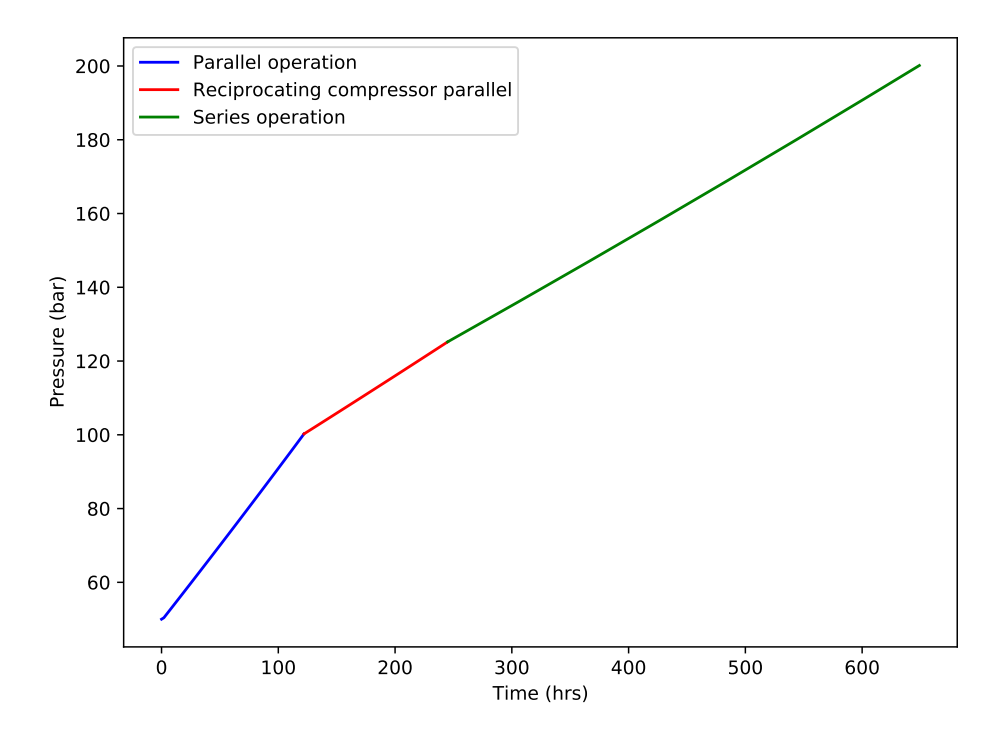


Figure 4.2: Cavern filling based on pressure increase when the hydrogen gas is compressed and injected using the existing compressors when the centrifugal compressor operated in parallel until 100 bar and the reciprocating compressor operated in parallel until 125 bar

From Figure 4.2 the slope corresponding to the increase in the cavern pressure decreases when the compressors start to operate in series and it takes longer to increase the pressure in series operation than the parallel operation. This is because in parallel operation the mass that is compressed and injected in the cavern is higher than when it operates in series mode. So when the existing compressors are possible for utilization it takes 622 hrs to completely fill all the seven caverns provided the cavern is already pressurized till the cushion gas limits.

Injection with only reciprocating compressor

The current available centrifugal compressor cannot be used for hydrogen due to its low molecular weight as discussed in section 3.2.1. So only the reciprocating compressors can be utilized for the hydrogen compression and this will have an effect on the storage time of the cavern and this is shown in Figure 4.3.

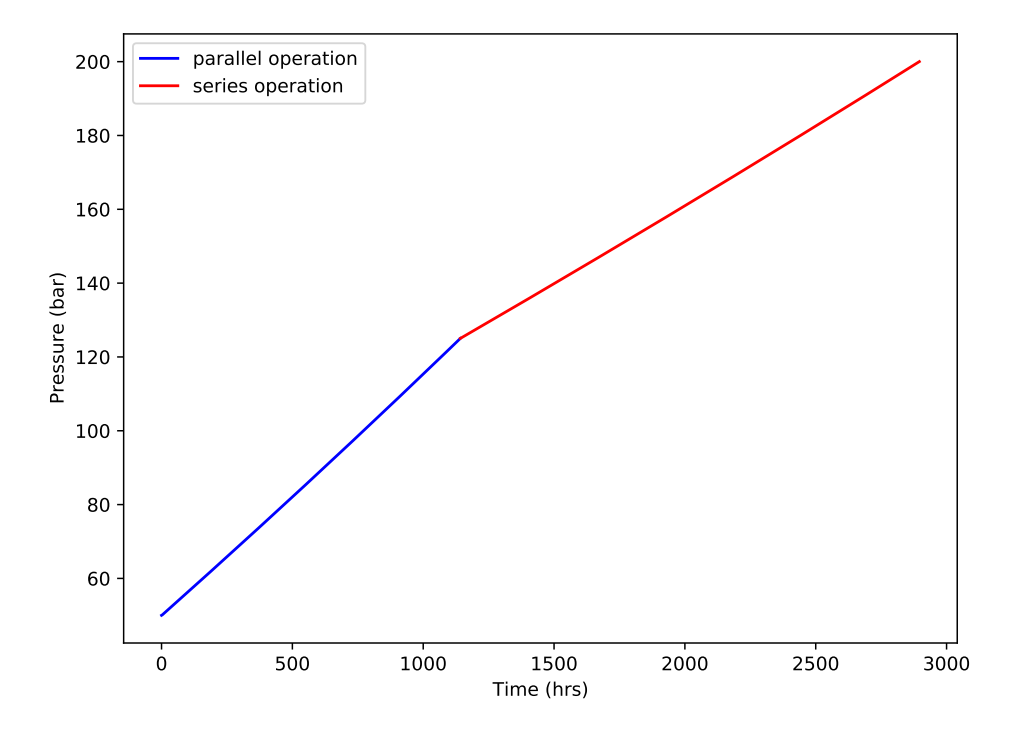


Figure 4.3: Cavern filling based on pressure increase when the hydrogen gas is compressed and injected using only the existing reciprocating compressors for all the seven caverns.

From Figure 4.3 it can be observed that when the centrifugal compressors are not available, the time taken to fill the cavern increases and it takes nearly 3000 hrs to fill the entire seven caverns each with a volume of 260,000 m³. The entire seven caverns cannot be utilized for hydrogen storage with only two reciprocating compressors so an increase in the number of compressors is required or initially, the number of caverns can be reduced.

Injection using single reciprocating compressor for a single cavern

In section 4.2 it could be observed that two reciprocating compressors were not sufficient for compressing and storing the gas in the seven caverns. So in this scenario, a single reciprocating compressor is used to inject hydrogen gas into a single cavern of volume 260,000 m³ and is given in Figure 4.4

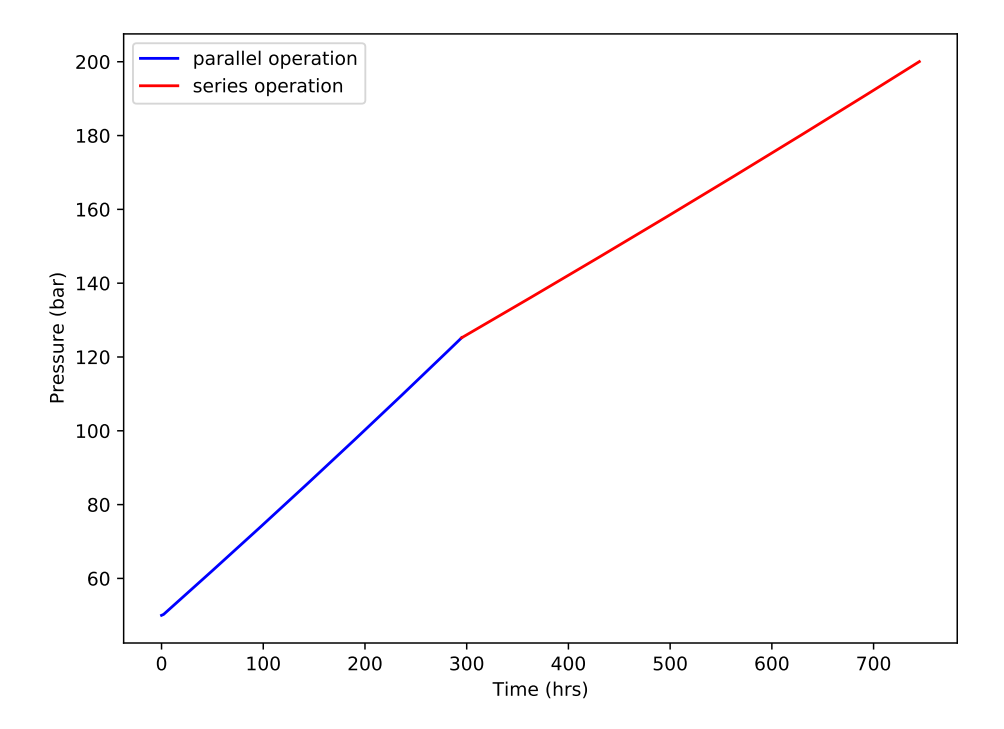


Figure 4.4: Cavern filling based on pressure increase when the hydrogen gas is compressed and injected with one reciprocating compressor for a single cavern

So from Figure 4.4 it can be seen that when a single reciprocating compressor is used to compress and store the gas in the cavern it takes around 700 hours to reach 200 bar. The time taken is still larger by 100 hrs when the centrifugal compressor was used for filling the seven caverns but the difference is acceptable. From this, it can be concluded that for operating in an acceptable time frame for each cavern a separate reciprocating compressor is required.

4.3. Results

4.3.1. Effect of cushion gas on LCHS present and future scenarios

To maintain the integrity of the cavern a minimum pressure should be maintained based on the time frame of the storage. This minimum pressure is maintained by keeping a certain quantity of working gas in the cavern this is known as cushion gas. The gas that remains in the cavern also depends on the operating pressure of the gas network as the withdrawal cycle purely works on the throttling effect where the gas flows from a high-pressure region to a low-pressure region. The cushion gas that is used in the cavern is approximately around 30% of the maximum cavern pressure. So the cushion gas will become an initial investment before the cavern is filled with the working gas. This cushion gas will have an effect on the levelized cost of hydrogen stored. To better understand this effect the following scenario is studied. Based on the type of hydrogen used for cushion gas the initial investment varies as shown in Figure 4.5. This difference is due to the cost of hydrogen used and is given by Table 4.11.

Table 4.11: Different colours of hydrogen cost [57, 61]

Hydrogen	Cost €/kg
Green	6.03
Blue	2.1

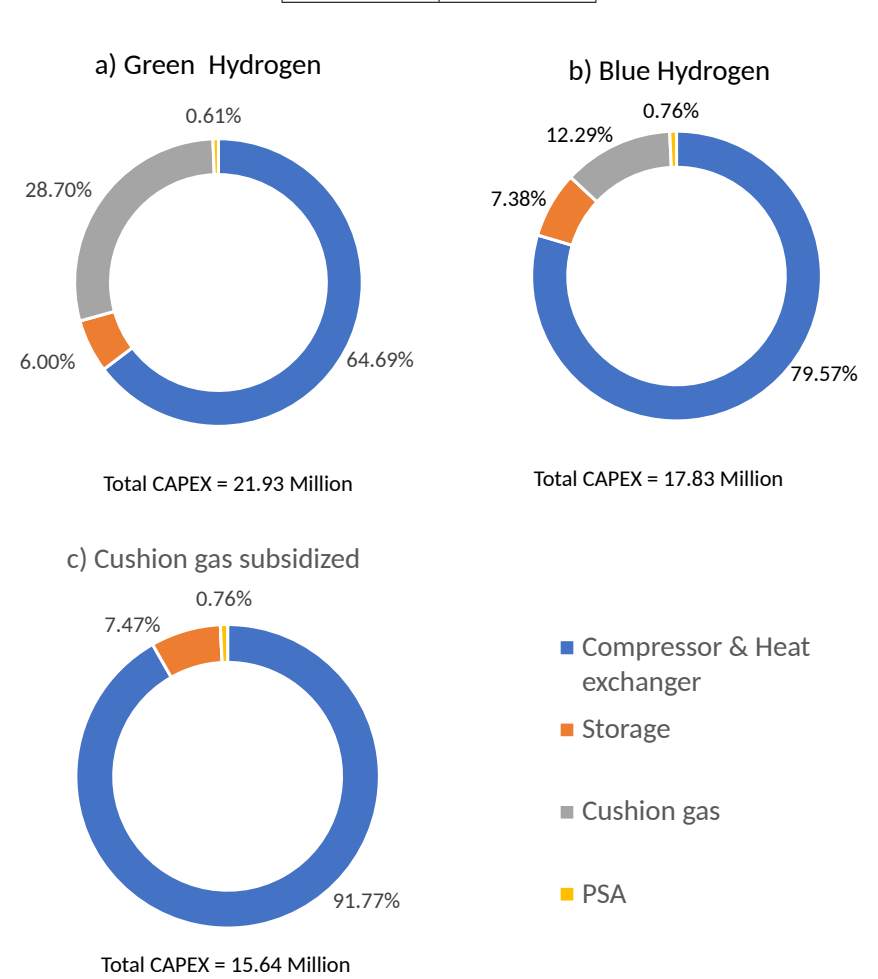


Figure 4.5: Distribution of the CAPEX based on cushion gas investment. The scenarios are studies based on the cost of hydrogen used, in (a) green hydrogen is used as cushion gas, in (b) blue hydrogen is used as cushion gas and in (c) cushion gas is subsidized. When the cost of cushion gas is reduced the capital investment reduces as well.

The study is performed for a single cavern with a volume of 260,000 m³ and filled using a single compressor and heat exchanger setup. The scenario study was performed for three cases of CAPEX based on the type of hydrogen used as cushion gas. In case(a) green hydrogen is used as cushion gas in the cavern using the current green hydrogen prices. In case(b) the blue hydrogen is used as the cushion gas and in case(c) the hydrogen required for the cushion gas is subsidized i.e. the cost for the cushion gas hydrogen is considered as $0 \in \text{kg}$. From Figure 4.5 it can be observed that the cushion gas was the second most contributor to the capital expense in case(a) and case(b) when green and blue hydrogen were used in satisfying the cushion gas requirement.

The economics namely the annualized cost and the LCHS were determined using the equation 3.38 and 3.40. The discount rate assumed in the calculation is 7% and the costs were estimated for three different lifetime scenarios, for all the three cushion gas cases. The hydrogen loss assumed in the purification step using the adsorption is assumed to be 2% and the loss is calculated in the OPEX using the cost of green hydrogen.

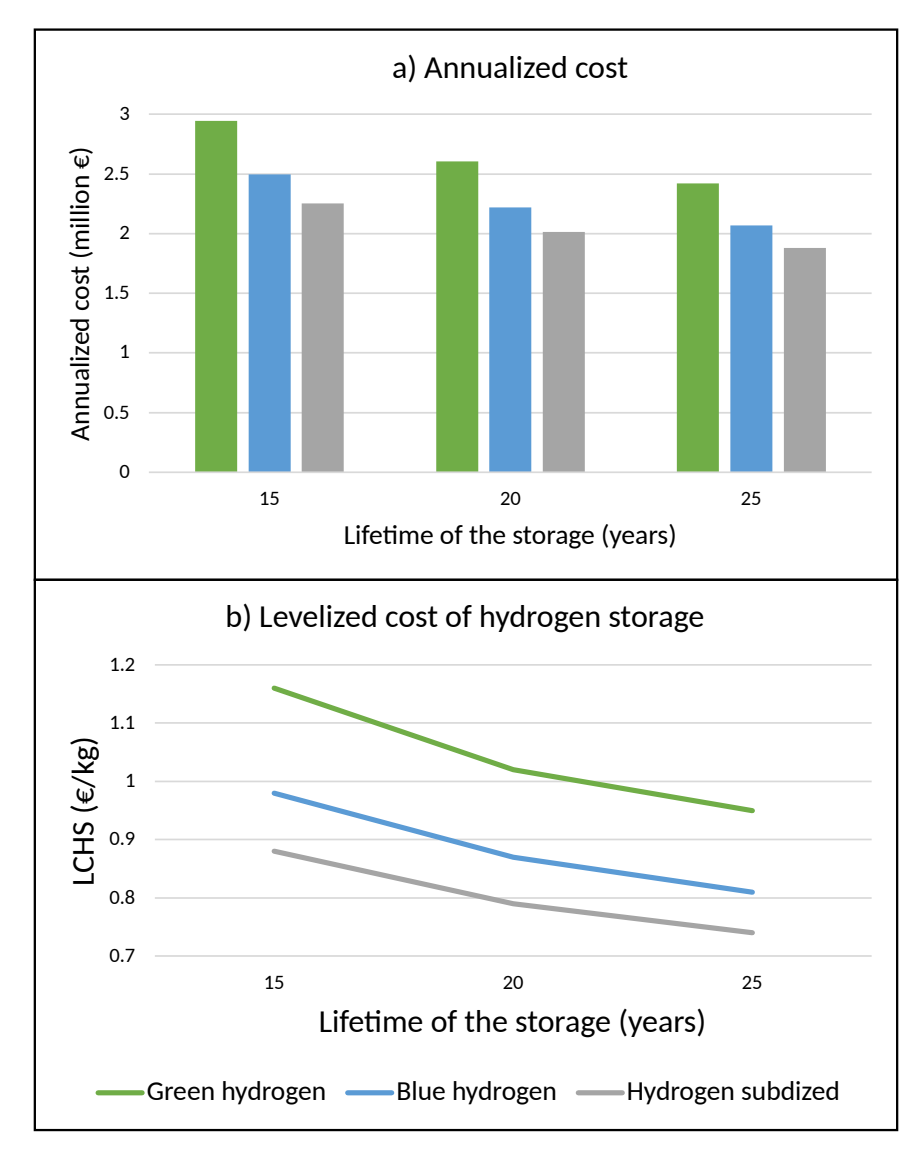


Figure 4.6: Distribution of a) annualized cost and b) levelized cost of Hydrogen storage, over three different lifetimes

From Figure 4.6 it can be observed that when the lifetime of storage is higher and when the initial investment towards the cushion gas is lower both the annualized cost and the levelized cost for the hydrogen storage

reduces. The maximum cost was obtained when the plant life is operated for 15 years and green hydrogen is used as cushion gas, the minimum cost was obtained when the plant is operated for 25 years and when the cushion gas is subsidized. The costs are given in Table 4.12

Table 4.12: Maximum and minimum distribution of cost for the cushion gas scenarios

Parameter	Annual Cost (million €)	LCHS(€/kg)
Minimum	1.8	0.74
Maximum	2.94	1.16

Effect of the future price of green hydrogen on the LCHS

In this scenario, the future cost of green hydrogen is considered and with the same operating inputs of the previous section, the economics were determined. The green hydrogen cost considered is $3 \in \text{/kg}$ [62]. The capital investment for the storage and the cost distribution is given by Figures 4.7 and 4.8.

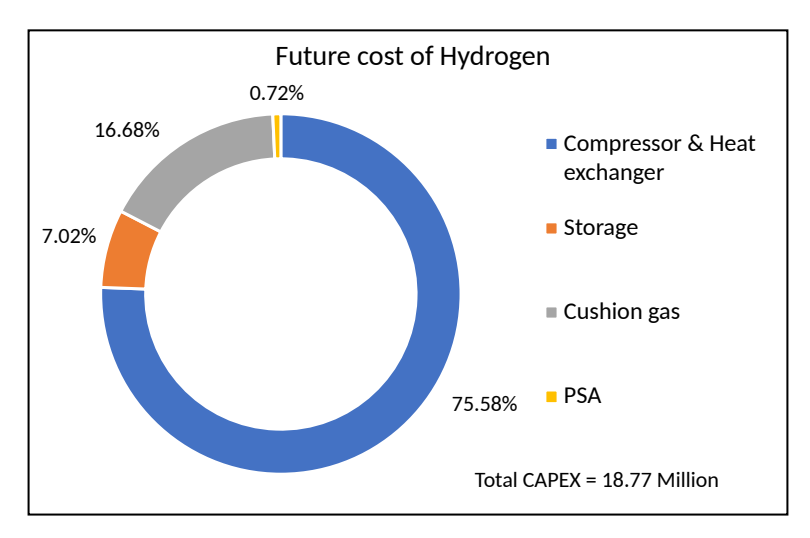


Figure 4.7: Distribution of the CAPEX based on future scenario of green hydrogen

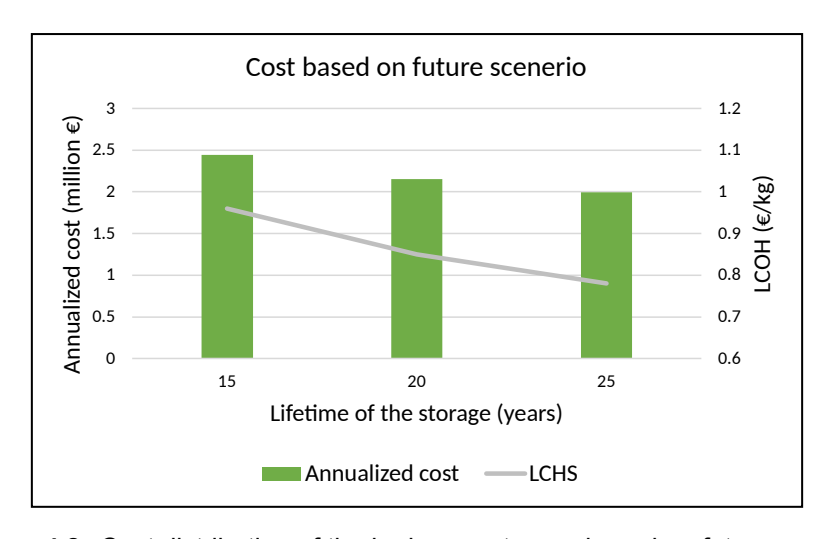


Figure 4.8: Cost distribution of the hydrogen storage based on future scenario

From Figure 4.8 it can be observed that the cost is lower for a longer plant lifetime and higher for a smaller plant lifetime and the costs are close to the blue hydrogen case from the previous section.

4.3.2. Effect of different percentage of purge gas

During the purification step using the pressure swing adsorber, a purge gas is required to regenerate the loaded adsorbent (i.e.) to remove the water from the adsorbent. This purge gas is usually a percentage of purified gas obtained from the adsorption unit. The purge gas was considered to be 2% of the total purified gas and the calculations were performed by considering the loss of hydrogen into the operating expense of the plant. But the purge gas ratio for a pressure swing adsorber system varies between 5-15% of the total gas. So to understand the effect of the purge gas ratio on the LCHS, the cost distribution is studied for different percentages of the gas starting from 2 to 10%.

The study is performed for a single cavern of volume 260,000 m³ operated for a single cycle using a single compressor and heat exchanger setup. The lifetime of the plant is considered to be around 20 years with a discount rate of 7%. Figure 4.9 gives the cost distribution for different percentages of purge gas used for the regeneration cycle of the pressure swing adsorber(PSA). The annualized and levelized cost with on the CAPEX and OPEX based on different regeneration costs is shown in Figure 4.9

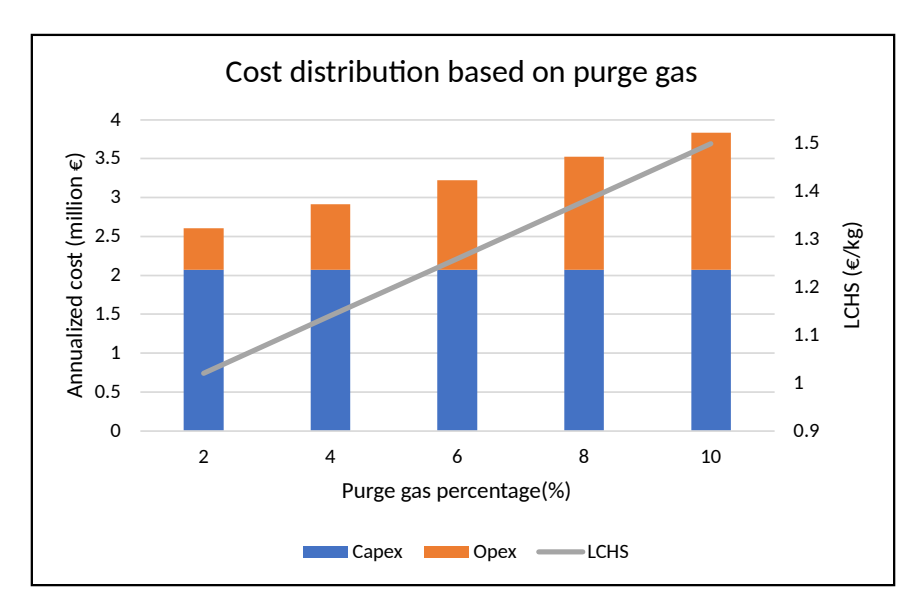


Figure 4.9: Levelized cost of hydrogen based on different percentages of regeneration mass. The CAPEX remains the same but the OPEX increases significantly in higher regeneration percentage

From Figure 4.9 it can be observed that when the percentage of the purge gas is increased the annualized cost associated with the storage increases and this increase is mainly due to the increase in the operating expense due to hydrogen loss in the PSA. So for the case studied the minimum cost is obtained for 2% purge gas and the maximum cost is obtained for 10% purge gas. The cost is given in Table 4.13

 Table 4.13: Maximum and minimum costs based on different regeneration percentages

Parameter	Annual Cost (million €)	LCHS(€/kg)
Minimum	2.6	1.02
Maximum	3.8	1.5

4.3.3. Effect on LCHS when two caverns and three compressors are used

In the subsection 4.3.2 the cost was studied when a single compressor is used for storing hydrogen in a single cavern. But from a maintenance and operation point of view, a standby compressor will be present and this will increase the cost associated with the storage. So in this section, the percentage of the purge gas used for the regeneration cycle will be fixed at a maximum of 10% and the discount rate is fixed at 7%. The study is performed for two caverns with each cavern having a volume of 260,000 m³ and three compressor & heat exchanger setup, with a single compressor on standby for operational safety and maintenance point of view. Green hydrogen is used as a cushion gas in this case. The capital distribution for the selected scenario is shown in Figure 4.10.

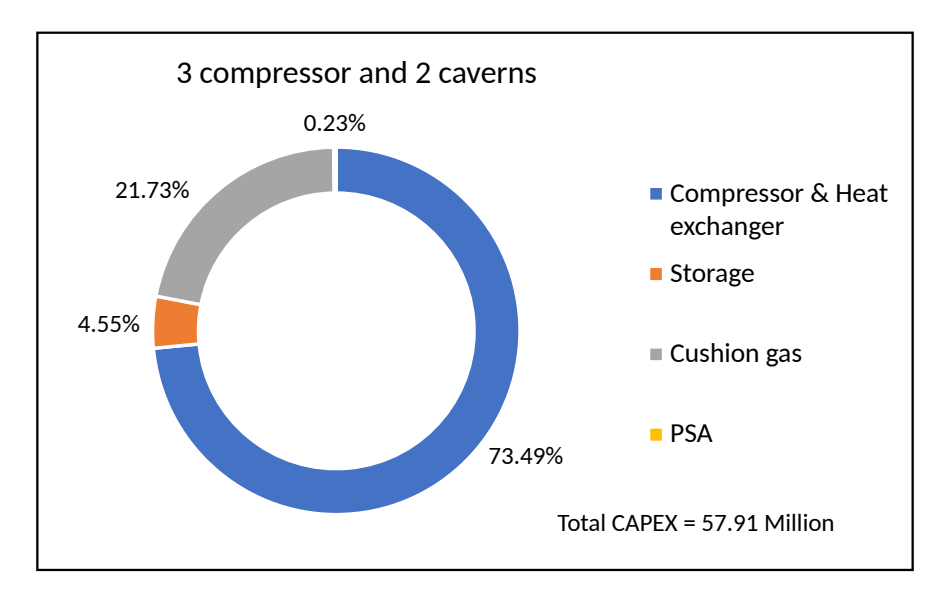


Figure 4.10: Capex distribution based on 2 caverns and 3 compressors & heat exchanger setup

From Figure 4.10 it can be observed that the capital involved with the compressor & heat exchanger is the most dominant one with cushion gas being the second dominant. The adsorption system does not play a major role in capital distribution but will have an impact on the operating expense. So based on the cost distribution operated for a single complete injection cycle of 700 hr with a 10% loss in the PSA is shown in Figure 4.11.

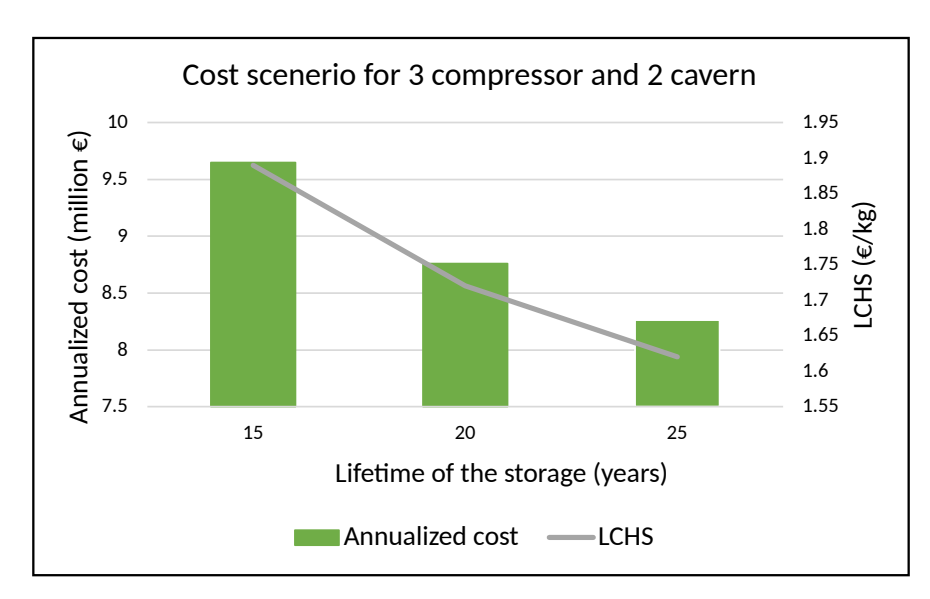


Figure 4.11: Cost distribution for 2 caverns and 3 compressors & heat exchanger setup

From Figure 4.11 it can be observed that the annualized and the levelized cost for the hydrogen storage are studied across the lifetime of the storage. From the results maximum cost was obtained for 15 years and the minimum was obtained for 25 year lifetime with the levelized cost of the hydrogen storage ranging between $1.94 \in / \text{kg}$ and $1.64 \in / \text{kg}$.

4.3.4. Effect of purge gas compression on LCHS

In the cases studied till now, the percentage of purified product hydrogen gas used in the purge gas is considered as a loss and this loss was accounted as an increase in the operating expense. This case specifically focuses on studying the economics involved in compressing and injecting the purge gas back into the storage process. This effect is studied for two cases and they are a) single cavern and single compressor and b) two cavern and three compressor system. The capital distribution between the components in the storage process for the two cases is given in Figure 4.12.

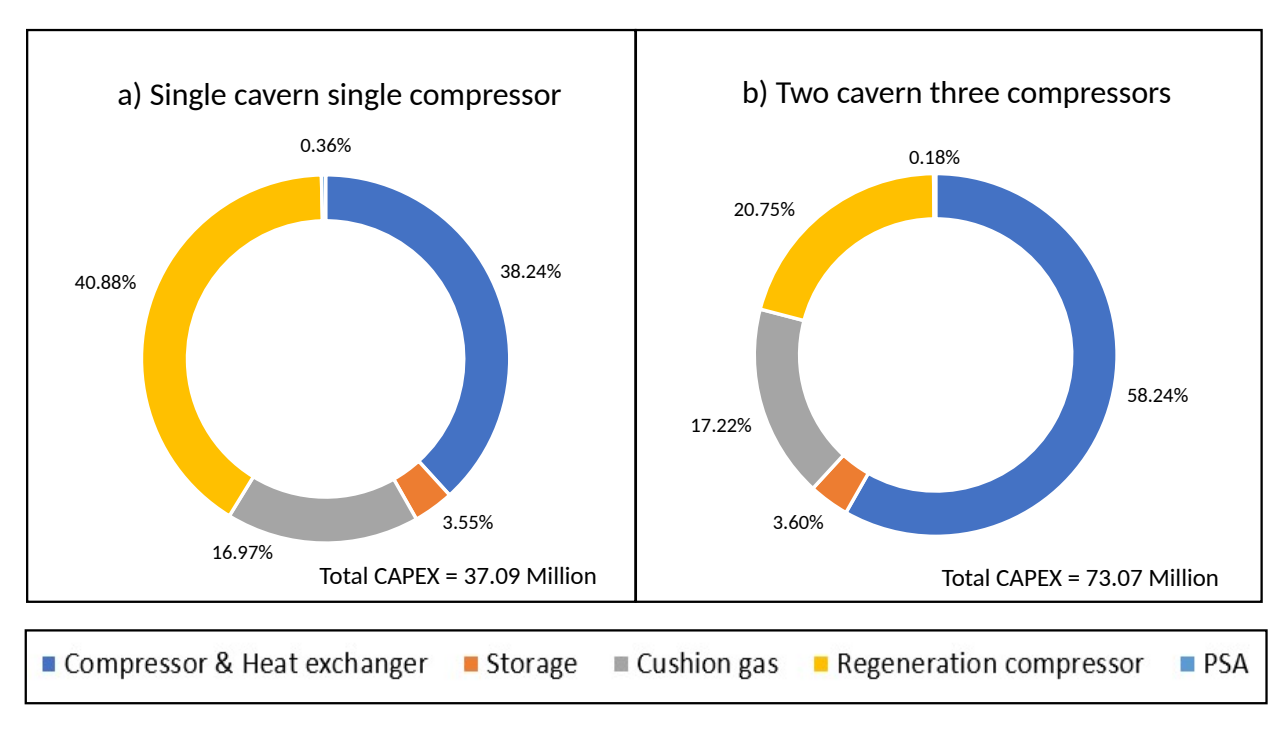


Figure 4.12: Capex distribution when 10% regeneration gas is compressed and reinjected into the grid

From Figure 4.12 the capital comparison between the two cases can be observed. In both cases, it can be observed that the capital investment towards the purge gas compression becomes the second most dominant factor just after the compressor & heat exchanger system used for injection. In case(a) the capital cost of the regeneration compressor is larger than the capital cost of the main compressor and in case(b) the capital investment for the purge gas compression is the second most dominating factor and is slightly greater than the cushion gas investment.

To better understand the effect of the purge gas compression on the cost associated with the storage a comparison for the two cases between hydrogen loss and without hydrogen loss is considered. The case without the hydrogen loss considers the process of compressing and re-injecting the purge gas back into the storage process, this process will include another operating expense relating towards the extra compressors utilized. For this study, the cavern volume is kept constant at 260,000 m³ and the calculations were performed for a 7% discount rate and a 20-year lifetime. The cost of electricity considered is 70 €/MWh. The comparison between the cost distribution for case(a) and case(b) is given in Figure 4.13. The storage is operated for a single complete cycle for a certain year.

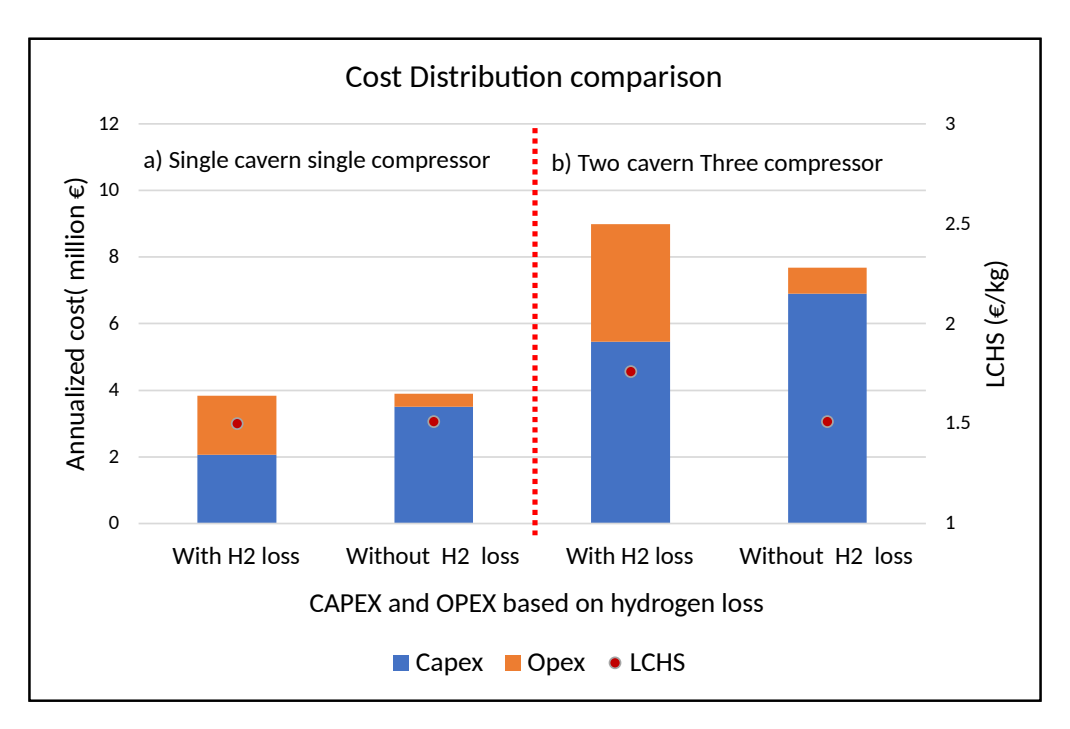


Figure 4.13: Cost comparison when there is H_2 loss vs without H_2 loss for a single cycle of operation based on two cases where case (a) is a single cavern single compressor and case (b) is two caverns and three compressors. From the figure, it could be observed that when the volume of stored hydrogen is lower investing in the regeneration compression is not useful in reducing the LCHS.

From Figure 4.13 it can be observed that the operating expense for the hydrogen storage in both case(a) and case(b) is reduced when the purge gas is compressed and injected back into the line. But it is to be noted that for a single cavern single compressor setup with a single cycle operation, the cost with and without the H_2 loss is nearly the same with an LCHS value of 1.5 \in /kg. But if the number of caverns is increased the hydrogen loss is increased as well and this is clearly shown in case(b) where there is a difference between the cost with and without H_2 loss and the LCHS is lower when the purge gas is compressed where the cost reduces from 1.7 \in /kg to 1.5 \in /kg.

4.3.5. Effect of cycle of operation and no of caverns on LCHS

The cycle of operation for the hydrogen storage was fixed at one cycle per year in the previous scenarios and the impact of the different cycles of operation was not assessed. To study the impact of the cycles in this scenario the number of caverns in the operation is fixed at two caverns, with the cavern operating in an alternate cycle i.e. when one cavern is in injection the other cavern will be in withdrawal cycle. As per the previous scenarios the capital, the annualized and levelized cost based on the lifetime time was determined and is given in Figures 4.14 and 4.15. From Figure 4.4 it can be found that it takes nearly a month for injection, and based on the withdrawal rate of hydrogen it takes nearly a month for emptying the working gas. So based on that, each cavern is operated for a maximum of 6 cycles of injection and withdrawal per year (i.e.) there is a net of 12 cycles of injection and 12 cycle withdrawal during an operational year. Both the cavern is assumed to be of a similar volume of 260,000 m³ two caverns, 10% regeneration loss. Two compressor & Heat exchanger setup was selected because only one cavern will be in injection mode and a single compressor & Heat exchanger setup is enough to operate during the injection cycle and the other compressor will be in standby mode. The capital distribution involved for the current storage scenario is given in Figure 4.14.

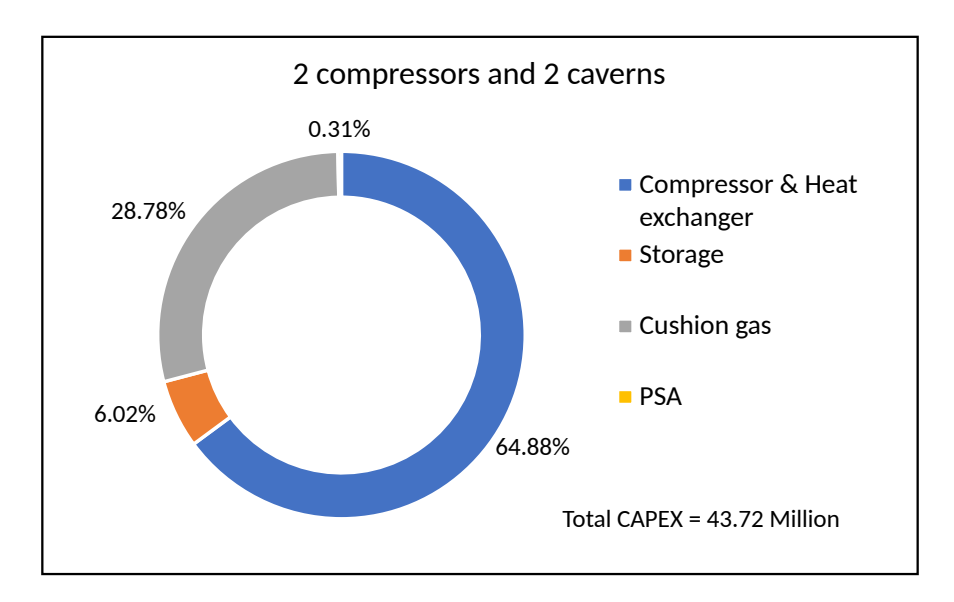


Figure 4.14: CAPEX distribution based on 2 caverns and 2 compressors with green hydrogen as cushion gas

From Figure 4.14 it can be observed that for a two-cavern system, the cost of cushion gas is larger and is still the second most dominant contributor in the CAPEX. To understand the cost distribution for the storage when operated for 12 cycles, the annualized and levelized costs were studied for a different operating lifetime of the plant and are given in Figure 4.15. For the operating expense, the cost of electricity considered is $70 \in MWh$ and the hydrogen loss is considered in the operating expense by considering the cost of green hydrogen to be $6.03 \in MWh$.

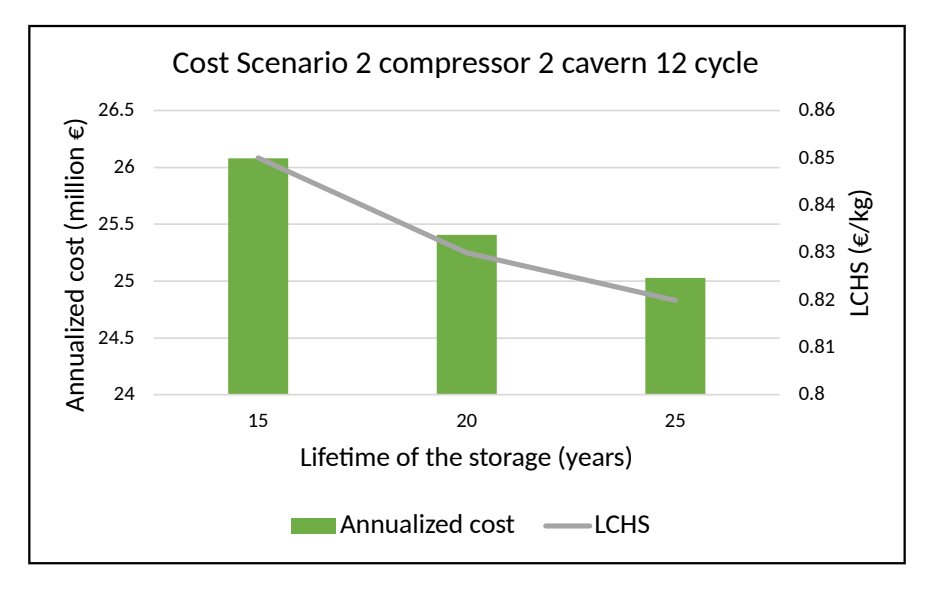


Figure 4.15: Cost distribution for the hydrogen storage for 2 cavern and 2 compressors & heat exchanger setup based on the different lifetimes of storage operated for 12 cycles per year.

From Figure 4.15 it can be observed that the cost reduces when the operated for a longer time. The levelized cost for hydrogen storage varies from $0.85 \in /kg$ to $0.82 \in /kg$. The difference between the cost based on the lifetime of the storage is not that large when a twelve-cycle operation is considered with each cavern operating for a maximum of 6 complete cycles per year. To understand the impact of the operational cycle on the LCHS, the following scenario was conducted while fixing the plant's lifetime at 20 years. This analysis takes into consideration the operational expenses associated with hydrogen loss. Figure 4.16 gives the effect of the number of cycles on the cost of hydrogen storage.

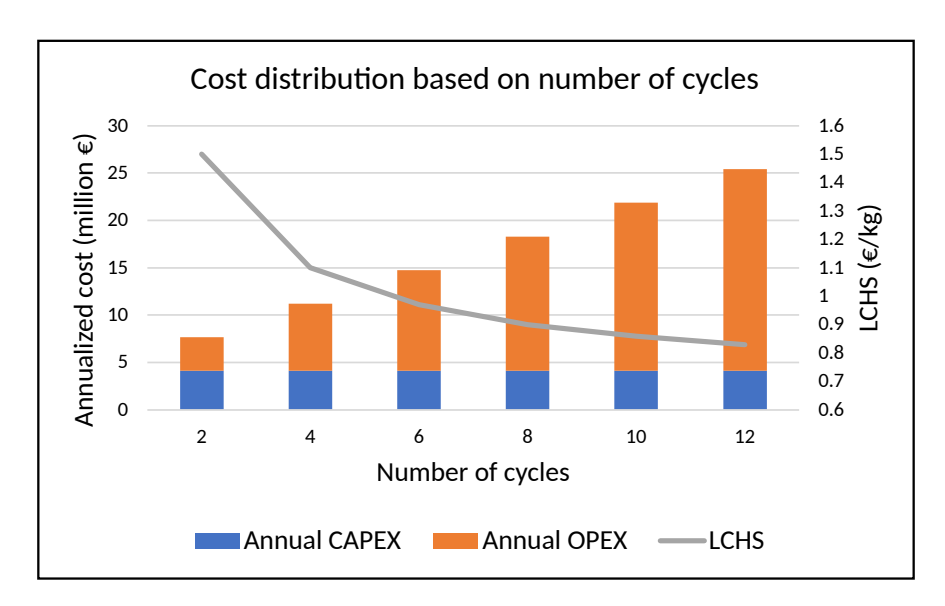


Figure 4.16: Cost distribution for the hydrogen storage for 2 cavern and 2 compressor & heat exchanger setup based on different cycle of operation.

From Figure 4.16 it can be observed that when the number of storage cycles is increased the operating expense becomes a dominating factor over the capital expense and the annual cost reaches nearly 25 million at maximum cycle operation. From the levelized cost is observed that when the number of cycles is larger than 4 the difference in LCHS becomes more linear. The maximum levelized cost is observed when the storage is operated for 2 cycles and the minimum levelized cost is observed when the storage is operated for 12 cycles and the cost varies between $1.5 \in /kg$ to $0.83 \in /kg$.

4.3.6. Effect of regeneration gas utilization on LCHS in increased cycles of operation

In the section 4.3.5 the hydrogen used as a purge gas was considered a complete loss and was included in the operating expense of the storage. So in this section together with the same conditions as in section 4.3.5 the regeneration compressors were also included. Figure 4.17 gives the capital distribution between the different contributing factors in the storage process.

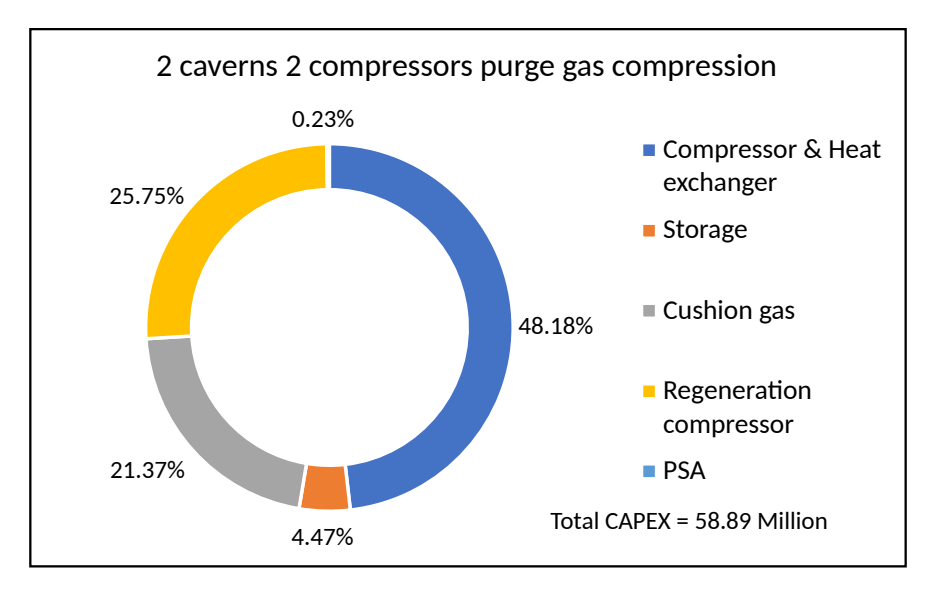


Figure 4.17: CAPEX distribution when the regeneration gas is compressed and reinjected into the storage process for a 2 cavern and 2 compressor & heat exchanger setup with green hydrogen as cushion gas.

From Figure 4.17 it can be observed that the capital expense of the compressor used in the injection mode of the storage dominates followed by the cost of the regeneration compressor and the cushion gas. Since the purge gas is compressed there will be an operating expense associated with it but it is not associated with loss of hydrogen. The annualized and levelized cost distribution based on the number of cycles is studied and is shown in Figure 4.18.

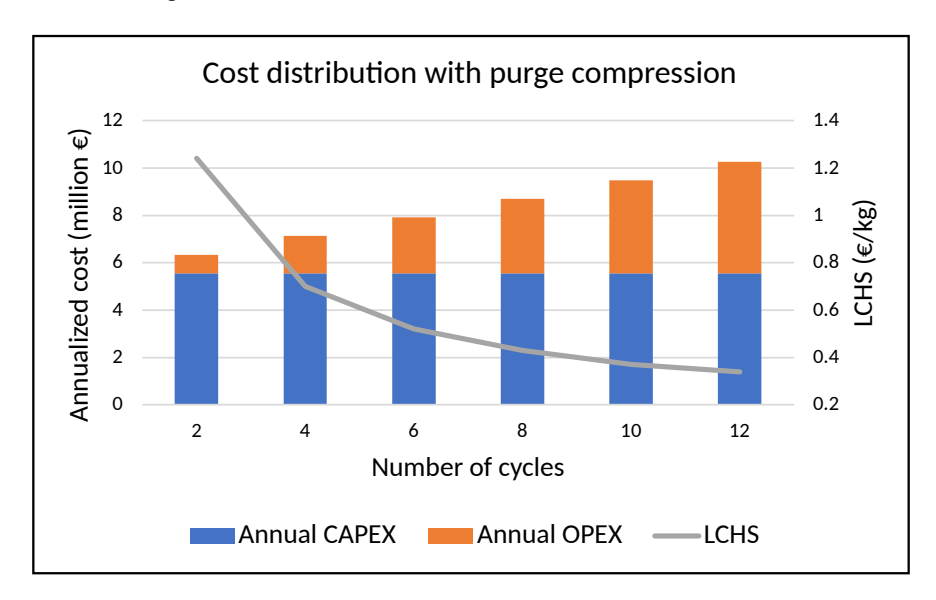


Figure 4.18: Cost distribution for the hydrogen storage for 2 cavern and 2 compressor & heat exchanger setup when the purge gas is compressed based on different cycles of operation.

From Figure 4.18, the first thing to observe is that the in the annualized cost the operating expense does not become more dominant than the annual CAPEX even if the plant is operated for 12 cycles, the next thing to be identified is that the levelized cost of hydrogen is less when compared to the other cases studied till now. The LCHS varies based on the operating cycles and it ranges from a maximum of $1.24 \in \text{kg}$ to a minimum of $0.34 \in \text{kg}$.

4.3.7. Sensitivity analysis

To understand the effect of the different parameters on the levelized cost for hydrogen storage a sensitivity analysis was performed. For the base case scenario for the sensitivity analysis the parameters given in Table 4.14 was assumed.

Table 4.14: Sensitivity base case input parameters

Parameter	Values
No of caverns	2
Hydrogen cost(€/kg)	6.03
Discount rate (%)	7
Regeneration (%)	10
Electricity price (€/MWh)	70
No of cycles	4
Lifetime (years)	20

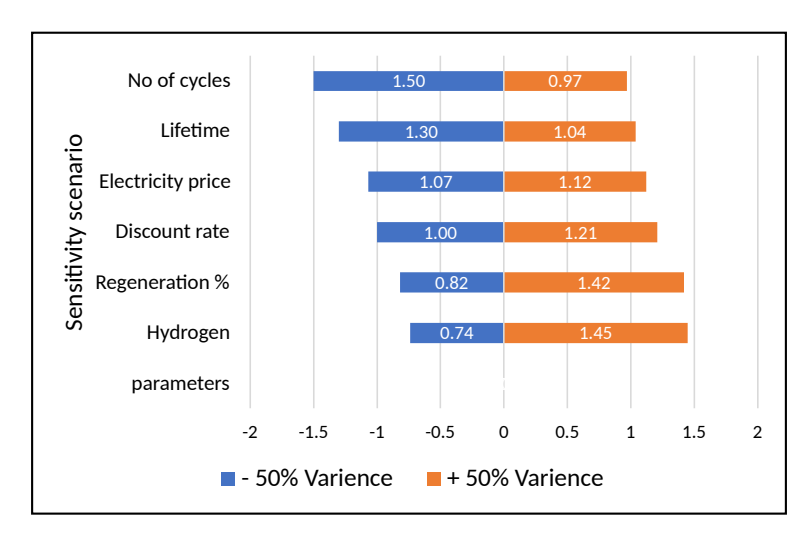


Figure 4.19: Tornado plot displaying the LCHS variation when a certain parameter is increased and decreased by 50% variance when the other parameters of the base case are kept constant.

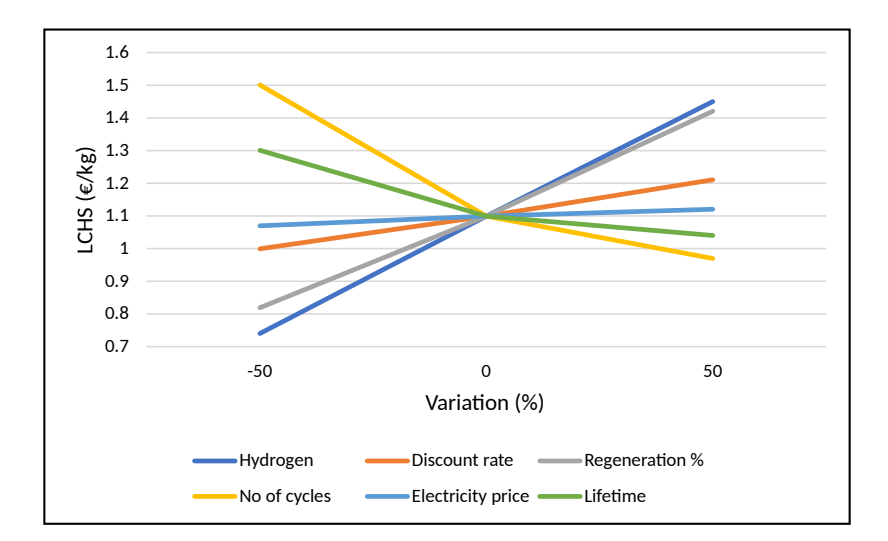


Figure 4.20: Spider plot displaying the LCHS variation based on the slope when a certain parameter is increased and decreased by 50% when the other base parameters are kept constant. The most dominating factor was found to be the cycle of operation and hydrogen cost.

Figures 4.19 and 4.20 gives the outputs of the sensitivity analysis, the analysis is performed when a particular scenario parameter is increased and decreased by 50% and the other parameters are kept at the base case. From Figure 4.20 it can be observed that the number of cycles of operation and the cost of hydrogen play an important role in the levelized cost of hydrogen storage. From the analysis, the levelized cost ranged from $0.74 \in /kg$ to $1.5 \in /kg$.

4.3.8. Effect of increase in LCHS on the NPV of the storage

The plant will not generate any profit when it is operated based on the levelized cost calculated from the previous scenarios the reason being that the cost is calculated by assuming the net present value as zero across its lifetime. To understand this the LCHS of the hydrogen storage is increased in percentage and the effect on the NPV is studied. From the sensitivity analysis, it was observed that the no of cycles of operation of the storage plant had a major effect on the LCHS, so a comparison between two and four cycles of operation was performed and is shown in Figures 4.21 and 4.22 for studying the NPV. The other model inputs are the same values as given in Table 4.14.

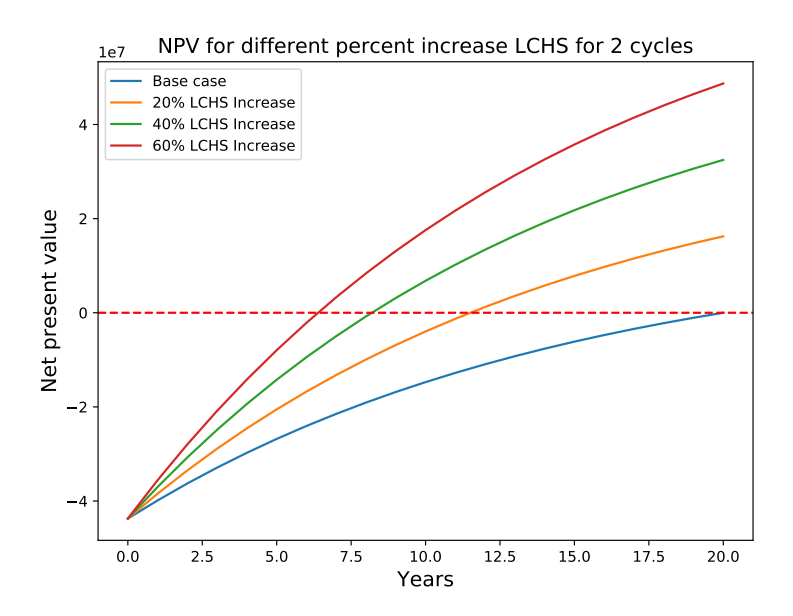


Figure 4.21: NPV analysis for 2 cycles of operation with different increase in LCHS percentage

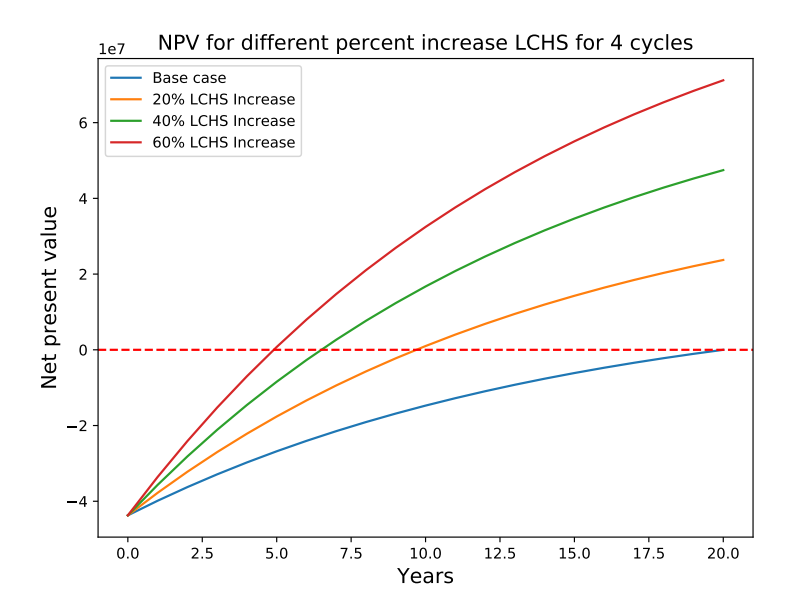


Figure 4.22: NPV analysis for 4 cycles of operation with different increase in LCHS percentage

From Figures 4.21 and 4.22 it can be observed that the NPV for storage is based on different percentage increases in the LCHS and the profile varies based on the operating cycle of the plant. When the storage is operated for two cycles and the levelized cost is increased by 60% (2.4 $\[\in \]$ /kg) it takes nearly 6.5 years to reach the profitable regime. When the storage is operated for four cycles and the levelized cost is increased by 60% (1.76 $\[\in \]$ /kg) it takes nearly five years to reach the profitable regime. So the larger cycle of operation increases the productivity of the plant which in turn helps in reaching positive NPV faster.

4.3.9. Effect on LCHS when new caverns are utilized for storage

The scenarios focused till now are studied for repurposing existing salt caverns and the cost was not observed for newly created caverns. In this section, the costs are observed for storing green hydrogen in newly created caverns.

The base case scenario from the previous studies is taken for this case as well. The scenario study is performed for two new caverns consisting of two compressor & heat exchanger setups. The current green hydrogen price of $6.03 \in /kg$ is assumed for calculating the cushion gas investment. The caverns are operated alternatively with a maximum of 12 cycles per year with each cavern operating six cycles and the loss due to regeneration is assumed to be 10% of the working gas. The cost for the creation of the cavern is given by the graph from the appendix 4.7 and from the graph for a volume of 260,000 m³ the cost of creation is around $70 \in /m³$. Based on the assumptions the capital distribution for the storage is shown in Figure 4.23.

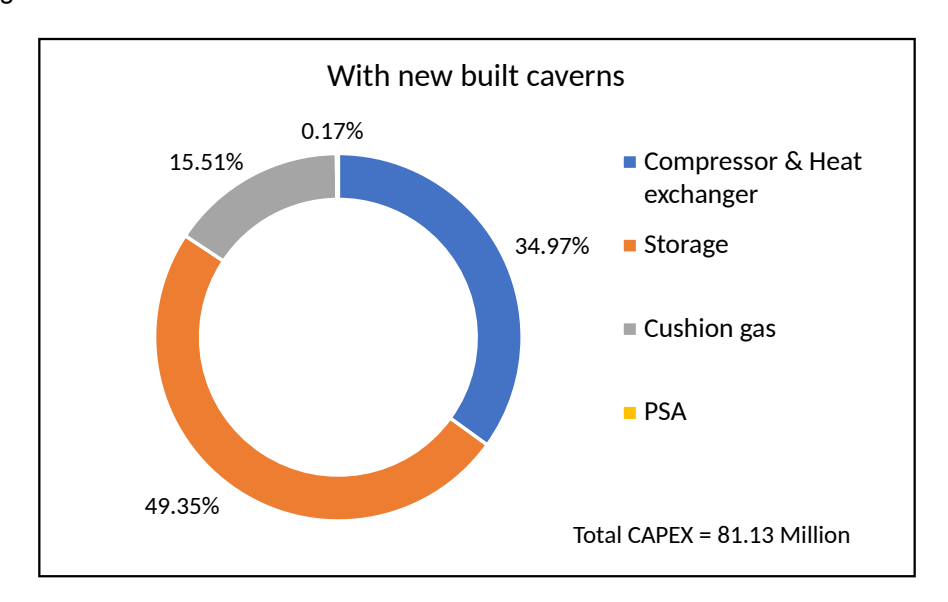


Figure 4.23: CAPEX distribution for two newly created caverns consisting of two compressors & heat exchanger setup.

From Figure 4.23 it can be observed that the cost associated with the storage increases and becomes the most dominating factor followed by the compressor & heat exchanger setup. When the new caverns are created the lifetime of the storage is between 30-50 years, so to understand the cost distribution across the lifetime, the annualized and levelized costs are studied for a 12-cycle operation and are shown in Figure 4.24.

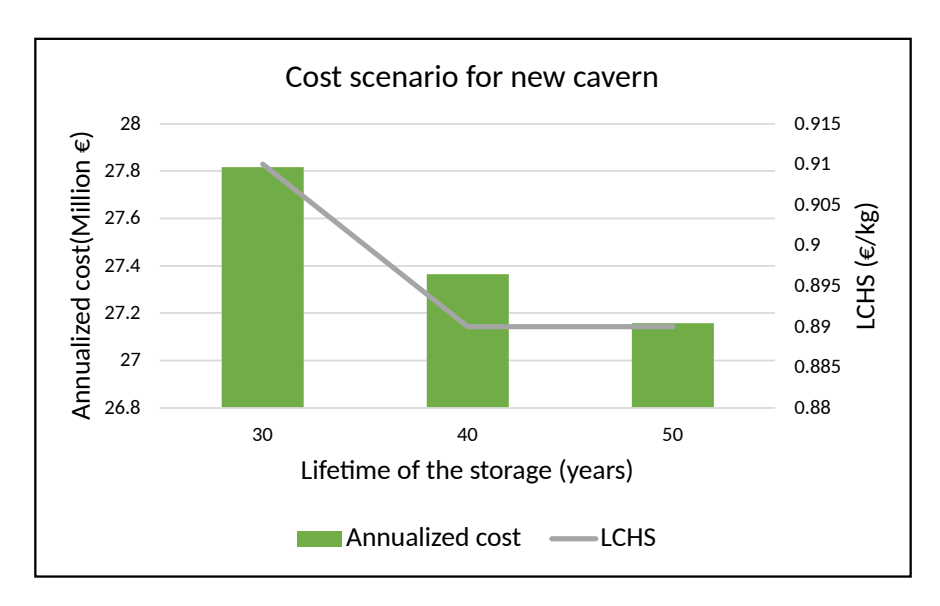


Figure 4.24: Cost distribution of the storage for 2 new caverns and 2 compressors heat exchanger setup, based on different lifetimes of storage operated for 12 cycles per year

From Figure 4.24 it can be observed that the levelized cost decreases until 40 years and after 40 years the change in the levelized cost is not large. As per the previous results based on the cost is estimated based on the number of cycles of operation and when the lifetime of the plant is fixed at 40 years and is given in Figure 4.25.

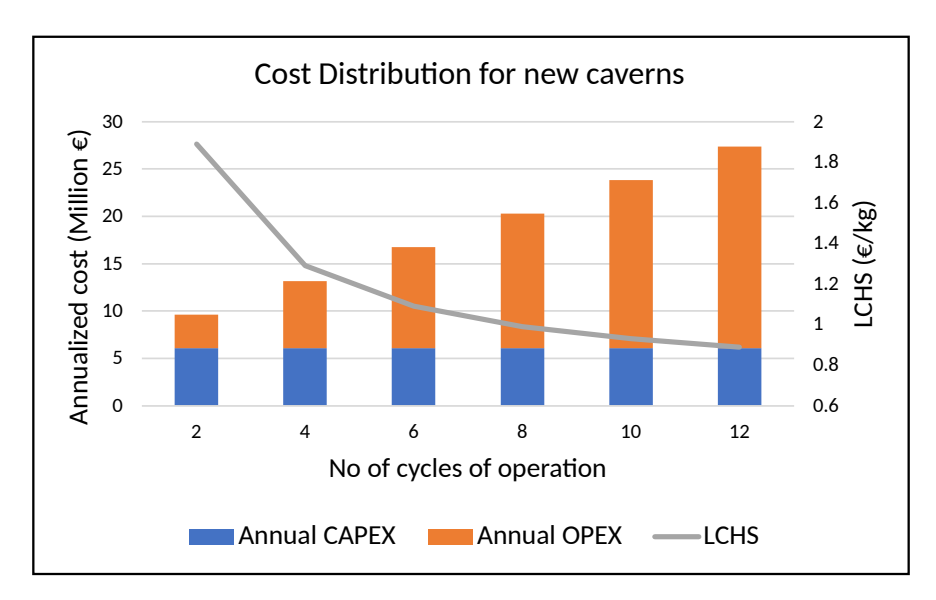


Figure 4.25: Levelized cost based on different cycles of operation for new caverns

From Figure 4.25 it can be observed that the levelized cost for the operation of the cavern for fewer cycles is higher when compared with the repurposing caverns but this closed the gap and the LCHS for the new cavern with a lifetime of 40 years is 0.89 /kg and the repurposed cavern with a lifetime of 20 years for 12 cycles is 0.83 /kg. So for lower operating cycles, the LCHS difference is larger and for higher operating cycles the LCHS difference is lower.

4.3. Results 52

4.3.10. Effect of cavern shrinkage on LCHS

Cavern when operated in cycles tends to create creep and this results in relative volume loss, the scenarios till now did not consider the impact of the cavern shrinkage on the LCHS, for a good operation of the cavern this needs to be maintained at less than 1% per year [63]. In this section, the impact of the shrinkage on the levelized cost of hydrogen storage is studied for a repurposed cavern with a lifetime of 20 years and for a new cavern with a lifetime of 40 years. The LCHS in both cases is compared together with the results case when the cavern shrinkage was not considered. The effect of cavern shrinkage on the LCHS is shown in Figures 4.26 and 4.27. There are two caverns with two compressor ad heat exchanger setups operated alternatively and the results are shown for the different cycles of operation.

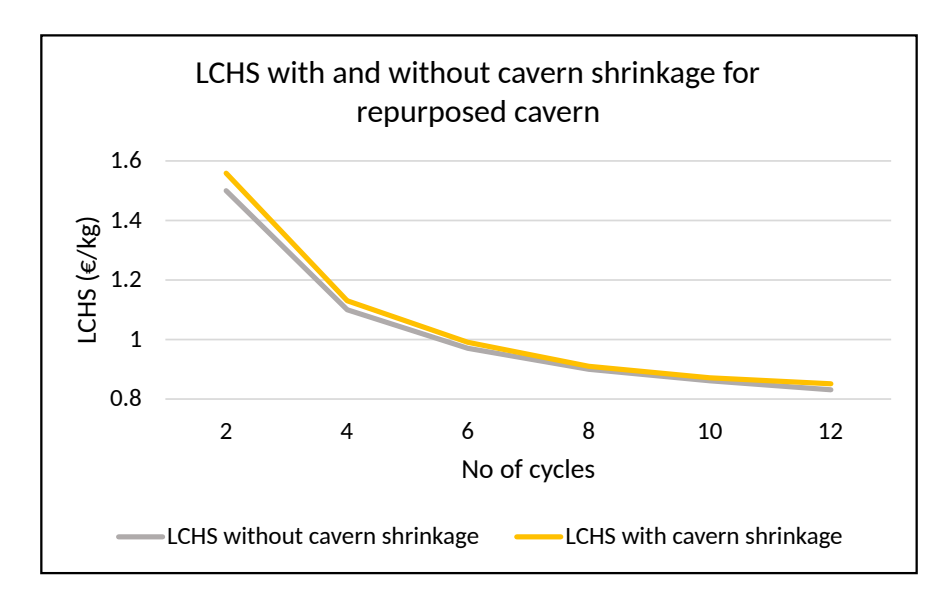


Figure 4.26: Effect of cavern shrinkage on LCHS when an existing cavern is used for a lifetime of 20 years based on different cycles of operation

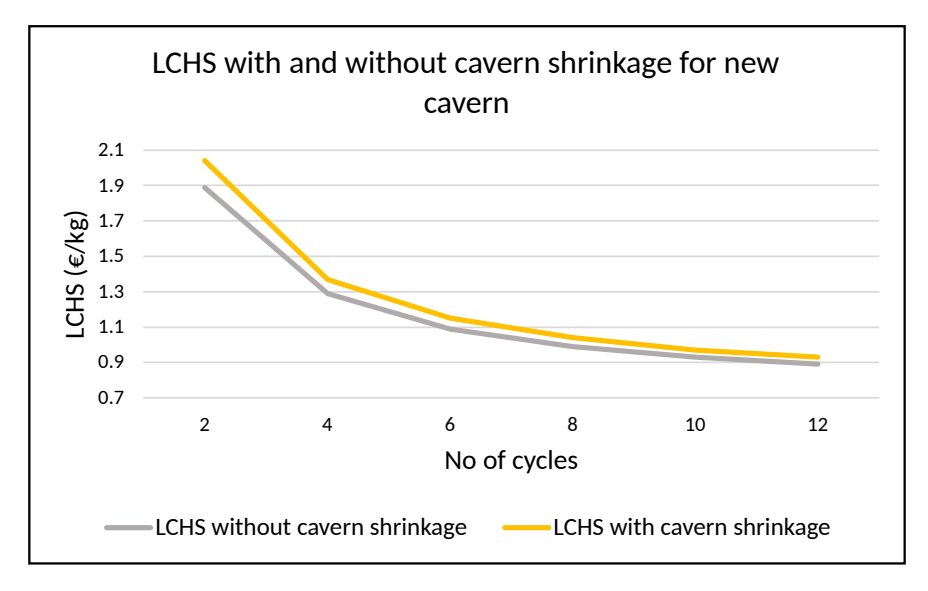


Figure 4.27: Effect of cavern shrinkage on LCHS when a new cavern is used for a lifetime of 40 years based on different cycles of operation

From Figures 4.26 and 4.27 it can be observed that the LCHS does not have a huge impact because of the shrinkage and this is because the operating expense is directly related to the working gas and this is a

4.3. Results 53

function of cavern volume, so the cavern shrinkage will have a direct effect on the OPEX of the storage. From equation 4.4 it could be observed that the shrinkage will only have an effect on the initial CAPEX and when this is large as in the case of new cavern creation the LCHS has a higher deviation.

$$LCHS_{shrinkage} = \frac{CAPEX}{\sum_{t=1}^{I} \frac{W \downarrow}{(1+i)^{t}}} + \frac{\sum_{t=1}^{I} \frac{OPEX \downarrow}{(1+i)^{t}}}{\sum_{t=1}^{I} \frac{W \downarrow}{(1+i)^{t}}}$$
(4.4)

4.3.11. Electrolyser capacity estimation for hydrogen storage

The scenarios were studied based on the assumption that there is green hydrogen available for storage. But with the current infrastructure this might not be possible and to understand hydrogen requirement based on the electrolyser capacity the following scenario was performed. The calculation is based on the assumption that a cavern with a volume of 260,000 m³, containing an existing 50-bar cushion gas, can store a working gas capacity of around 2.73 kilotons of green hydrogen. From Figure 4.4 it can be taken that the injection process takes 700 hours to completely fill the cavern, which is approximately equivalent to 30 days. This indicates that approximately of 3,900 kg hydrogen per hour is required for the storage to function continuously.

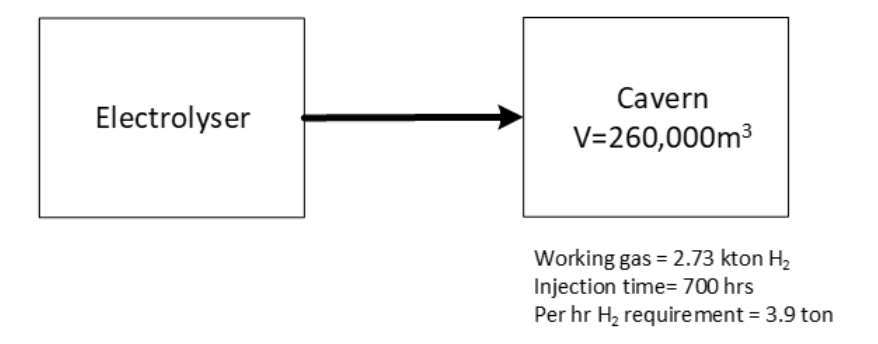


Figure 4.28: Input parameters used to estimate the electrolyser requirement for hydrogen storage in a single salt cavern

Given the current available green hydrogen production technologies, a 100 MW electrolyser produces 1.7 tons per hour. To meet the hourly hydrogen requirement, it would require running a 230 MW electrolyser to run continuously at full capacity, producing green hydrogen for the storage operation. If the electrolyser is operated at 70% capacity, the required electrolyser capacity would be around 330 MW. Consequently, the electricity needed for the production of hydrogen using the 230 MW electrolyser (operated at 70% electrical efficiency) is approximately 130 GWh. Considering the Lower Heating Value (LHV) of hydrogen and the energy capacity of the working gas within the storage it is around 90 GWh.

At present, the largest planned electrolyser has a capacity of 200 MW, and if other projects were taken into account, the total electrolyser capacity is expected to reach a maximum of 500 MW by 2028. These electrolysers will primarily satisfy base requirements, with peak production occurring during the winter months when offshore wind production is high. However, this presents a challenge as it would require operating the storage with only one or two cycles per year, leading to increased costs and a higher levelized cost of hydrogen. Alternatively, operating the electrolyser as seasonal storage with lower capacity seems nonviable due to the presence of other storage facilities in the Netherlands, which will be connected to the hydrogen network initially. Moreover, the hydrogen gas network connection to the storage location at Epe is not expected until after 2030. Given this information, the use of hydrogen storage will likely become feasible only when the electrolyser capacity reaches Gigawatt scales and a proper hydrogen network is established and connected to the storage location. But if the storage does not rely purely on the hydrogen network from the Netherlands but also relays on imports from other countries this could change the type of operation of the storage.

Conclusion and Recommendation

5.1. Conclusions

The following research question was answered with this thesis project

1. What are the challenges involved in storing hydrogen in the salt cavern?

Due to the low volumetric energy density of hydrogen compared to natural gas, the energy stored in hydrogen per cavern is three times less than the energy density of natural gas. Since the storage process is in high pressure and hydrogen is susceptible towards hydrogen embrittlement high strength material cannot be used and new alloys need to be investigated. Due to purity requirements, the existing gas within the storage needs to be extracted. The presence of water and microbial activity withdrawn gas needs to be purified.

2. What technical measures are needed for making Epe fit for hydrogen?

The current surface equipment used for natural gas storage cannot be utilized for storing hydrogen. so new investment needs to be made towards the surface equipment which is suitable for hydrogen application. The natural gas emptying process poses some challenges in itself as there is less availability of brine solution and the process of fluting the cavern occurs at a rate of 50 m³/hr. The timeline required for the storage conversion is shown in Figure 5.1.

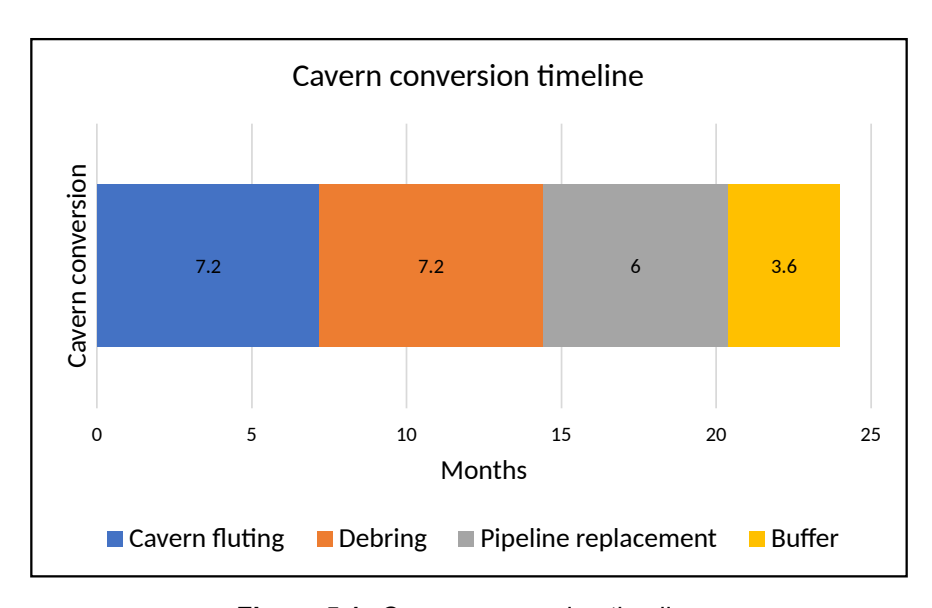


Figure 5.1: Cavern conversion timeline

From Figure 5.1 it can be observed that when the storage is converted it takes approximately a minimum 2 years for a single cavern to be converted to store hydrogen and the cavern can be converted one by one as the water availability might be an issue for converting together. So

5.2. Recommendations 55

repurposing all seven caverns might take nearly 14 years and, if the conversion starts immediately all the caverns will be repurposed around 2038 and this will reduce the available lifetime of some caverns which in turn will affect the LCHS. So from the results, if the lifetime of the repurposed cavern is expected below 20 years the cost increases so it is better to invest in new caverns when the lifetime is shorter.

3. What will be the CAPEX and OPEX involved in converting the storage and operating it with Hydrogen?

The major contributing factor towards the capital expenditure is the cost associated with the compressor and heat exchanger setup followed by the cushion gas investment which almost takes up to 70% of the total investment costs. When the cavern is operated at lower cycles, the operating expense does not play a major role unless the gas loss due to the purification step is higher.

4. What will be the Levelized cost of hydrogen storage(LCHS) in salt cavern?

The levelized cost of hydrogen varied based on different cases, the highest range occurred when a stand-by compressor was utilized for a single cycle and single cavern, the LCHS ranged from $1.68 \in /kg$ to $1.94 \in /kg$. The best case was obtained when two caverns were operated in alternate injection and withdrawal cycles and when the purification gas is sent back into the storage process, the LCHS varied from $1.24 \in /kg$ to $0.34 \in /kg$. Through sensitivity analysis, the most sensitive part identified is the number of cycles of operation and the cost associated with hydrogen loss. The number of cycles of operation also affects the NPV.

5. When will be the storage required and at what electrolyser capacity will it be feasible?

A 230 MW electrolyser operated continuously in full operation is required for a single cavern filling within 700hrs of injection. The storage is possible when the hydrogen gas network is connected to the storage location which is expected after 2030 but importing hydrogen for storage from overseas and other countries is a possible option and the storage can be utilized based on that option.

To conclude there are technological gaps involved with the storage equipment that can be used for hydrogen storage, and the green hydrogen production and transportation infrastructure are still in the initial stages and when this is further developed in future, the hydrogen storage becomes reasonable.

5.2. Recommendations

The following recommendations are proposed for future work

- The purification step is focused on proven technology for hydrogen purification i.e. PSA but further research can be done in looking for other purification options.
- The cushion gas used is hydrogen but the cost can be studied for different cushion gas and how the purification step needs to be modified.
- The cost estimation did not include the leak testing of the cavern and the economic loss incurred during the storage conversion timeframe.
- The entire hydrogen backbone can be studied based on the electrolyser capacity.
- There is microbial activity present in the salt cavern and this needs to be accounted and a multi-component purification must be studied.

- [1] Energy Transition Outlook. Tech. rep. DNV, 2022.
- [2] Hydrogen Supply Capacity and Demand. Tech. rep. Fuel Cell and Hydrogen Observatory, 2022.
- [3] Netherlands entreprise agency. english.rvo.nl,offshore-wind-energy-plans-2030-2050. 2022.
- [4] Excelling in Hydrogen. Tech. rep. rvo.
- [5] Anthony Wang et al. "Analysing future demand, supply, and transport of hydrogen". In: (2021).
- [6] CBS Statline. opendata.cbs.nl. 2022.
- [7] HyWay27,Realisation of national hydrogen network. rijksoverheid.nl.
- [8] A Amid et al. "Seasonal storage of hydrogen in a depleted natural gas reservoir". In: *International journal of hydrogen energy* 41.12 (2016), pp. 5549–5558.
- [9] N Heinemann et al. "Hydrogen storage in saline aquifers: The role of cushion gas for injection and production". In: *International Journal of Hydrogen Energy* 46.79 (2021), pp. 39284–39296.
- [10] Nasiru Salahu Muhammed et al. "A review on underground hydrogen storage: Insight into geological sites, influencing factors and future outlook". In: *Energy Reports* 8 (2022), pp. 461–499.
- [11] Radoslaw Tarkowski. "Underground hydrogen storage: Characteristics and prospects". In: *Renewable and Sustainable Energy Reviews* 105 (2019), pp. 86–94.
- [12] Alvaro Sáinz-García et al. "Assessment of feasible strategies for seasonal underground hydrogen storage in a saline aquifer". In: *International journal of hydrogen energy* 42.26 (2017), pp. 16657–16666.
- [13] Wolf Tilmann Pfeiffer et al. "Subsurface porous media hydrogen storage–scenario development and simulation". In: *Energy Procedia* 76 (2015), pp. 565–572.
- [14] M. Panfilov. "4 Underground and pipeline hydrogen storage". In: *Compendium of Hydrogen Energy*. Ed. by Ram B. Gupta et al. Woodhead Publishing Series in Energy. Woodhead Publishing, 2016, pp. 91–115. URL: https://www.sciencedirect.com/science/article/pii/B9781782423621000043.
- [15] Leszek Lankof et al. "Assessment of the potential for underground hydrogen storage in bedded salt formation". In: *International journal of hydrogen energy* 45.38 (2020), pp. 19479–19492.
- [16] Xin Liu et al. "Maximum gas production rate for salt cavern gas storages". In: *Energy* 234 (2021), p. 121211.
- [17] Alexander Lemieux et al. "Preliminary assessment of underground hydrogen storage sites in Ontario, Canada". In: *International Journal of Hydrogen Energy* 44.29 (2019), pp. 15193–15204.
- [18] Richard L Wallace et al. "Utility-scale subsurface hydrogen storage: UK perspectives and technology". In: *International Journal of Hydrogen Energy* 46.49 (2021), pp. 25137–25159.
- [19] Davood Zivar et al. "Underground hydrogen storage: A comprehensive review". In: *International journal of hydrogen energy* 46.45 (2021), pp. 23436–23462.
- [20] Wei Liu et al. "Feasibility evaluation of large-scale underground hydrogen storage in bedded salt rocks of China: A case study in Jiangsu province". In: *Energy* 198 (2020), p. 117348.
- [21] BENT Sorensen. "Underground hydrogen storage in geological formations, and comparison with other storage solutions". In: *Hydrogen Power Theoretical and Engineering International Symposium VII*", *Merida, Mexico, Paper HU-02, CDROM.* 2007.

[22] Jan Michalski et al. "Hydrogen generation by electrolysis and storage in salt caverns: Potentials, economics and systems aspects with regard to the German energy transition". In: *International Journal of Hydrogen Energy* 42.19 (2017), pp. 13427–13443.

- [23] Laura M Valle-Falcones et al. "Green Hydrogen Storage in an Underground Cavern: A Case Study in Salt Diapir of Spain". In: *Applied Sciences* 12.12 (2022), p. 6081.
- [24] Ahmet Ozarslan. "Large-scale hydrogen energy storage in salt caverns". In: *International journal of hydrogen energy* 37.19 (2012), pp. 14265–14277.
- [25] Office of Energy Efficiency and Renewable Energy: Hydrogen Storage. URL: https://www.energy.gov/eere/fuelcells/hydrogen-storage.
- [26] Sankara Papavinasam. "Chapter 5 Mechanisms". In: Corrosion Control in the Oil and Gas Industry. Ed. by Sankara Papavinasam. Boston: Gulf Professional Publishing, 2014, pp. 249–300. URL: https://www.sciencedirect.com/science/article/pii/B9780123970220000054.
- [27] Sandeep Kumar Dwivedi et al. "Hydrogen embrittlement in different materials: A review". In: International Journal of Hydrogen Energy 43.46 (2018), pp. 21603—21616. URL: https://www.sciencedirect.com/science/article/pii/S0360319918331306.
- [28] Ujwal Shreenag Meda et al. "Challenges associated with hydrogen storage systems due to the hydrogen embrittlement of high strength steels". In: *International Journal of Hydrogen Energy* (2023). URL: https://www.sciencedirect.com/science/article/pii/S036031992300530X.
- [29] Niklas Heinemann et al. "Enabling large-scale hydrogen storage in porous media—the scientific challenges". In: *Energy & Environmental Science* 14.2 (2021), pp. 853–864.
- [30] A. Davoodi et al. "A comparative H2S corrosion study of 304L and 316L stainless steels in acidic media". In: Corrosion Science 53.1 (2011), pp. 399–408. URL: https://www.sciencedirect.com/ science/article/pii/S0010938X10004816.
- [31] Pierre-André Jacques et al. "HyCoRA–Hydrogen Contaminant Risk Assessment Grant agreement no: 621223 Review on the impact of impurities on PEMFC and". In: ().
- [32] Edward P Bartlett. "The concentration of water vapor in compressed hydrogen, nitrogen and a mixture of these gases in the presence of condensed water". In: *Journal of the American Chemical Society* 49.1 (1927), pp. 65–78.
- [33] Mohammad-Reza Tahan. "Recent advances in hydrogen compressors for use in large-scale renewable energy integration". In: *International Journal of Hydrogen Energy* (2022).
- [34] Giuseppe Sdanghi et al. "Review of the current technologies and performances of hydrogen compression for stationary and automotive applications". In: *Renewable and Sustainable Energy Reviews* 102 (2019), pp. 150–170.
- [35] A Peschel. "Industrial perspective on hydrogen purification, compression, storage, and distribution". In: *Fuel cells* 20.4 (2020), pp. 385–393.
- [36] Ahmed M Elberry et al. "Large-scale compressed hydrogen storage as part of renewable electricity storage systems". In: *International journal of hydrogen energy* 46.29 (2021), pp. 15671–15690.
- [37] Christoph Windmeier et al. *Ullmann's Encyclopedia of Industrial Chemistry: Cryogenic Technology*. 2013.
- [38] Ulrich Bünger et al. "Large-scale underground storage of hydrogen for the grid integration of renewable energy and other applications". In: *Compendium of hydrogen energy*. Elsevier, 2016, pp. 133–163.
- [39] Justin Hollingsworth et al. "Reciprocating compressors". In: *Compression Machinery for Oil and Gas*. Elsevier, 2019, pp. 167–252.
- [40] Office of Energy Efficiency and Renewable Energy: Hydrogen Compression. URL: https://www.energy.gov/eere/fuelcells/gaseous-hydrogen-compression.

[41] Jiaxing Liu et al. "Overview of hydrogen-resistant alloys for high-pressure hydrogen environment: on the hydrogen energy structural materials". In: *Clean Energy* 7.1 (2023), pp. 99–115.

- [42] Christopher W San Marchi. "Austenitic stainless steels in Gaseous Hydrogen Embrittlement of High Performance Metals in Energy Systems." In: (2011).
- [43] Thorsten Michler et al. "Hydrogen embrittlement of Cr-Mn-N-austenitic stainless steels". In: *International Journal of Hydrogen Energy* 35.3 (2010), pp. 1485–1492.
- [44] Steel properties. URL: https://www.finetubes.co.uk/products/materials/stainless-steel-tubes/alloy-316-uns-s31600-wnr-14401.
- [45] Thermal conductivity of steel. URL: https://thermtest.com/thermal-conductivity-of-steel.
- [46] Gavin Towler et al. Chemical engineering design: principles, practice and economics of plant and process design. Butterworth-Heinemann, 2021.
- [47] Philip Kosky et al. *Exploring engineering: an introduction to engineering and design*. Academic Press, 2012.
- [48] Heat exchanger fouling factor. URL: https://powderprocess.net/Tools_html/Data_Diagrams/Heat Exchanger Fouling Factor.html.
- [49] Stainless Steel allowable pressures. URL: https://www.engineeringtoolbox.com/stainless-steel-pipes-pressure-ratings-d_346.html.
- [50] Gasuni Hydrogen purity. URL: https://www.gasunie.nl/en/expertise/hydrogen/hydrogen-and-industry/hydrogen-quality-for-the-dutch-network.
- [51] Thorsten Agemar et al. "Subsurface temperature distribution in Germany". In: *Geothermics* 44 (2012), pp. 65–77.
- [52] Humza Bin Navaid et al. "A comprehensive literature review on the challenges associated with underground hydrogen storage". In: *International Journal of Hydrogen Energy* 48.28 (2023), pp. 10603–10635.
- [53] John Morgan Campbell. "Chapter-18, Gas conditioning and processing. Vol. 2". In: (1979).
- [54] Zainul Abdin et al. "Projecting the levelized cost of large scale hydrogen storage for stationary applications". In: *Energy Conversion and Management* 270 (2022), p. 116241.
- [55] Hydrogen Network. Tech. rep. URL: https://www.hynetwork.nl/en/news/quality-specification-for-hydrogen/.
- [56] Chemical Engineering Plant Cost Index. URL: https://personalpages.manchester.ac.uk/staff/tom.rodgers/Interactive_graphs/CEPCI.html?reactors/CEPCI/index.html.
- [57] Fuel cell and observatory. URL: https://www.fchobservatory.eu/observatory/technology-and-market/levelised-cost-of-hydrogen-green-hydrogen-costs.
- [58] TE, EU natural gas. URL: https://tradingeconomics.com/commodity/eu-natural-gas.
- [59] FE, Stainless Steel cost. URL: https://www.fastwell.in/3161-stainless-steel-supplier-manufacturer.html.
- [60] Adsorbent cost. URL: https://www.made-in-china.com/products-search/hot-china-products/Zeolite_4a_Price.html.
- [61] IEA Blue Hydrogen Cost. URL: https://www.iea.org/data-and-statistics/charts/global-average-levelised-cost-of-hydrogen-production-by-energy-source-and-technology-2019-and-2050.
- [62] IEA North West hydrogen monitot. URL: https://www.iea.org/reports/northwest-european-hydrogen-monitor.
- [63] Jie Chen et al. "Stability study and optimization design of small-spacing two-well (SSTW) salt caverns for natural gas storages". In: *Journal of Energy Storage* 27 (2020), p. 101131.

- [64] Nicholas P Chopey. "Handbook of chemical engineering calculations". In: (No Title) (2004).
- [65] Fritz Crotogino. "Traditional bulk energy storage—Coal and underground natural gas and oil storage". In: *Storing energy*. Elsevier, 2022, pp. 633–649.



Appendix

A.1. Heat exchanger sizing

Table 19.3 Standard Dimensions for Steel Tubes					
Outside Diameter (mm)	Wall Thickness (mm)				
16	1.2	1.7	2.1	_	_
19	_	1.7	2.1	2.8	_
25	_	1.7	2.1	2.8	3.4
32	_	1.7	2.1	2.8	3.4
38	_	_	2.1	2.8	3.4
50	_	_	2.1	2.8	3.4

Figure A.1: Standard tube diameters [46]

		Face velocity, ft/min (m/s)	
Number of tube rows	8 fins/in (315 fins/m), 2.375-in (0.0603-m) pitch	10 fins/in (394 fins/m), 2.375-in (0.0603-m) pitch	10 fins/in (394 fins/m), 2.5-in (0.0635-m) pitch
3	650 (3.30)	625 (3.18)	700 (3.56)
4	615 (3.12)	600 (3.05)	660 (3.35)
5	585 (2.97)	575 (2.92)	625 (3.18)
6	560 (2.84)	550 (2.79)	600 (3.05)

Figure A.2: Face velocity design assumption [64]

A.2. PSA sizing 61

A.2. PSA sizing

Basic Type	Nominal Pore Diameter (Angstroms)	Available Form	Equilibrium H ₂ O Capacity (% wt)	Molecules Adsorbed	Molecules Excluded	Applications
3A	3	Powder 1/16 in Pellets 1/8 in Pellets 8-12 Beads 4-8 Beads	26 21 21 21 21 21	Molecules with an effective diameter <3 angstroms, including H ₂ O and NH ₃	Molecules with an effective diameter >3 angstroms, e.g., ethane, CO ₂ , H ₂ S, methanol	Selected to minimize co- adsorption of unwanted impurities, such as metha- nol or light olefins, and to reduce the formation of COS. Dry olefins, methanol, ethanol, and natural gas.
4A	4	Powder 1/16 in Pellets 1/8 in Pellets 8-12 Beads 4-8 Beads 14 × 30 Mesh	27.5 22 22 22 22 22 22 22	Molecules with an effective diameter <4 angstroms, including ethanol, H ₂ S, CO ₂ , SO ₂ , C ₂ H ₄ , C ₂ H ₆ , and C ₃ H ₆	Molecules with an effective diameter >4 angstroms, e.g., propane	Most commonly used for natural gas dehydration. Dry natural gas, remove H ₂ S. 4A sieve can also be manufactured to remove trace amounts of CO ₂ for LNG applications.
5A	5	Powder 1/16 in Pellets 1/8 in Pellets 8-12 Beads 4-8 Beads	26 21.5 21.5 21.5 21.5 21.5	Molecules with an effective diameter <5 angstroms, including n-C ₄ H ₉ OH, n-C ₄ H ₁₀ , C ₃ H ₈ to C ₂₂ H ₄₆	Molecules with an effective diameter >5 angstroms, e.g., iso compounds and all 4 carbon rings	Separates normal paraf- fins from branched-chain and cyclic hydrocarbons through a selective adsorption process, remove H ₂ S, and normal mercaptans.
13X	10	Powder 1/16 in Pellets 1/8 in Pellets 8-12 Beads 4-8 Beads	30 26 26 26 26 26	Molecules with an effective diameter < 10 angstroms	Molecules with an effective diameter > 10 angstroms	Remove mercaptans and H ₂ S from hydrocarbon liquids, remove H ₂ O and CO ₂ from air plant feed, remove iso-mercaptans from natural gas.

Note: 8-12 and 4-8 refers to the Tyler screen size.

4-8 beads is equivalent to a nominal diameter of 3.2 mm [1/8 in].

8-12 beads is equivalent to a nominal diameter of 3.2 mm [1/16 in].

Chart shows typical molecular sieve types only. It is common for vendors to customize these basic forms for specific use. Equilibrium H₂O Capacity taken at 2.333 kPa and 25°C (0.34 psia and 77°F).

Acid resistant sieves are available for dehydration of natural gas containing high concentrations of acid gas (H₂S + CO₂).

Each type adsorbs the molecules listed plus those in the preceding row.

Figure A.3: Adsorbent selection [53]

A.2. PSA sizing 62

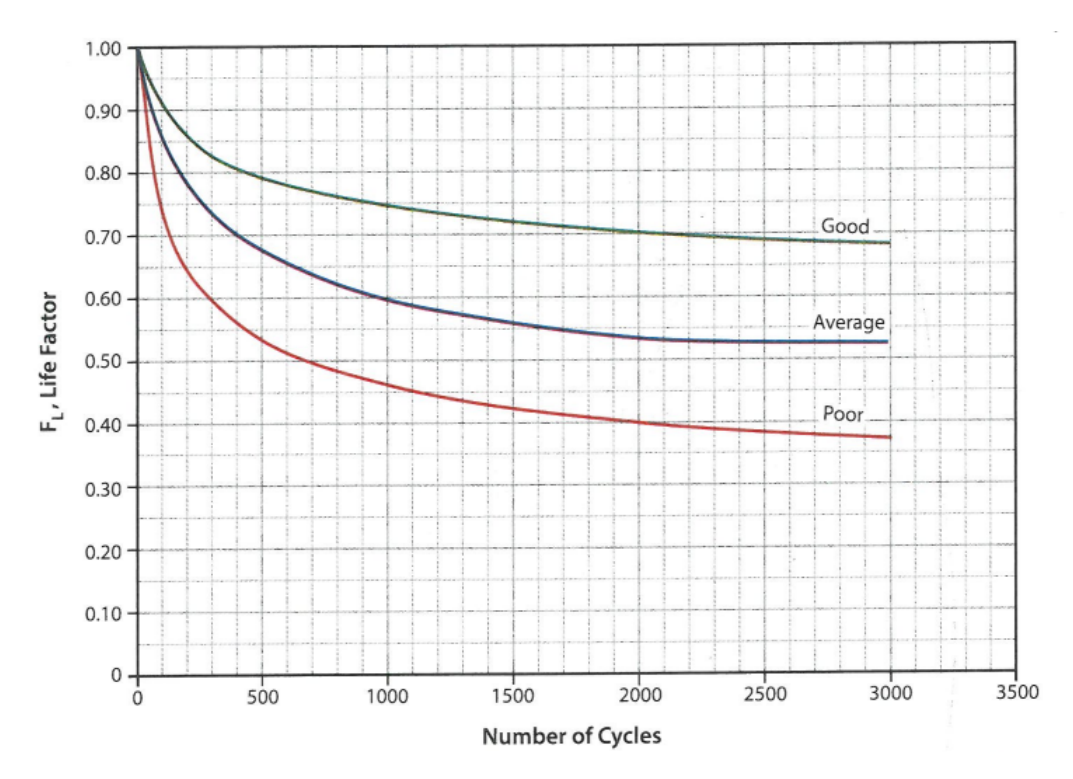


Figure A.4: Molecular sieve capacity decline curves [53]

	SI		FPS		
Desiccant Shape and Size	В	C	В	C	
4x8 bead	4.16	0.001 35	0.056 0	0.000 088 9	
3.2 mm (1/8") extrudate	5.36	0.001 89	0.072 2	0.000 124	
8x12 bead	11.3	0.002 07	0.152	0.000 136	
1.6 mm (1/16") extrudate	17.7	0.003 19	0.238	0.000 210	

Figure A.5: Pressure drop constant for molecular sieve based on sizes [53]

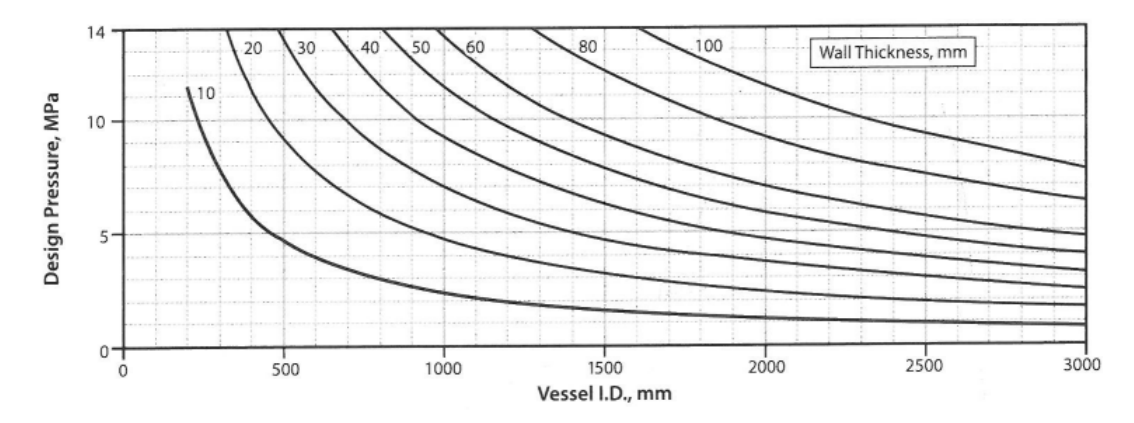


Figure A.6: Thickness of the column [53]

A.3. New cavern creation 63

A.3. New cavern creation

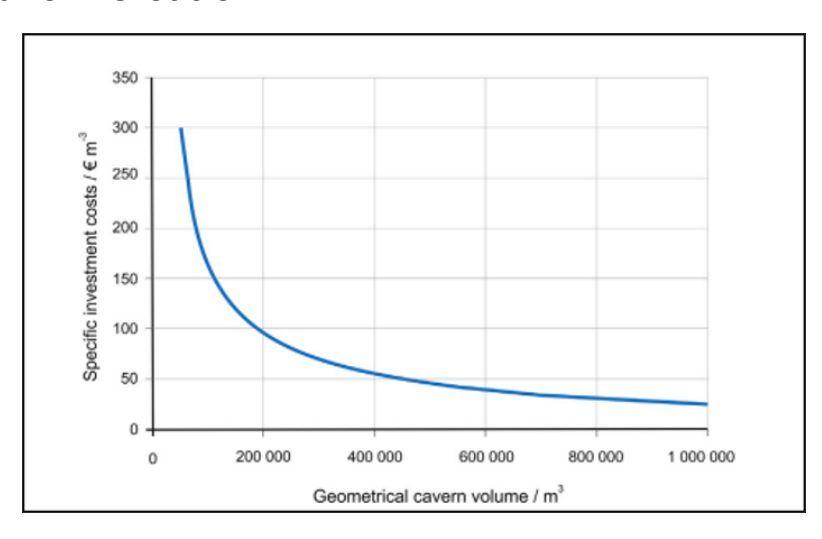


Figure A.7: Cavern creation cost [65]